Charge Carrier Transporting Molecular Materials and Their Applications in Devices

Yasuhiko Shirota*,† and Hiroshi Kageyama‡

Fukui University of Technology, 3-6-1, Gakuen, Fukui City, Fukui 910-8505, Japan, and Department of Applied Chemistry, Faculty of Engineering, Osaka University, Yamadaoka, Suita, Osaka 565-0871, Japan

Received August 11, 2006

Contents

* To whom correspondence should be addressed. Postal address: 3-6-1, Gakuen, Fukui City, Fukui 910-8505, Japan. E-mail: shirota@fukui-ut.ac.jp and shirota@ap.chem.eng.osaka-u.ac.jp.
† Fukui University of Technology.
‡ Osaka University.

1. Introduction

Electronic and optoelectronic devices using organic materials as active elements, for example, organic light-emitting diodes (OLEDs), organic photovoltaic devices (OPVs), organic field-effect transistors (OFETs), organic photorefractive devices, and so forth, have recently received a great deal of attention from the standpoint of potential technological applications as well as fundamental science.[1−4] The devices using organic materials are attractive because they can take advantage of organic materials such as light weight, potentially low cost, and capability of thin-film, large-area, flexible device fabrication. Photoreceptors in electrophotography using organic photoconducting materials have already established wide markets of copying and laser printers. OLEDs have also found practical applications in small displays such as mobile phones, digital camera finders, and car audios and are expected to expand their markets to flat-panel televisions and lighting in the future.

10.1021/cr050143+ CCC: $65.00
Published on Web 04/11/2007

Yasuhiko Shirota graduated from Osaka University in 1963, and received his Doctor of Engineering from Osaka University in 1968. He was appointed to be Research Associate at Osaka University in 1968 and promoted to Associate Professor in 1972 and full Professor in 1986. Since 2003, he has been Professor Emeritus of Osaka University and Professor at Fukui University of Technology. His research interest covers a wide field of organic materials science including the synthesis, structures, reactions, properties, functions, and device performance of both molecular materials and polymers.

Hiroshi Kageyama obtained his B. Eng. (1992), M. Eng. (1994), and Ph.D. (1997) degrees from Osaka University. He was appointed to be Research Associate at Osaka University in 1997 and has been Assistant Professor since 2006. He is interested in charge transport in organic disordered systems.

Organic materials for use in electronic and optoelectronic devices, in particular, OPVs and OFETs, are often called organic semiconductors, which play the role of the charge carrier transport as well as the charge carrier generation or injection. In contrast to inorganic semiconductors, organic semiconductors are essentially electrical insulators. All the devices described above involve charge transport as an essential operation process and hence, require charge-transporting materials. Therefore, the development of high-performance, charge-transporting materials is a key issue for the fabrication of high-performance devices. Charge-transporting materials are mostly based on π-electron systems, which are characterized by properties such as light absorption and emission in the ultraviolet-to-visible wavelength region, charge-carrier generation and transport, nonlinear optical properties, and so forth. Organic charge-transporting materials include both small molecules, that is, molecular materials, and polymers, the latter of which are mainly classified into π-conjugated polymers and nonconjugated polymers containing pendant π-electron systems.

Charge transport has been a subject of interest from the standpoints of both fundamental science and technology. Early studies of charge transport in organic materials were performed on both single crystals and disordered systems, for example, polymers and molecularly doped polymers, where small organic molecules are dispersed in a polymer binder. In particular, molecularly doped polymers have been studied extensively in view of their practical applications in photoreceptors in electrophotography. The recent development of small organic molecules that readily form stable amorphous glasses, namely, amorphous molecular materials, has enabled the studies of charge transport in the amorphous glassy state of small organic molecules without any binder polymers. Charge carrier mobilities of a number of organic polycrystals have also been determined from the performance of OFETs.

This review article focuses on charge-transporting molecular materials for use in electronic and optoelectronic devices such as OLEDs, OPVs, and OFETs. First, some basic aspects of charge transport and the operation processes of OLEDs, OPVs, and OFETs are described. Then, discussion is directed to the molecular design concepts of charge-transporting molecular materials and their synthesis, properties, and applications in devices. Charge-transporting molecular materials in each device are classified on the basis of their molecular structures. The device structures and performance using charge-transporting molecular materials are also described. Finally, charge transport in molecular materials is discussed in relation to their molecular structures and the performance of devices.

2. Basic Aspects of Charge Transport

This section describes the definition of charge carrier drift mobility, experimental methods for determining charge carrier drift mobilities, and a few models proposed for charge transport in organic disordered systems.

2.1. Charge Carrier Drift Mobility

When a voltage is applied to a sample sandwiched between two electrodes, charge carriers, that is, holes and electrons, are transported across the sample under the electric field. The main concerns with charge transport are how fast and by what mechanism charge carriers are transported.

The velocity of charge carriers is proportional to the strength of the applied electric field and is expressed as eq 1:

$$v = \mu F \tag{1}$$

where v is the velocity of charge carriers, F is the strength of electric field, and the proportional constant μ is the drift mobility of charge carriers, that is, the distance over which charge carriers are transported per second under the unit electric field. It should be noted that μ is dependent upon the electric field for organic disordered systems.

The charge carrier mobilities of organic materials greatly vary depending on the kind of charge carriers, namely, whether they are holes or electrons, molecular structures, and materials morphologies. Different transport mechanisms are operative depending on the aggregation states of materials, for example, crystalline and amorphous states.

2.2. Drift Mobility Measurements

The charge carrier drift mobility has been determined by several methods, which include time-of-flight (TOF) method;[5,6]

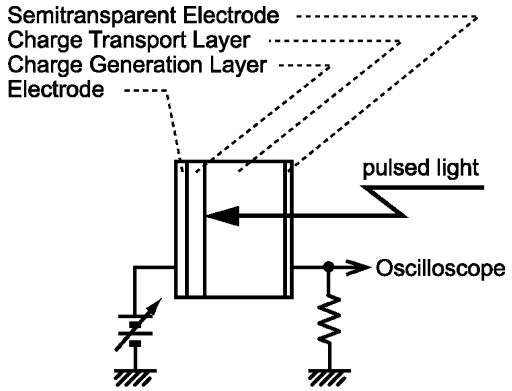

Figure 1. Schematic diagram of apparatus for a time-of-fight method.

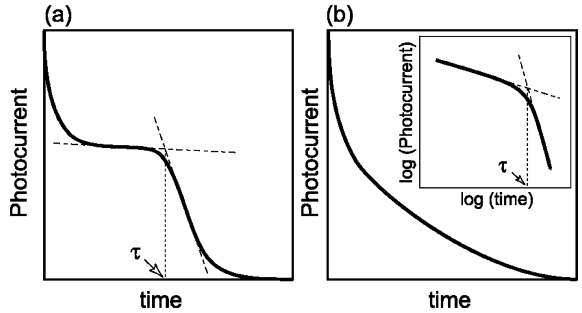

Figure 2. Typical transient photocurrents: (a) nondispersive; (b) dispersive. Inset: double logarithmic plot.

analysis of steady-state, trap-free, space-charge limited current (steady-state TF-SCLC method);[5,7] analysis of dark injection space-charge-limited transient current (DI-SCLC method);[5] analysis of the performance of OFETs (FET method);[8] measurement of transient electroluminescence (EL) by the application of step voltage (transient EL method);[9−12] and pulse radiolysis time-resolved microwave conductivity (PR-TRMC) technique.[13] Among these methods, the TOF technique and the analysis of the performance of OFETs have been most widely employed to determine the carrier drift mobility.

The TOF method is based on the measurement of the carrier transit time (τ), namely, the time required for a sheet of charge carriers photogenerated near one of the electrodes by pulsed light irradiation to drift across the sample to the other electrode under an applied electric field. Samples used for the measurement are either a single charge-transporting layer or double layers consisting of charge carrier generation and transport layers (CGL and CTL, respectively) sandwiched between the two electrodes, one of which is transparent. The thickness of samples is usually in the range from 5 to 20 μm. The samples are prepared using vacuum evaporation, solvent cast from solution, or by pressing melt samples with two ITO electrodes. In the case of the double layer structure (Figure 1), irradiated pulsed light is transmitted through the transparent CTL and absorbed by the CGL. Copper phthalocyanine and perylenebis(dicarboximide)s can be used as CGL materials. One of the charge carriers, either holes or electrons, photogenerated in the CGL is injected into the CTL and then drifts across the CTL to the electrode. Alternatively, photogeneration of charge carriers takes place at the interface between the CGL and CTL depending upon the kind of CGL materials. When charge carriers start to drift, photocurrents flow until the charge carriers arrive at the other electrode. Figure 2 shows a typical transient photocurrent as a function of time. The transit time (τ) is experimentally determined from the cusp of nondispersive photocurrent, as shown in the figure. In contrast to the nondispersive photocurrent in Figure 2a, the transient photocurrents observed for polymers and molecularly doped polymers are often dispersive without any definite cusp as shown in Figure 2b. In this case, τ is determined from the double logarithmic plots of transient photocurrents, according to the Scher−Montroll theory.[14]

The transit time (τ) is given by eq 2, where v is the velocity of charge carriers and d is the sample thickness. When eqs 1 and 2 are combined, the charge carrier drift mobility (μ) is expressed as eq 3.

$$\tau = \frac{d}{v} \tag{2}$$

$$\mu = \frac{d^2}{V\tau} \tag{3}$$

The measurement of carrier drift mobility by the steady-state TF-SCLC method is based on the analysis of current density (J)−applied voltage (V) characteristics in the dark. Generally, the $J-V$ characteristics are linear at low drive voltages, showing ohmic behavior. At high applied voltages, the $J-V$ characteristics become space-charge-limited because of the injection of charge carriers from one electrode. When the contact between the electrode and the organic layer is ohmic and the current is transport-limited instead of injection-limited, the space-charge-limited current J is given by eq 4, which is known as the Mott-Gurney equation,[5]

$$J = \frac{9}{8}\epsilon\mu\frac{V^2}{d^3}\theta = \frac{9}{8}\epsilon\mu\frac{1}{d}F^2\theta \tag{4}$$

where ϵ and d are the permittivity and thickness of the sample, and θ is a factor that considers the presence of charge carrier traps, that is, the ratio of the number of free carriers to the total number of carriers. When the current flow is in agreement with SCLC, J should be proportional to the square of the electric field (F^2), which is dependent upon the sample thickness. When θ is equal to 1, the current becomes trap-free SCLC. The charge carrier mobility can be evaluated from this equation on the basis of the assumption that the contact between the electrode and the organic layer is ohmic without any energy barrier for charge injection. In case the mobility data determined by other methods are available, one can calculate J. When the experimental value of J is equal to the calculated value, the contact between the organic layer and the electrode is regarded to be an ideal ohmic one.

Equation 4 applies for materials in which the mobility is independent of the electric field. Since the charge carrier mobility of organic disordered systems is usually electric-field dependent, in agreement with the Poole−Frenkel effect as described in section 2.3, eq 4 is modified as eq 5,[15]

$$J = \frac{9}{8}\epsilon\mu_0\exp(\beta F^{1/2})\frac{1}{d}F^2\theta \tag{5}$$

where μ_0 is the mobility when $F = 0$. If the mobility is independent of the electric field, $\beta = 0$.

In the DI-SCLC method, a step voltage is applied to the sample sandwiched between two electrodes, one of which forms an ohmic contact. An ideal transient current for trap-free materials is shown in Figure 3. The current increases

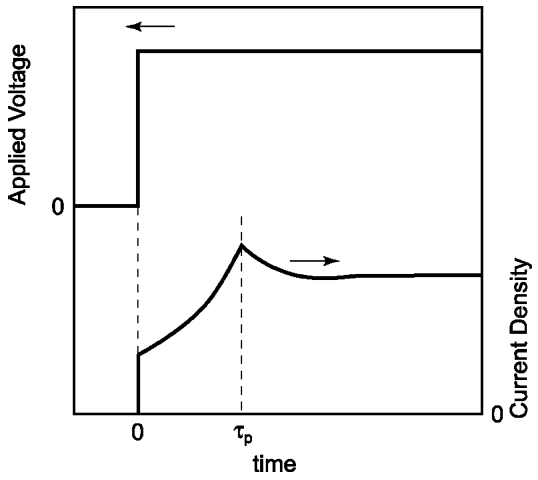

Figure 3. Typical DI-SCLC.

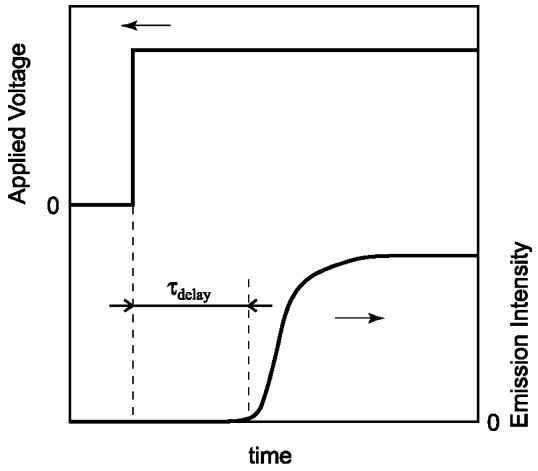

Figure 4. Typical transient emission behavior of OLEDs.

with time, reaches the maximum at time τ_p, and then gradually decreases to a constant current, which is steady-state SCLC. τ_p is related to space-charge-free transit time τ_0 as expressed by eq 6, and the mobility can be calculated from eq 7.

$$\tau_p \sim 0.786\tau_0 \tag{6}$$

$$\mu = \frac{d^2}{V\tau_0} \sim 0.786 \times \frac{d^2}{V\tau_p} \tag{7}$$

The transient EL method is based on the measurement of a time delay between the application of a step voltage and the onset of emission, as shown in Figure 4. The onset of emission is determined by the arrival of the slower charge carrier of the injected carriers at the emission zone.

The determination of charge carrier drift mobilities from the performance of OFETs is described in section 3.3.

2.3. Models for Charge Transport in Organic Disordered Systems

Both band and hopping models are available. The mechanisms of charge transport in organic materials are different from those for inorganic semiconductors. While inorganic semiconductors form energy band structures, namely, valence and conduction bands, organic materials in which only weak intermolecular interactions such as van der Waals forces are operative usually do not form energy bands. Charge carriers, that is, hole and electron, for organic materials correspond to the cation and anion radicals of a molecule. It has generally been accepted that charge transport in organic disordered systems, for example, polymers and molecularly dispersed polymers, takes place by a hopping process. That is, charge transport in organic disordered systems is understood as a sequential redox process over molecules; electrons are sequentially transferred from the anion radical of a molecule to the neutral molecule through the lowest unoccupied molecular orbital (LUMO) for electron transport, and electrons are sequentially transferred from a neutral molecule to its cation radical through the highest occupied molecular orbital (HOMO) for hole transport.

Charge transport in molecular crystals generally shows the following characteristics;[16] one is the mobility value being ca. 10^{-2} to 1 $cm^2\ V^{-1}\ s^{-1}$, and the other is a small temperature dependence of the mobility ($\mu \propto T^{-n}$, $0 < n < 2$). Both band and hopping models cannot satisfactorily explain this transport behavior observed for molecular crystals. On the other hand, charge transport in organic disordered systems such as polymers and molecularly dispersed polymer systems is generally characterized by the following features:[17] (a) transient photocurrents are usually dispersive in contrast to nondispersive photocurrents observed for organic crystalline materials, (b) drift mobilities are much lower (e.g., 10^{-7} $cm^2\ V^{-1}\ s^{-1}$ for poly(*N*-vinylcarbazole)[17]) compared to those of organic crystals ($\sim$1 $cm^2\ V^{-1}\ s^{-1}$ for anthracene single crystal), (c) charge transport is thermally activated, and (d) charge carrier drift mobilities are electric-field-dependent. It should be noted, however, that recent studies on amorphous molecular materials have revealed that they exhibit almost nondispersive photocurrents and much higher drift mobilities ($10^{-4} \sim 10^{-2}$ $cm^2\ V^{-1}\ s^{-1}$).

A few models have been proposed to explain the temperature and electric-field dependencies of charge carrier drift mobilities of organic disordered systems, which include the Poole−Frenkel model,[17,18] small-polaron model,[19] and disorder formalism.[20]

An empirical equation (eq 8), which takes into account the Poole−Frenkel model, has been presented to explain the temperature and electric-field dependencies of charge carrier drift mobilities,[17]

$$\mu = \mu_0 \exp\left(-\frac{E_0 - \beta_{PF}F^{1/2}}{kT_{eff}}\right), \quad T_{eff} = T^{-1} - T_0^{-1} \tag{8}$$

where, E_0, β_{PF}, F, k, T_0, and μ_0 are the activation energy in the absence of electric field, the Poole−Frenkel coefficient, electric field, the Boltzmann constant, the temperature at which the extrapolated data of Arrhenius plots for various electric fields intersect with one another, and the mobility at T_0, respectively. This model shows that the activation energy for charge transport is lowered by $\beta_{PF}F^{1/2}$, but does not provide any physical meanings for μ_0 and T_0. The experimental results obtained for many organic disordered systems have been reported to fit this empirical equation well.

The small-polaron theory is based on the idea that charge carrier transport takes place via the hopping of small polarons, that is, charge carriers accompanied by the lattice deformation, between localized states, and that hopping is

assisted by phonons. According to this theory, mobility is given by eq 9,

$$\mu(F=0) = (e\rho^2/kT)P(\omega/2\pi)\exp\left[-\left(\frac{E_p}{2}-J\right)/kT\right] \quad (9)$$

adiabatic regime: $P = 1$
nonadiabatic regime: $P < 1$

where, e, ω, J, and E_P are the elementary charge, a phonon frequency, the overlap integral, and the polaron binding energy, respectively. P represents the probability that charge carriers hop once energy coincidence occurs.[19] The intersite distance dependence of activation energy for charge transport in molecularly doped polymer systems has been explained in terms of this model.[19,21,22]

The disorder formalism assumes that charge transport in disordered systems takes place by hopping through a manifold of localized states subject to the fluctuations of both hopping site energy and intermolecular wavefunction overlap and that both the hopping site energy and the intermolecular distance follow the Gaussian distributions. The disorder formalism is given by eq 10,

$$\mu = \mu_0 \exp\left[-\left(\frac{2\sigma}{3kT}\right)^2\right]\exp\left\{C\left[\left(\frac{\sigma}{kT}\right)^2-\Sigma^2\right]F^{1/2}\right\} \quad (10)$$

where σ and Σ are parameters that characterize the energetic and positional disorders, respectively, μ_0 represents a hypothetical mobility in the energetic disorder-free system, F is the electric field, and C is an empirical constant.[20] The charge-transport parameters involved in eq 10, μ_0, σ, and Σ, have been obtained for a variety of amorphous molecular glasses, as described in section 6.

3. Principles and Operation Processes of Electronic and Optoelectronic Devices Involving Charge Transport

This section describes the principles and operation processes of OLEDs, OPVs, and OFETs.

3.1. Organic Light-Emitting Diodes (OLEDs)

Electroluminescence (EL) in organics was first reported using single crystals of anthracene in the 1960s.[23] However, the fabricated device required a high drive voltage of 400 V to obtain blue emission resulting from anthracene. Then, the use of vacuum-deposited anthracene thin films led to a significant reduction of drive voltage.[24] In 1987, a double-layer OLED using thin films of 1,1-bis{4-[di(*p*-tolyl)amino]-phenyl}cyclohexane (TAPC) as a hole-transporting material and tris(8-quinolinolato)aluminum (Alq_3) as an emitting material sandwiched between transparent indium tin oxide (ITO) and an alloy of magnesium and silver was reported to exhibit a luminance of over 1000 cd m^{-2} at a drive voltage of ca. 10 V.[25,26] Subsequently, a single-layer OLED using a thin film of poly(*p*-phenylene vinylene), ITO/polymer/Ca, was reported in 1990.[27] These two reports have triggered extensive research and development of OLEDs from the standpoints of both fundamental science and potential technological applications for full-color, flat-panel displays and lighting. Furthermore, the recent finding of triplet emitters has led to remarkable improvements in the EL quantum efficiency.[28−30] OLEDs are characterized by low drive voltage, high brightness, full-color emission, rapid response, and easy fabrication of large-area, thin-film devices.

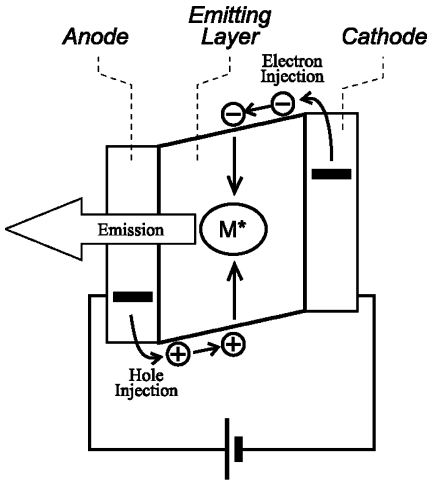

Figure 5. Operation principles of OLEDs.

OLEDs are current-driven devices that utilize emissions from the electronically excited states of molecules. The operation of OLEDs involves charge injection from the anode and the cathode into the adjacent organic layers, transport of injected charge carriers through the organic layers, exothermic recombination of holes and electrons to generate electronically excited states of molecules, which are often called excitons, followed by their deactivation by the emission of either fluorescence or phosphorescence, which is taken out of the device as EL (Figure 5).

The luminous power efficiency (L_{eff}) [lm W^{-1}] is defined as eq 11,

$$L_{eff} = \frac{\pi L}{JV} \quad (11)$$

where L is the luminance [cd m^{-2}], and J and V are the current density [A m^{-2}] and applied voltage [V] needed to obtain the luminance. The external quantum efficiency (Φ_{ext}) of EL is defined as the number of photons emitted per number of injected charge carriers and is expressed as eq 12,[31]

$$\Phi_{ext} = \frac{\pi L \int \frac{F'(\lambda)\lambda}{hc}\,d\lambda}{\int F'(\lambda)K_m y(\lambda)d\lambda} \div \frac{J}{e} \quad (12)$$

where λ is the wavelength, e is elementary charge [C], h is the Planck constant [J s], c is the velocity of light [m s^{-1}], $F'(\lambda)$ is the EL spectrum, K_m is the maximum luminous efficacy, and $y(\lambda)$ is the normalized photopic spectral response function.

The main factors that determine L_{eff} and Φ_{ext} are as follows: efficiency of charge carrier injection from the anode and the cathode at low drive voltage, charge balance, spin multiplicity of the luminescent state, photoluminescence (PL) quantum yield, and extraction of the emission out of the device. Therefore, Φ_{ext} is understood as the value multiplied by these factors: $\Phi_{ext} = \alpha\Phi_{re}\Phi_{spin}\Phi_{em}$, where α is the light extraction factor, Φ_{re} represents the recombination probability of injected holes and electrons, namely, the ratio of the number of injected minority charge carriers used for recombination to the total number of injected charge carriers, Φ_{spin} is the generation probability of either electronically excited singlet or triplet state, which is 0.25 and 0.75 for the singlet and triplet formation, respectively, and Φ_{em} is the PL

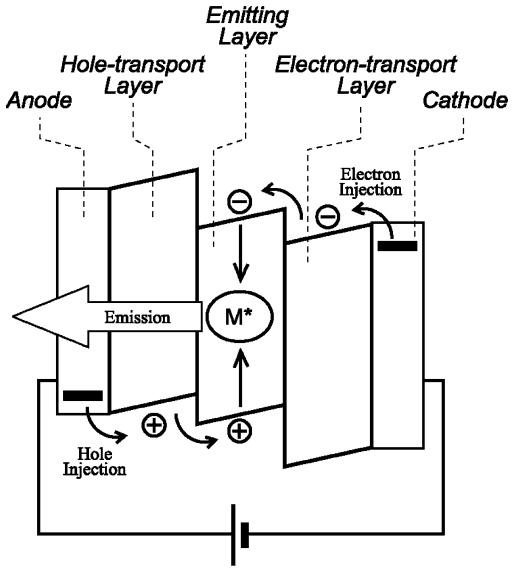

Figure 6. Structure of multilayer OLEDs.

quantum yield from either the electronically excited singlet or the triplet state. When fluorescent emitters are employed, only 25% of the generated excitons are utilized. However, when phosphorescent emitters are used, an internal quantum efficiency up to 100% can be achieved in principle since the phosphorescent emitters, which are usually doped in a host material, can capture both singlet and triplet excitons generated by the recombination of injected holes and electrons.[28,32]

To attain high quantum efficiency for EL, it is necessary to achieve efficient charge injection from both the anode and the cathode into the adjacent organic layers at low drive voltage, good charge balance, and confinement of the injected charge carriers within the emitting layer to increase the probability of the desired emissive recombination. The insertion of hole-transport and electron-transport layers between the electrodes and the emitting layer reduces the energy barriers for the injection of charge carriers from the electrodes into the emitting layer by a stepwise process, resulting in efficient charge injection and charge balance. That is, charge carriers injected from the electrodes into the adjacent charge-transport layers are transported through the charge-transport layers and then injected into the emitting layer. The hole- and electron-transport layers can also act as electron- and hole-blocking layers, respectively, thus, confining the electrons and holes within the emitting layer and preventing them from escaping to the adjacent carrier-transport layers. A structure of multilayer OLEDs consisting of the emitting and hole- and electron-transport layers sandwiched between the ITO anode and the metal cathode is shown in Figure 6.

The performance of OLEDs, therefore, depends upon various materials functioning in specialized roles such as charge-injection and -transporting, charge-blocking, and emission. Generally, materials for use in OLEDs should meet the following requirements: (a) Materials should possess suitable ionization potentials and electron affinities, that is, well-matched energy levels for the injection of charge carriers from the electrodes or the organic layer into the adjacent organic layers. (b) They should be capable of forming smooth, uniform thin films without pinholes. (c) They should be morphologically and thermally stable. (d) In addition to these general requirements, materials should meet further specialized needs depending upon the roles that they play in devices, for example, hole transport, electron transport, charge blocking, and light emission.

3.2. Organic Photovoltaic Devices (OPVs)

Solar energy has a great potential as a clean and inexhaustible new energy source. Solar cells are devices that directly convert light energy into electrical energy. Devices for such photoelectric conversion with organic photoactive materials are mainly classified into photoelectrochemical cells and photovoltaic devices. Photoelectrochemical cells consist of two electrodes immersed in an electrolyte solution containing a redox couple. Dye-sensitized organic solar cells using nanocrystalline, porous TiO_2, on which an organic dye is adsorbed, and I_3^-/I^- redox species in solution or gels have been a topic of current intensive research and development because of the high conversion efficiencies reaching 10%.[33,34]

Organic solid-state photovoltaic devices (OPVs) consist of thin films of organic photoactive materials sandwiched between two metal electrodes. Both Schottky-type and *pn*-heterojunction cells have been studied. In Schottky-type cells, a single-layer organic photoactive material is sandwiched between two dissimilar electrodes to form a Schottky barrier in the organic layer at the interface with the metal electrode. On the other hand, *pn*-heterojunction cells are typically based on the double layers of organic thin films, where the organic/organic interface plays an important role in the performance, the electrodes simply providing ideally ohmic contacts with the organic layers. Generally, higher quantum yields for the photogeneration of charge carriers have been attained for *pn*-heterojunction cells compared with Schottky-type devices because of electron donor−acceptor interactions between the two kinds of organic semiconductors, that is, *p*-type and *n*-type organic semiconductors. *P*-type and *n*-type organic semiconductors generally mean electron-donating and -accepting organic materials, respectively. The main driving force for the photogeneration of charge carriers in *pn*-heterojunction devices is the chemical potential at the organic donor/organic acceptor interface.

Studies on OPVs performed before the mid 1980s showed very low power conversion efficiencies. In 1986, it was reported that a bilayer *pn*-heterojunction cell consisting of copper phthalocyanine (CuPc) and a perylene pigment sandwiched between the ITO and Ag electrodes gave a power conversion efficiency as high as 0.95% for simulated AM2 white light at 75 mW cm^{-2}.[35] Extensive studies have since been performed on OPVs, resulting in significant improvements in the power conversion efficiency, as described in section 5.2.

The performance of OPVs is evaluated by power conversion efficiency (η) and fill factor (FF). They are defined as eqs 13 and 14,

$$\eta = \frac{(VJ)_{\max}}{I} \tag{13}$$

$$\mathrm{FF} = \frac{(VJ)_{\max}}{V_{\mathrm{OC}} J_{\mathrm{SC}}} \tag{14}$$

where I, V_{OC}, and J_{SC} are the incident light power, the open circuit voltage, and the short-circuit current, respectively (Figure 7). The equivalent circuit of OPVs is shown in Figure 8, where R_s is a series resistance, R_{sh} is a shunt resistance,

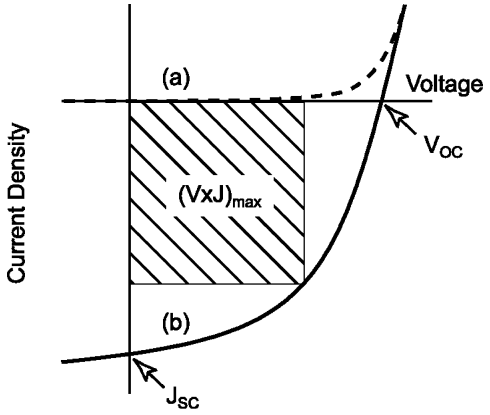

Figure 7. Typical $J-V$ curves of OPVs: (a) in dark; (b) under illumination.

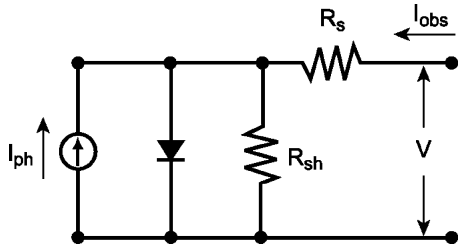

Figure 8. Equivalent circuit of OPVs.

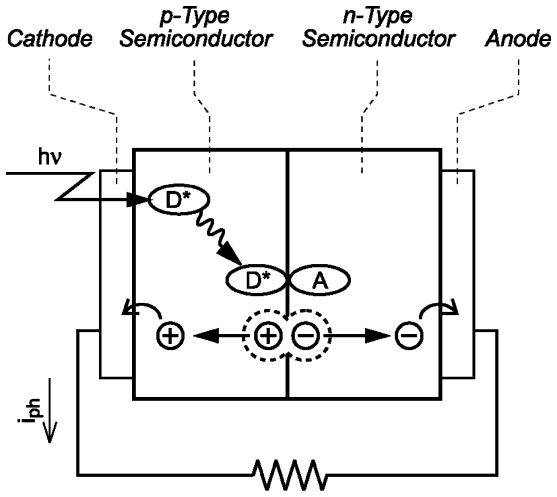

Figure 9. Operation processes of *pn*-heterojunction OPVs.

and I_{ph} is a photocurrent. The observed current (I_{obs}) is given by eq 15,

$$I_{obs} = I_0 \left[\exp\left\{ \frac{q(V - I_{obs}R_s)}{nkT} \right\} - 1 \right] + \frac{V - I_{obs}R_s}{R_{sh}} - I_{ph} \quad (15)$$

where I_0 is the reverse saturated dark current, q is the elementary charge, V is the cell voltage, n is the diode ideal factor, and k is the Boltzmann constant.

The mechanisms for the operation of OPVs have been interpreted in terms of the energy band model applied for inorganic semiconductor PV devices, which may not be applicable to molecular organic solids with well-localized energy levels. The basic operation processes of *pn*-heterojunction OPVs are as follows (Figure 9): (a) light absorption by organic semiconductors to form excitons, (b) diffusion of excitons, (c) charge carrier generation and separation at the organic/organic interface, (d) charge transport through the organic layers, and (e) charge collection at both electrodes. These processes are just the opposite to those of OLEDs, namely, (a) charge injection from the electrodes into the organic layers, (b) charge transport through the organic layers, (c) charge recombination to form excitons, (d) emission from excitons, and (e) light extraction out of devices.

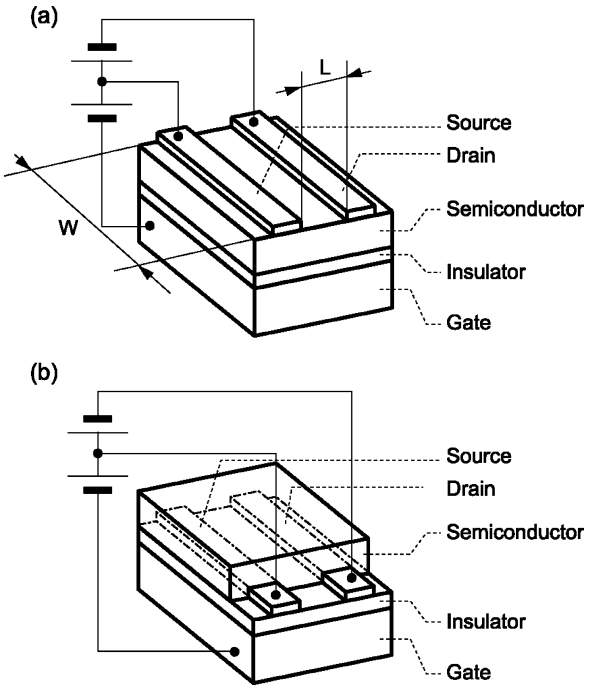

Figure 10. Structures of OFETs: (a) top contact configuration; (b) bottom contact configuration.

3.3. Organic Field-Effect Transistors (OFETs)

Organic field-effect transistors (OFETs) are expected to be a promising technology for large-area, low cost, and flexible electronics for applications in displays, sensors, and memories.[36] In addition, they have an advantage over silicon FETs in that the processing temperature is lower. Since the reports on OFETs using polythiophene[37] and phthalocyanine[38] appeared, there have been extensive studies on OFETs using oligothiophenes and other numerous kinds of organic semiconductors. The recent finding of high performance for CuPc- and pentacene-based OFETs has directed the studies of this field to a new stage of research and development.

OFETs consist of conductors, that is, source, drain, and gate electrodes, an insulator, that is, a gate dielectric, and an organic semiconductor as an active element. The materials used as the gate dielectric are either inorganic dielectric materials, for example, SiO_2, or organic dielectric materials such as insulating organic polymers. Two types of structures, that is, top-contact and bottom-contact electrode configurations, have been adopted for the fabrication of OFETs (Figure 10). When there is no voltage application to the gate electrode, only small currents flow between the source and drain electrodes; this state is referred to as the off-state of transistor. When negative voltage, for example, is applied to the gate electrode, hole carriers in the organic semiconductor layer become accumulated at the interface with the gate dielectric, and hence, hole transport takes place from the source to the drain electrode; this state corresponds to the on-state of transistor. This type of device is called a *p*-channel device. Likewise, application of positive voltage

to the gate electrode causes electron transport in the case of *n*-channel devices. Since the so-called organic semiconductors are essentially electrical insulators, charge carriers in organic semiconductors are usually supplied by injection from the source electrode into the organic layer. The current flow (I_{SD}) can be modulated by the magnitude of both the gate voltage (V_G) and the source/drain voltage (V_{SD}).

The current that flows from the source to the drain electrode (I_{SD}) under a given V_G increases almost linearly with the increasing V_{SD} and gradually becomes saturated as shown in Figure 11. The current (I_{SD}) is given by eq 16,

$$I_{SD} = \frac{C_i W \mu_{FET}}{L}\left[(V_G - V_T)V_{SD} - \frac{{V_{SD}}^2}{2}\right] \qquad (16)$$

where, μ_{FET} is the field-effect mobility of the charge carrier, L is the channel length, W is the channel width, C_i is the capacitance per unit area of the gate dielectric, and V_T is the threshold voltage. The current I_{SD} in the linear and saturation regions are given by eqs 17 and 18, respectively.

$$I_{SD,linear} = \frac{C_i W \mu_{FET}}{L}(V_G - V_T)V_{SD} \qquad (17)$$

$$I_{SD,sat} = \frac{C_i W \mu_{FET}}{2L}(V_G - V_T)^2 \qquad (18)$$

The field-effect mobility (μ_{FET}) can be determined from the slope of the linear plots of $(I_{SD,sat})^{1/2}$ versus V_G, according to eq 18. The performance of OFETs is evaluated by μ_{FET}, V_T, and the on/off ratio of I_{SD}. Not only organic semiconductors, but also the gate dielectric materials greatly affect the device performance.[39]

4. General Aspects of Charge Carrier Transporting Molecular Materials

Charge-transporting materials often function as emitting materials in OLEDs. Likewise, charge-transporting materials in OPVs play a role of the photogeneration of charge carriers in addition to charge transport. Thus, a number of charge-transporting materials have dual functions, for example, charge transport and light emission in OLEDs, and charge carrier photogeneration and transport in OPVs. In fact, materials in OLEDs often function as either hole-transporting or electron-transporting light emitters.

4.1. Classifications and Characterization

Both small organic molecules and polymers have been used as charge-transporting materials in the devices described above. Usually, vacuum deposition and spin-coating methods are used for small molecules and polymers, respectively, for the preparation of thin films.

Molecular materials are classified into single crystals, polycrystals, liquid crystals, and amorphous glasses according to their organization states. As device performance is highly dependent on materials' morphology, control over materials' morphology is of crucial importance in materials science and practical applications.

Charge-transporting materials are classified into hole- and electron-transporting materials depending upon the kind of charge carriers transported. Since the properties of charge-transporting materials used in OLEDs, OPVs, and OFETs greatly affect the device performance, the design and synthesis of high-performance, charge-transporting materials are of great importance for the development of high-performance devices.

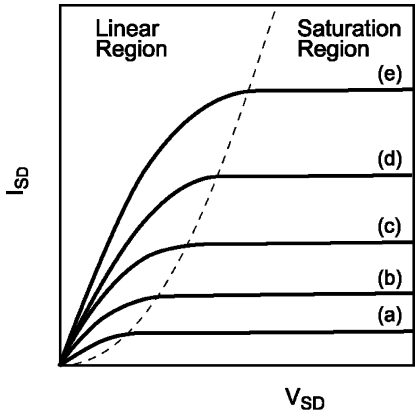

Figure 11. Schematic of $I_{SD}-V_{SD}$ curves of OFETs. V_G increases in the order of (a) → (b) → (c) → (d) → (e).

4.1.1. Crystalline, Liquid Crystalline, and Amorphous Materials

Charge-transporting materials with different morphologies have been used depending upon the kind of devices. Generally, organic crystalline materials exhibit larger charge carrier mobilities than those of organic amorphous materials. Devices using organic single crystals, for example, EL[23] and OFETs,[40,41] have been reported; however, the single-crystal growth on the plane of a large-area substrate for device applications is not easy. Polycrystalline materials have been used mostly in OFETs and OPVs. The grain size, grain boundaries, and molecular orientations affect the device performance. Amorphous materials have advantages over crystalline materials in device fabrication because of their good processability, transparency, and isotropic and homogeneous properties. Amorphous molecular materials have recently constituted a new class of organic materials for use in various applications, in particular, OLEDs.[1b,d] Liquid crystalline materials have also been studied for emitters or a host matrix for emitters in OLEDs to obtain polarized emission from the devices.[42−46]

4.1.2. Hole-Transporting and Electron-Transporting Materials

Hole-transporting materials are those that accept hole carriers with a positive charge and transport them. Likewise, electron-transporting materials are those that accept electron carriers with a negative charge and transport them. Therefore, materials which have low ionization potentials together with low electron affinities usually function as hole-transporting materials, whereas materials which have high electron affinities together with high ionization potentials usually function as electron-transporting materials. In other words, charge-transporting materials with electron-donating and -accepting properties usually serve as hole- and electron-transporting materials, respectively. It should be noted, however, that there are a number of materials that exhibit ambipolar character, that is, materials that can transport both holes and electrons, as described in sections 5 and 6. In addition to the role of charge transport, hole- and electron-transporting materials used in OLEDs play a role of facilitating hole and electron injection from the anode and the cathode, respectively, into the emitting layer by a

Chart 1. Examples of Crystalline Materials for Electronic and Optoelectronic Devices

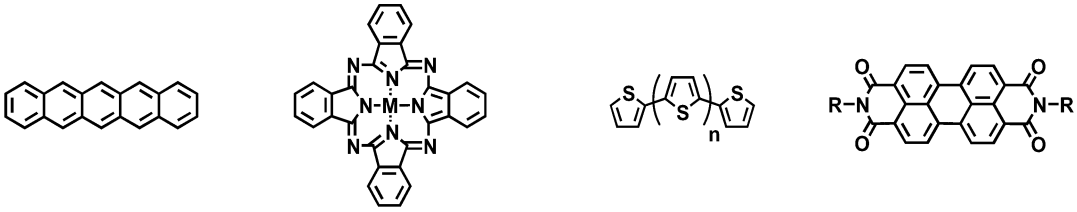

pentacene (**1**) | metal phthalocyanines **2** (CuPc) : M=Cu, **3** (TiOPc) : M=TiO | oligothiophenes (**4**) | perylene-bis(dicarboximide)s (**5**)

stepwise process. Hole- and electron-transporting materials also play the role of blocking electrons and holes, respectively, from escaping from the emitting layer in OLEDs.

4.1.3. Role of Hole Blocking Played by Electron-Transporting Materials in OLEDs

When materials with hole-transporting properties are used as emitters in OLEDs, the presence of an electron-transport layer with an effective hole-blocking ability is required to facilitate electron injection from the cathode into the emitting layer and to block hole carriers from escaping from the emitting layer. However, some electron transporters do not necessarily function well as effective hole blockers.

An effective approach for the fabrication of OLEDs using emitters with hole-transporting properties is the use of an additional hole-blocking layer inserted between the emitting and electron-transport layers, where the electron-transporting and hole-blocking layers play the roles of facilitating electron injection from the cathode and blocking holes from escaping from the emitting layer to confine holes within the emitting layer, respectively. The materials for use as the hole-blocking layer in OLEDs should have both weak electron-accepting properties to be able to accept electrons and electron-transporting properties. Such materials are referred to as hole-blocking materials.

4.1.4. Characterization of Charge-Transporting Materials

The key characteristics of charge-transporting materials are charge carrier drift mobility, solid-state ionization potential or anodic oxidation potential, electron affinity or cathodic reduction potential, and optical band gap. The methods for the measurement of charge carrier drift mobility are described earlier in section 2.2. The glass-transition temperature (Tg) is also an important factor in evaluating the thermal stability of amorphous molecular materials, which can be measured by differential scanning calorimetry (DSC).

The ionization potential and the electron affinity of organic materials are determined directly by ultraviolet photoelectron spectroscopy (UPS) and inverse photoelectron spectroscopy. The ionization potential or oxidation potential and the electron affinity or reduction potential correspond to the HOMO and LUMO energy levels of a molecule, respectively. The LUMO energy level can also be estimated from the ionization potential or oxidation potential and the optical band gap. The oxidation and reduction potentials are determined by cyclic voltammetry for solution. The solid-state ionization potential, which is lowered by the polarization energy (ca. 1.7 eV for organic molecules) relative to the gas-phase ionization potential, has been correlated with the oxidation potential: $E_{HOMO} = -(4.8 + qV_{CV})$, where q is the elementary charge, and V_{CV} is the oxidation potential versus Fc (ferrocene)/Fc^+ (ferrocenium cation) reference electrode determined by solution-based cyclic voltammetry.[47] Recently, the following relationship between the solid-state ionization potential and the oxidation potential (vs Fc/Fc^+ reference electrode) has been reported: $E_{HOMO} = -(1.4 \pm 0.1) \times (qV_{CV}) - (4.6 \pm 0.08)$ eV.[48] The ionization potentials or oxidation potentials of materials give information on the strength of electron-donating properties and how much of the energy barriers exist for the injection of holes from the ITO electrode into an adjacent hole-transport organic layer in OLEDs. Likewise, the electron affinities or reduction potentials of materials give information on the strength of electron-accepting properties and the energy barriers for the injection of electrons from the cathode into an adjacent electron transport layer in OLEDs. The HOMO/LUMO energy levels of organic materials are also of essential importance in discussing efficiencies of the photogeneration of charge carriers and open-circuit voltages in OPVs, and charge injection in OFETs.

4.2. Crystalline Molecular Materials

4.2.1. Representative Classes of Crystalline Materials

Representative classes of organic crystals for use in electronic and optoelectronic devices include polycyclic aromatic hydrocarbons, macrocycles such as phthalocyanines, fused heterocyclic aromatic compounds, oligothiophenes, oligoarylenes, oligoarylenevinylenes, fullerenes, perylene pigments, and so forth. Violanthrone, a low-molecular-weight model for graphite, was first studied as an electrically conducting molecular material,[49] and perylene was studied as an electron donor component for conducting charge-transfer complexes.[50] Pentacene (**1**) and related condensed aromatic hydrocarbons have recently attracted attention as a new class of promising materials for use in OFETs.[51] The molecular structures of such representative classes of crystalline materials are shown in Chart 1.

Metal- and metal-free phthalocyanines, for example, CuPc (**2**), are typical *p*-type organic semiconductors for use in OLEDs, OPVs, and OFETs. Phthalocyanines are known to take up different crystalline morphologies: solvent vapor exposure treatment transforms the morphology from one crystalline form into another crystalline form, as exemplified by zinc phthalocyanine (ZnPc)[52] and magnesium phthalocyanine (MgPc).[53] Titanyl phthalocyanine (TiOPc (**3**)) also assumes several crystalline forms, which has been widely used as a charge carrier generation material in electrophotographic photoreceptors for laser printers. Perylene pigments (**5**) and C_{60} are typical examples of *n*-type organic semiconductors and have been used for OPVs.

Oligothiophenes with well-defined structures (**4**), which are highly crystalline in nature, constitute a new class of

Scheme 1. Synthetic Routes of Oligothiophenes

Coupling reactions

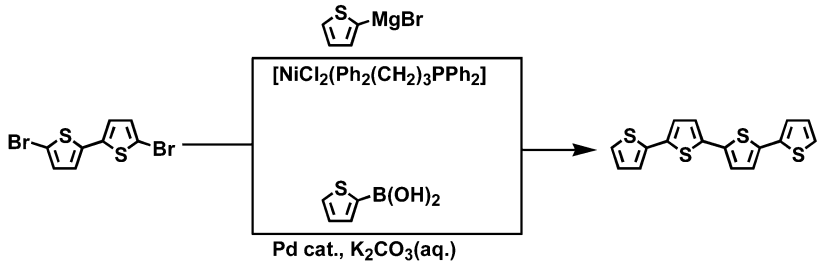

Cyclization reactions

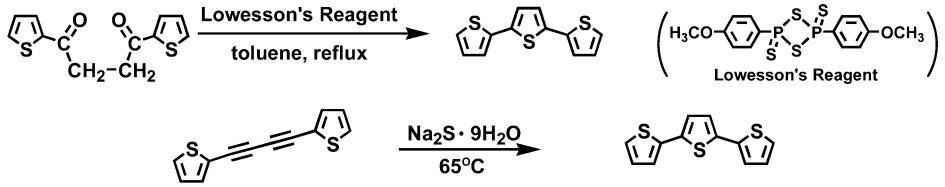

organic π-electron systems for various potential applications. They also serve as model compounds for electrically conducting polythiophenes. A number of unsubstituted and alkyl-substituted oligothiophenes with varying conjugation lengths have been synthesized. Oligothiophenes with long conjugation lengths, for example, 16-, 20-, and 27-mers, are expected to serve as molecular wires.[54−56] In addition, cyclic oligothiophenes[57] and selenium analogues of oligothiophenes[58,59] have also been synthesized. Although oligothiophenes are highly crystalline, amorphous molecular materials containing oligothiophenes have been designed and synthesized.[60−63] There have been extensive studies on the molecular and crystal structures, and optical, electrochemical, and electrical properties of oligothiophenes[64−76] and their applications in OPVs,[77] OLEDs, and OFETs.[78−81]

Some crystalline materials, for example, polycyclic aromatic hydrocarbons and phthalocyanines, form thin films with amorphous nature by vacuum deposition on substrates kept at moderate to low temperatures. However, these initially amorphous thin films are readily transformed into polycrystalline films upon solvent vapor exposure. The examples are given by TiOPc,[82,83] perylene pigment,[83,84] tris(8-quinolinolato)aluminum (Alq_3),[85] and so forth. These amorphous thin films are distinguished from amorphous molecular materials described later in that the definite glass-transition phenomena have not been observed, whereas amorphous molecular materials exhibit well-defined Tg's and readily form smooth, uniform amorphous thin films by spin coating from solution as well as vacuum deposition.

4.2.2. Synthesis of Oligothiophenes

Oligothiophenes with well-defined structures have been synthesized by the C−C coupling reactions of bromo-substituted oligothiophenes with thiophen-2-yl magnesium bromide[86,87] or thiophen-2-yl boronic acid in the presence of transition metal complexes as catalysts. The C−C coupling reactions of oligothiophenes using *n*-butyllithium in the presence of $CuCl_2$ also produce oligothiophenes with an extended π-conjugation.[88] The cyclization reactions of butanediones or butadiynes have also been employed for the synthesis of oligothiophenes.[89,90] A few synthetic routes of oligothiophenes are described in Scheme 1.

4.3. Amorphous Molecular Materials

Small organic molecules generally tend to crystallize very readily, and hence, they usually exist as crystals below their melting temperatures. However, recent extensive studies have revealed that small organic molecules can also form stable amorphous glasses above room temperature if their molecular structures are properly designed. Small organic molecules that readily form stable amorphous glasses above room temperature are referred to as amorphous molecular glasses or amorphous molecular materials.[91] They constitute a new class of functional organic materials for various applications.[1b,d] Several new concepts for photo- and electroactive molecular materials have been presented, which include electrically conducting amorphous molecular materials,[92] photochromic amorphous molecular materials,[93] amorphous molecular resists,[94] and amorphous molecular materials for use in a variety of electronic, optoelectronic, and photonic devices. Amorphous molecular materials have found successful applications as materials for OLEDs. Photochromic amorphous molecular materials have potential applications for image formation and molecular memories.[95,96] Azobenzene-based photochromic amorphous molecular materials have been shown to form photoinduced surface relief gratings.[97,98] Amorphous molecular resists have been demonstrated to be promising candidates for future nanolithography.[94,99,100]

4.3.1. Characteristic Features of Amorphous Molecular Materials

Usually, amorphous molecular materials are obtained as polycrystals by recrystallization from solution. They readily form amorphous glasses when the melt samples are cooled on standing in air or rapidly cooled with liquid nitrogen. Some compounds have been obtained as amorphous glasses despite attempted recrystallization from solution. The forma-

Chart 2. Typical Classes of Amorphous Molecular Materials

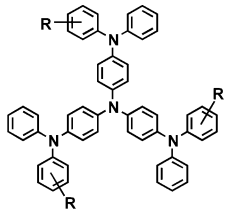

6 (TDATA) : R=H
7 (*o*-MTDATA) : R=*o*-CH_3
8 (*m*-MTDATA) : R=*m*-CH_3
9 (*p*-MTDATA) : R=*p*-CH_3

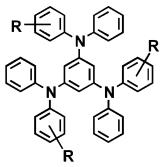

10 (*o*-MTDAB) : R=*o*-CH_3
11 (*m*-MTDAB) : R=*m*-CH_3
12 (*p*-MTDAB) : R=*p*-CH_3

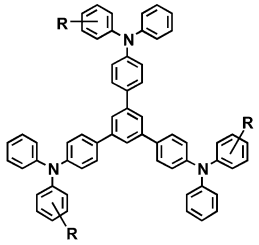

13 (TDAPB) : R=H
14 (*o*-MTDAPB) : R=*o*-CH_3
15 (*m*-MTDAPB) : R=*m*-CH_3
16 (*p*-MTDAPB) : R=*p*-CH_3

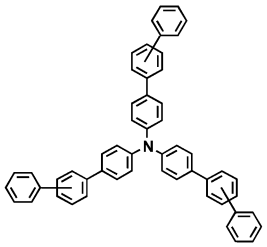

17 (*o*-TTA) : *o*-Ph
18 (*m*-TTA) : *m*-Ph
19 (*p*-TTA) : *p*-Ph

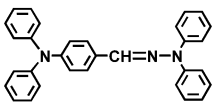

20 (DPH)

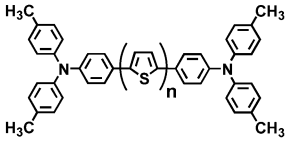

21 (BMA-1T) : n=1
22 (BMA-2T) : n=2
23 (BMA-3T) : n=3
24 (BMA-4T) : n=4

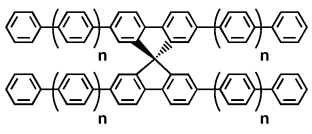

25 (spiro-4Φ) : n=0
26 (spiro-8Φ) : n=2
27 (spiro-10Φ) : n=3

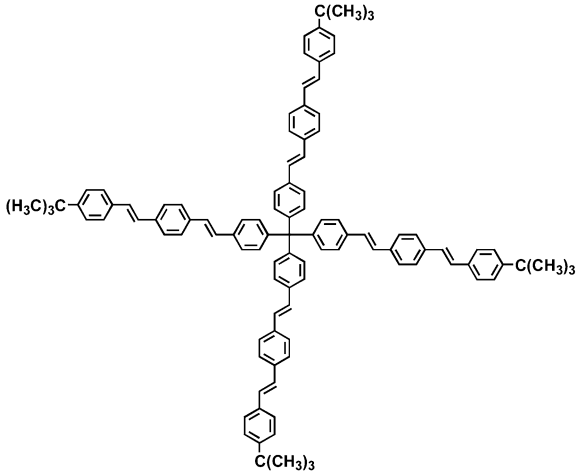

28

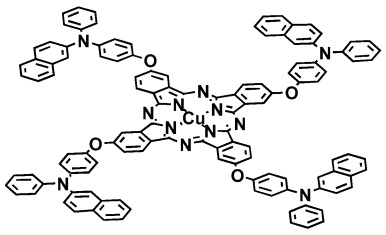

29

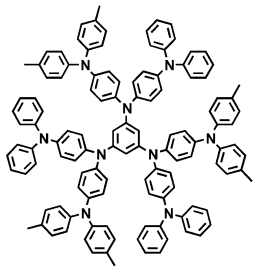

30 (MTBDAB)

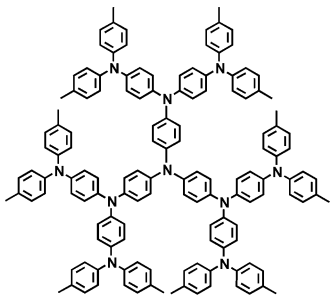

31

tion of amorphous glasses is evidenced by X-ray diffraction, DSC, and polarizing light microscopy.

Amorphous molecular materials are characterized by the following features.[1b,d] They take up several different organization states, such as single crystal, polycrystal, isotropic liquid, supercooled liquid, and amorphous glass. Amorphous molecular glasses are in the state of thermodynamic nonequilibrium, and hence, they tend to undergo structural

Chart 3. Examples of Structural Modifications of TDATA, TDAB, and TDAPB

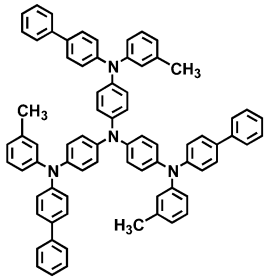

32 (*p*-PMTDATA)

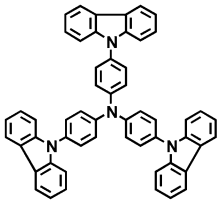

33 (TCTA)

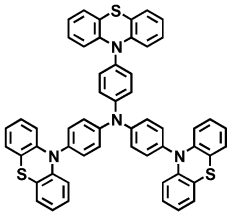

34 (TPTTA)

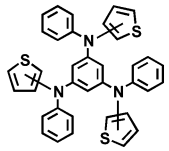

35 (α-TPTAB) : α-thienyl
36 (β-TPTAB) : β-thienyl

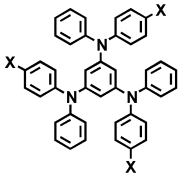

37 (*p*-FTDAB) : X = F
38 (*p*-ClTDAB) : X = Cl
39 (*p*-BrTDAB) : X = Br

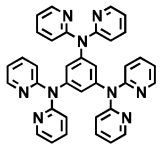

40

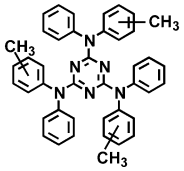

41 : *o*-CH_3
42 : *m*-CH_3
43 : *p*-CH_3

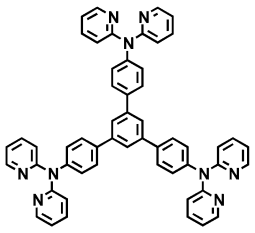

44

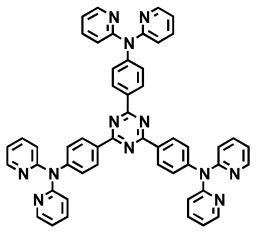

45

relaxation, exhibiting well-defined Tg's. Amorphous molecular glasses tend to crystallize on heating above their Tg's, frequently exhibiting polymorphism.[1b,101−103] Amorphous glasses show isotropic and homogeneous properties without grain boundaries. They are characterized by the presence of free volume and disorder in both molecular distance and orientation. Like polymers, amorphous molecular materials readily form uniform amorphous thin films by themselves by vacuum deposition and spin coating from solution. They contrast polymers in that they are pure materials with well-defined molecular structures and definite molecular weights without any distribution. They can be purified by column chromatography, followed by recrystallization from solution or by vacuum sublimation.

The stability of amorphous glasses greatly differ depending on the molecular structures of materials. Certain materials form very stable amorphous glasses that do not undergo any crystallization even upon heating above Tg's. The absence of grain boundaries in amorphous films allows uniform contact between organic/metal electrode and organic/organic layers. The isotropic and homogeneous properties of amorphous molecular materials prevent $\pi-\pi$ stacking of π-electron systems. These characteristic features of amorphous molecular materials provide advantages for device applications.

4.3.2. Molecular Design and Representative Classes of Amorphous Molecular Materials

Several guidelines for the molecular design of amorphous molecular materials have been presented,[1b] which include nonplanar molecular structures[91,101] as evidenced by X-ray crystal structure analysis,[1b,103] existence of different conformers,[101−103] incorporation of bulky and heavy substituents,[104,105] and the enlargement of molecular size.[106] The latter two guidelines also serve as the ones for increasing Tg's and for enhancing the stability of the amorphous glassy state. The introduction of structurally rigid moieties to form nonplanar molecules is another important guideline for increasing Tg's.[92,107]

Nonplanar molecular structures are responsible for the glass formation; however, all the compounds with nonplanar molecular structures do not necessarily lead to glass forma-

Chart 4. Spiro and Related Compounds and Tetraarylmethanes

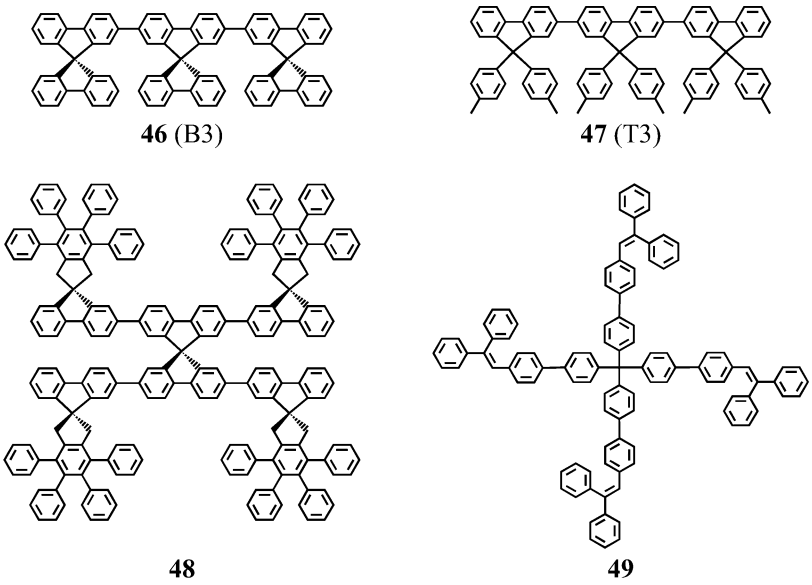

Scheme 2. Synthesis of *p*-TTA

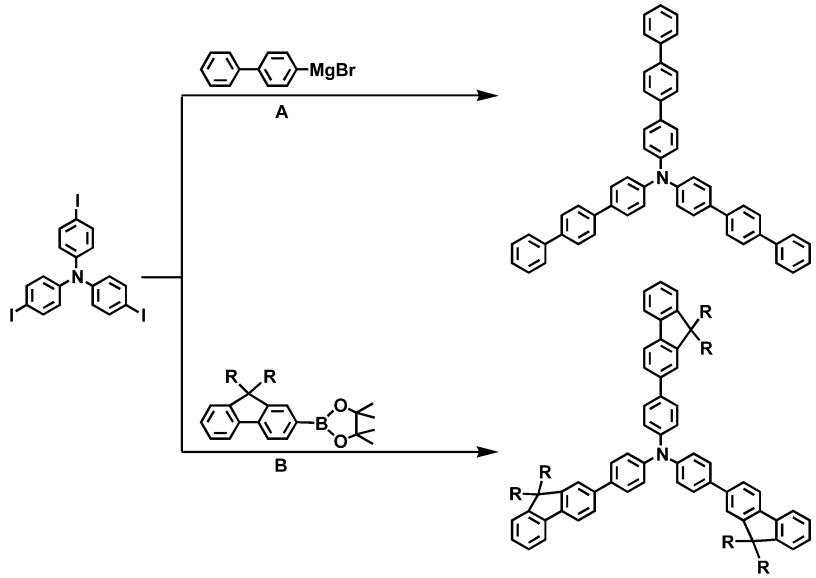

A = $Ni(dppp)Cl_2$, THF, reflux
B = $Pd(PPh_3)_4$, toluene, 2N K_2CO_3, PTC, 50-80 °C

tion. For example, triphenylamine and 1,3,5-triphenylbenzene with nonplanar molecular structures instantly crystallize instead of forming amorphous glasses even when their melt samples are rapidly cooled with liquid nitrogen. Likewise, 1,3,5-tris(diphenylamino)benzene (TDAB) with a nonplanar structure also instantly crystallizes even when its melt sample is rapidly cooled with liquid nitrogen.[101] On the other hand, the incorporation of aryl substituents into the triphenylamine or 1,3,5-triphenylbenzene moiety allows the formation of amorphous glasses, as exemplified by tri(biphenyl-4-yl)amine (TBA),[108,109] tri(*p*-terphenyl-4-yl)amine (*p*-TTA (**19**)),[108] and 1,3,5-tri(biphenyl-4-yl)benzene (TBB).[110] The incorporation of an alkyl or halogeno substituent into TDAB also permits the formation of amorphous glasses.[101,105] They form amorphous glasses when the melt samples are rapidly cooled with liquid nitrogen. These results imply that not only nonplanar molecular structures, but also the existence of different conformers are responsible for the formation of amorphous glasses. One approach for the existence of different conformers is to make nonplanar molecules unsymmetrical by the introduction of substituents.

4.3.2.1. Typical Key Compounds for Amorphous Molecular Glasses. On the basis of the above-mentioned molecular design concepts, a variety of amorphous molecular materials have been created. Typical key compounds that readily form amorphous glasses are π-electron starburst molecules, for example, families of 4,4′,4″-tris(diphenylamino)-triphenylamine (TDATA (**6**−**9**)),[91,92,111] 1,3,5-tris(diphenylamino)benzene (TDAB (**10**−**12**)),[101,112] and 1,3,5-tris[4-(diphenylamino)phenyl]benzene (TDAPB (**13**−**16**)).[113] Tris-(oligoarylenyl)amines, for example, tri(terphenylyl)amines (*o*-, *m*-, and *p*-TTA (**17**−**19**)),[108] and diarylaminophenylaldehyde arylhydrazones, for example, 4-diphenylaminobenzaldehyde diphenylhydrazone (DPH (**20**)),[114] constitute other families of amorphous molecular materials. Oligothiophenes are very crystalline in nature; however, oligothiophenes end-

Table 1. Glass-Transition Temperatures (Tg's), Oxidation Potentials, Ionization Potentials (IPs), and Electron Affinities (EAs) of Representative Classes of Amorphous Molecular Materials

compound	Tg (°C)	oxidation potential	IP (eV)	EA (eV)	ref
		TDATA Derivatives			
6 (TDATA)	89	0.11 V vs Ag/Ag^+ (0.01 mol dm^{-3}) in CH_2Cl_2			91
7 (*o*-MTDATA)	76				1b
8 (*m*-MTDATA)	75	0.06 V vs Ag/Ag^+ (0.01 mol dm^{-3}) in CH_2Cl_2			91
	75		5.1	1.9	111
9 (*p*-MTDATA)	80				1b
33 (TCTA)	151	0.69 V vs Ag/Ag^+ in CH_2Cl_2 (irreversible)			1b, 107
		0.69 V vs Fc/Fc+ in DMF	5.71		48
34 (TPTTA)	141				92
31	169	−0.050 V vs $Ag/AgNO_3$ in THF			121
		TDAB Derivatives			
10 (*o*-MTDAB)	42	0.55 V vs Ag/Ag^+ (0.01 mol dm^{-3}) in CH_2Cl_2 (irreversible)			112
11 (*m*-MTDAB)	49	0.55 V vs Ag/Ag^+ (0.01 mol dm^{-3}) in CH_2Cl_2 (irreversible)			112
12 (*p*-MTDAB)	58	0.50 V vs Ag/Ag^+ (0.01 mol dm^{-3}) in CH_2Cl_2 (irreversible)			112
37 (*p*-FTDAB)	54				105
38 (*p*-ClTDAB)	64				105
39 (*p*-BrTDAB)	72				105
35 (α-TPTAB)	38				103
36 (*β*-TPTAB)	46				103
30 (MTBDAB)	134	0.10 V vs Ag/Ag^+ (0.01 mol dm^{-3})			106
40	80		5.09	1.64	123
		TDAPB Derivatives			
13 (TDAPB)	121	0.67 V vs Ag/Ag^+ (0.01 mol dm^{-3}) in CH_2Cl_2 (irreversible)			113
14 (*o*-MTDAPB)	109	0.72 V vs Ag/Ag^+ (0.01 mol dm^{-3}) in CH_2Cl_2 (irreversible)			113
15 (*m*-MTDAPB)	105	0.66 V vs Ag/Ag^+ (0.01 mol dm^{-3}) in CH_2Cl_2 (irreversible)			113
16 (*p*-MTDAPB)	110	0.64 V vs Ag/Ag^+ (0.01 mol dm^{-3}) in CH_2Cl_2			113
44	128		5.55	2.13	123
45	121		4.99	1.93	123
		Tris(oligoarylenyl)amines			
17 (*o*-TTA)	81	0.61 V vs Ag/Ag^+ (0.01 mol dm^{-3}) in CH_2Cl_2			1b
18 (*m*-TTA)	80	0.64 V vs Ag/Ag^+ (0.01 mol dm^{-3}) in CH_2Cl_2			1b
19 (*p*-TTA)	132	0.58 V vs Ag/Ag^+ (0.01 mol dm^{-3}) in CH_2Cl_2			108
		Arylhydrazones			
20 (DPH)	50				114
		π-Electron Systems End-Capped with Triarylamines			
21 (BMA-1T)	86	0.39 V vs Ag/Ag^+ (0.01 mol dm^{-3}) in CH_2Cl_2			61
	86		5.10		115
22 (BMA-2T)	90	0.39 V vs Ag/Ag^+ (0.01 mol dm^{-3}) in CH_2Cl_2			61
	90		5.08		115
23 (BMA-3T)	93	0.38 V vs Ag/Ag^+ (0.01 mol dm^{-3}) in CH_2Cl_2			60, 61
	93		5.07		115
24 (BMA-4T)	98	0.35 V vs Ag/Ag^+ (0.01 mol dm^{-3}) in CH_2Cl_2			60, 61
	98		5.05		115
		Spiro and Related Compounds			
25 (Spiro-4Φ)	184				116
26 (Spiro-8Φ)	254				116
46 (B3)	>200		∼5.6	∼2.54	125
47 (T3)	>200		5.4∼5.5	2.34∼2.44	125
48	296				127
		Tetraphenylmethane Derivatives			
49	142				128
		Macrocycles			
29	128				118

capped with a triarylamine group, α,*ω*-bis[bis(4-methylphenyl)aminophenyl]oligothiophenes (BMA-nT (**21**−**24**)), readily form amorphous glasses.[60−62,115] Spiro compounds, for example, spiro-4Φ (**25**), spiro-8Φ (**26**), and spiro-10Φ (**27**),[116] tetraarylmethane derivatives, for example, **28**,[117] and macrocycle-based compounds, for example, **29**,[118] are also important classes of amorphous molecular materials. Oligo(diphenylsilane)s have also been found to show morphologies with amorphous nature, exhibiting interesting even−odd effects; while the oligo(diphenylsilane)s with even number of silicon atoms tend to readily crystallize, those with the odd numbers of silicon atoms form amorphous glasses.[119] The enlargement of molecular size leads to dendrimers with higher Tg's, as exemplified by 1,3,5-tris[4-bis(4-methylphenyl)aminophenyl-4-diphenylaminophenylamino]benzene (MT-BDAB (**30**)) and **31**.[106,120,121] The structures of these compounds are shown in Chart 2.

4.3.2.2. Structural Modifications of the Key Compounds. A variety of structural modifications of the key compounds in Chart 2 have been made. One is the replace-

Scheme 3. Synthesis of *m*-MTDATA

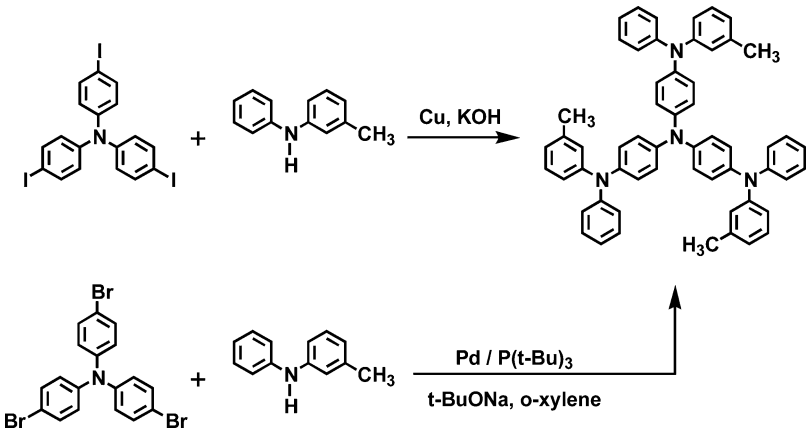

Scheme 4. Synthesis of TDAB

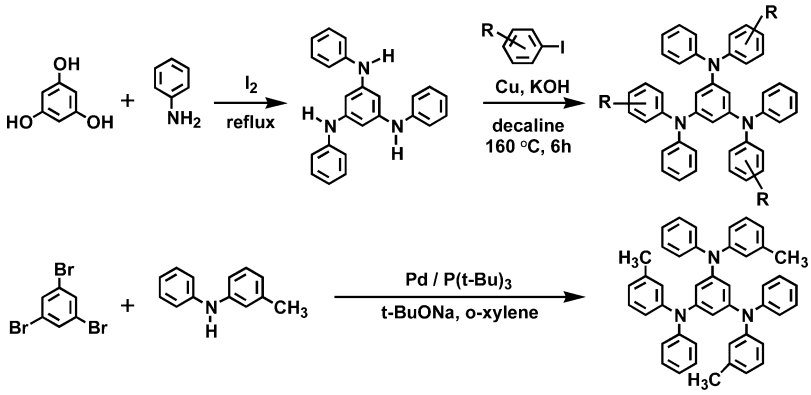

Scheme 5. Synthesis of TDAPB

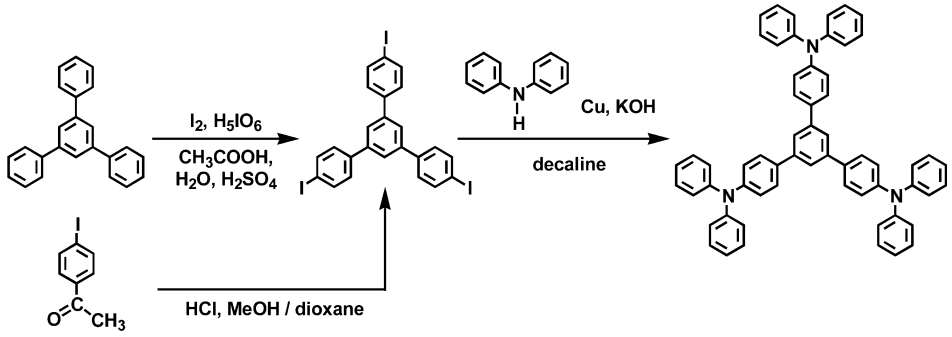

Scheme 6. Synthesis of Spiro Compound

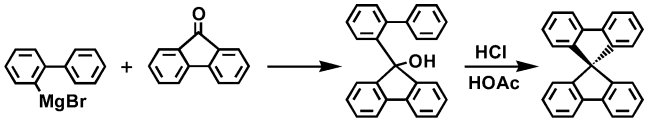

ment of the phenyl group by thienyl, pyridyl, biphenylyl, naphthyl, fluorenyl, phenanthryl, and oxadiazolyl groups. Another is the replacement of the diphenylamino group by the carbazolyl, benzocarbazolyl, or phenothiazinyl group. The central core structures of triphenylamine, benzene, and 1,3,5-triphenylbenzene have also been replaced by triazine and 1,3,5-triphenyltriazine moieties.

Examples of such structural modifications of the TDATA, TDAB, and TDAPB families are shown in Chart 3. The replacement of the diphenylamino group in TDATA by the biphenylyl, carbazolyl, or phenothiazinyl group afforded 4,4′,4″-tris[biphenyl-4-yl(3-methylphenyl)amino]triphenylamine (*p*-PMTDATA (**32**)),[122] 4,4′,4″-tri(*N*-carbazolyl)triphenylamine (TCTA (**33**)),[107] and 4,4′,4″-tri(*N*-phenothiazinyl)triphenylamine (TPTTA (**34**)).[92] The introduction of structurally rigid biphenylyl, carbazolyl, and phenothiazinyl groups significantly increased Tg's.[92,107,122] The replacement of the phenyl group in TDAB and TDAPB by the thienyl or pyridyl group afforded 1,3,5-tris(phenyl-2-thienylamino)benzene (α-TPTAB (**35**)), 1,3,5-tris(phenyl-3-thienylamino)benzene (β-TPTAB (**36**)),[103] **40**, and **44**.[123] The replacement of the benzene core in TDAB and TDAPB by the triazine core gave **41**−**43**, and **45**.[123,124] A few examples of spiro and related compounds, for example, B3 (**46**) and T3 (**47**),[125,126] and tetraarylmethanes, for example, **48**[127] and **49**,[128] are shown in Chart 4.

The Tg's, the oxidation potentials determined by cyclic voltammetry (CV), and the solid-state ionization potentials (IPs) which are determined by UPS or estimated from the CV data and the electron affinities (EAs) of the compounds shown in Chart 2−4 are listed in Table 1.

Scheme 7. Synthesis of Tetraphenylmethanes

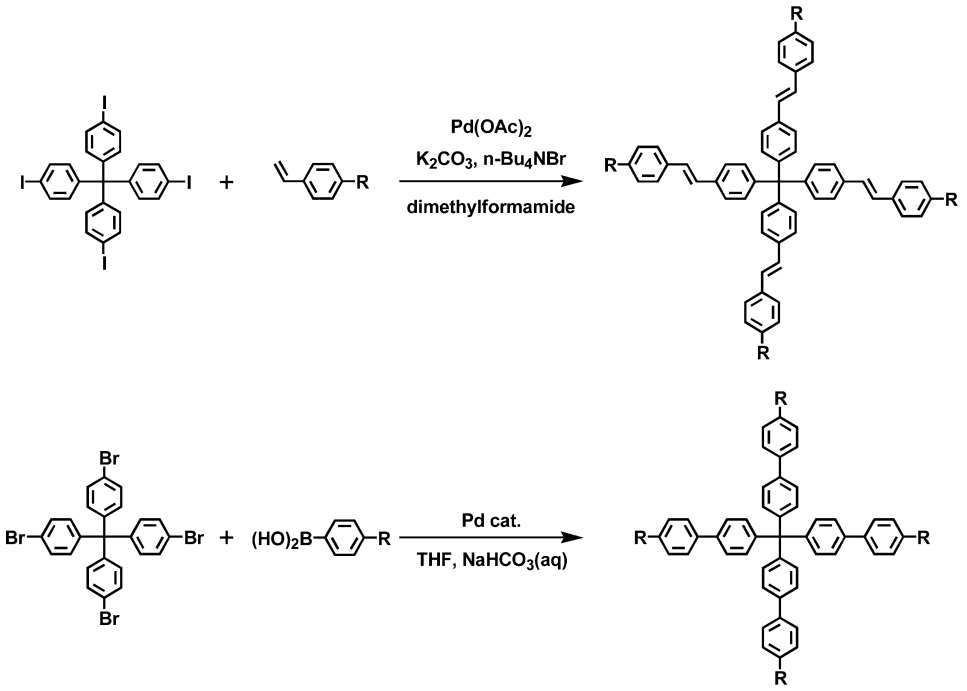

Chart 5. Hole Injection Buffer Layer Materials: TDATA Family

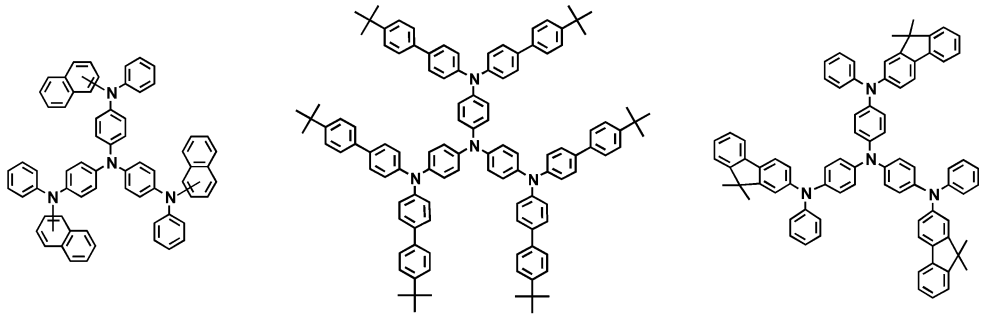

50 (1-TNATA)
51 (2-TNATA)
52 (t-Bu-TBATA)
53 (TFATA)

4.3.3. Synthesis of Several Classes of Amorphous Molecular Materials

Cross-coupling reactions of aromatic compounds, for example, Grignard coupling reaction, Ullmann coupling reaction, Suzuki coupling reaction, and palladium-catalyzed amination reaction, are frequently employed for the synthesis of π-electron-based charge-transporting materials.

p-TTA and its analogues have been synthesized either by the Grignard coupling reaction of tris(4-iodophenyl)amine with a Grignard reagent derived from 4-bromobiphenyl in THF in the presence of $NiCl_2$(dppp)[108] or by the Suzuki coupling reaction of tris(4-iodophenyl)amine with corresponding arylboronic acids in toluene in the presence of Pd catalyst[129] (Scheme 2).

m-MTDATA has been synthesized by the Ullmann coupling reaction between tris(4-iodophenyl)amine and 3-methylphenyl(phenyl)amine[91] or by the Pd-catalyzed amination reaction[130] (Scheme 3).

The synthesis of TDAB and its derivatives has been performed by the reaction of 1,3,5-trihydroxybenzene (phloroglucinol) with aniline in the presence of iodine under reflux to give 1,3,5-tris(phenylamino)benzene, followed by the Ullmann coupling reaction with iodobenzenes in decalin.[101] The Pd-catalyzed amination reaction between 1,3,5-tribromobenzene and 3-methylphenyl(phenyl)amine also gives TDAB[130] (Scheme 4).

TDAPB has been synthesized by the Ullmann coupling reaction of 1,3,5-tris(4-iodophenyl)benzene with diphenylamine in decalin in the presence of copper powder and potassium hydroxide.[113] 1,3,5-Tris(4-iodophenyl)benzene has been prepared either by the iodonation of 1,3,5-triphenylbenzene with iodine and H_5IO_6 in acetic acid or by the acid-catalyzed cyclization of *p*-iodoacetophenone in methanol/dioxane[131] (Scheme 5).

Spiro compounds have been synthesized by the reaction of biphenyl-2-ylmagnesium bromide with 9-fluorenone, followed by intramolecular dehydration reaction (Scheme 6).[132] Tetraphenylmethanes have been synthesized by palladium-catalyzed coupling reactions (Scheme 7).[128]

5. Charge Carrier Transporting Molecular Materials for Electronic and Optoelectronic Devices

While polycrystalline materials have been studied mostly for use in OPVs and OFETs, amorphous molecular glasses have been used in OLEDs.

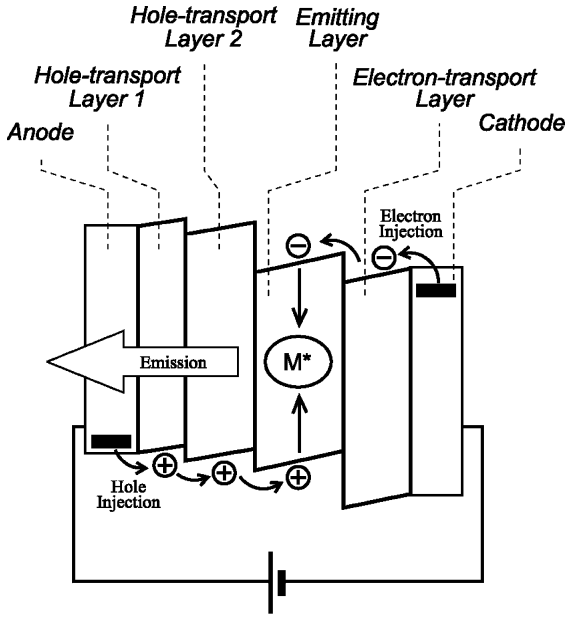

Figure 12. Multilayer OLEDs consisting of hole-injection and -transport layers, electron-transport, and emitting layers.

5.1. Amorphous Molecular Materials for Organic Light-Emitting Diodes (OLEDs)

Amorphous molecular materials have been proven to be excellent materials for use in OLEDs. They form uniform, smooth amorphous thin films without pinholes, allowing uniform contact with the metal electrodes and between organic layers because of their isotropic and homogeneous properties.

Charge-transporting amorphous molecular materials should have either high electron or hole (or both) drift mobilities to be capable of transporting charge carriers through them. Charge carriers, holes and electrons, which correspond to the cation and anion radicals of molecules, should be stable. Therefore, hole-transporting materials should undergo reversible anodic oxidation to form stable cation radicals. On the other hand, electron-transporting materials should undergo reversible cathodic reduction to form stable anion radicals. In addition, they should be morphologically and thermally stable and should not be easily crystallized.

Emitting materials emit either fluorescence or phosphorescence. Phosphorescence-based OLEDs attain higher EL quantum efficiencies than fluorescence-based OLEDs because the probability of the formation of the electronically excited triplet state resulting from the recombination of holes and electrons is 75% as compared with 25% for the formation of the electronically excited singlet state. Charge-transporting materials can be commonly used regardless of the kind of emitters.

5.1.1. Hole-Transporting Materials

An important requirement for high-performance OLEDs is efficient charge injection from the anode and the cathode at low drive voltage. A hole-transport layer is used for attaining efficient hole injection from the anode, which is usually a thin, transparent layer of ITO. Hole-transporting materials, namely, materials with relatively low solid-state ionization potentials are used as the hole-transport layer. Often a double hole-transport layer structure (Figure 12) is employed to more readily facilitate hole injection from the ITO into the emitting layer, where materials with very low

Chart 6. Hole-Transporting Materials: Modified TDATAs

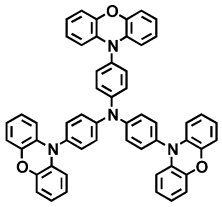

54 (TPOTA)

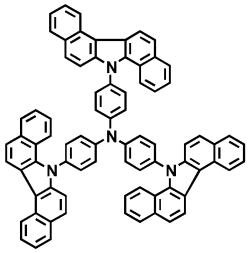

55 (TDCTA)

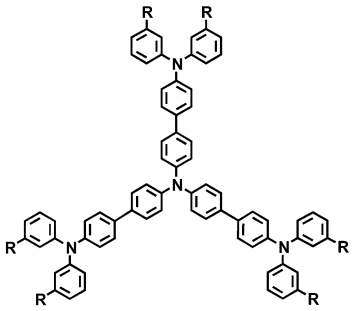

56 : R = H
57 (TPTE(S)) : R=CH_3

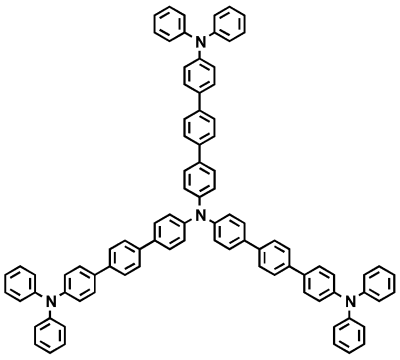

58

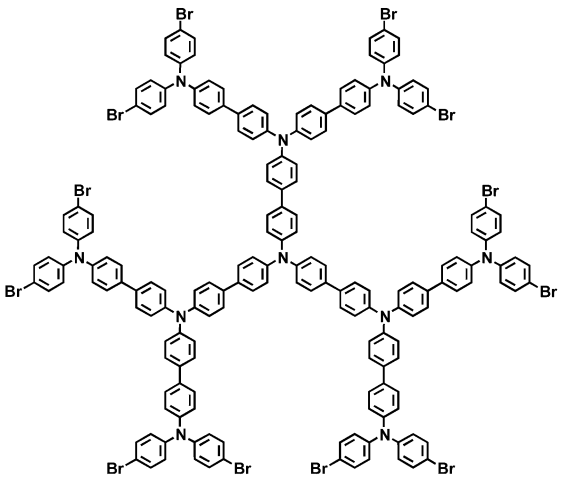

59

Chart 7. Hole-Transporting Materials: TDAB Family

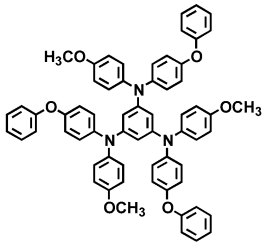

60

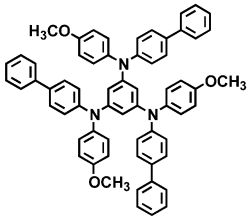

61

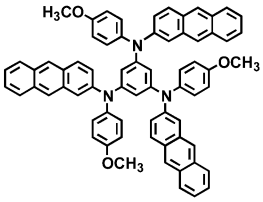

62

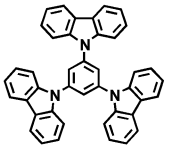

63 (TCB)

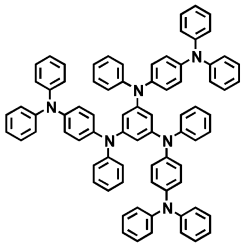

64 (*p*-DPA-TDAB)

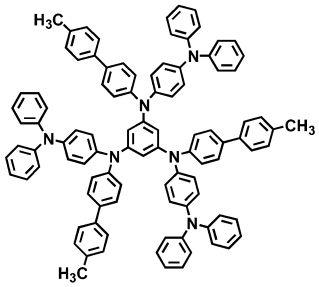

65 (MTDBB)

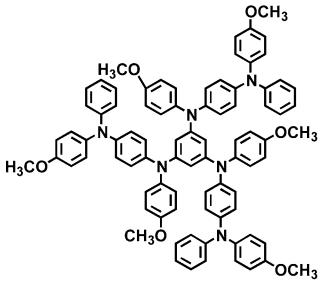

66

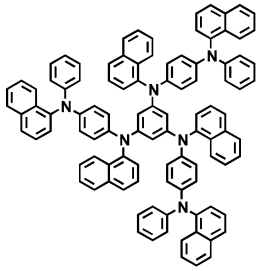

67

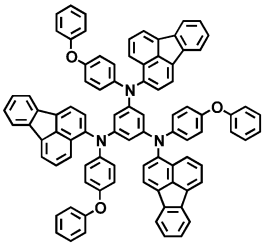

68

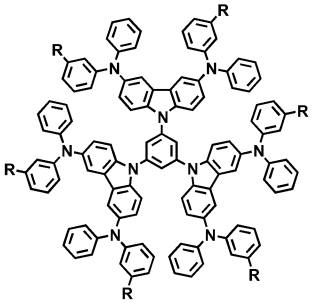

69 : R=H
70 : R=CH_3

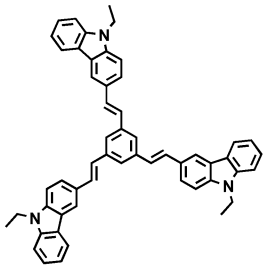

71 (TECEB)

solid-state ionization potentials and higher ionization potentials are used as the first hole-transport layer (HTL1) in contact with the ITO anode and as the second hole-transport layer (HTL2), respectively. Hole carriers are injected in a stepwise process from the anode to the HTL1, from the HTL1 to HTL2, and then from the HTL2 to the emitting layer. The energy barriers for hole injection are lowered by the use of this double hole-transport layer structure. The HTL1 is referred as a hole-injection buffer layer.

Most of the hole-transporting materials contains triarylamine moieties in their molecular structures. They are used either as HTL1 in contact with the ITO electrode or as HTL2, depending on their ionization potentials or oxidation potentials. Hole-transporting materials with very low solid-state ionization potentials, for example, *m*-MTDATA (**8**),[111,133−135] CuPc (**2**),[136] and an electrically conducting polymer, poly(3,4-ethylenedioxythiophene) doped with poly(4-styrene sulfonate) (PEDOT:PSS),[137] have been widely used as a hole-injection buffer layer (HTL1) in OLEDs.

The analysis of the current density−voltage characteristics for the hole-only device using *m*-MTDATA showed that the *m*-MTDATA/ITO interface is capable of providing TF-SCLC, and that *m*-MTDATA forms nearly an ohmic contact with the ITO electrode.[138−140] The contact between the ITO and CuPc has also been understood as ohmic.[141] It has been reported that when the energy barrier height is lower than ca. 0.3 eV, the metal/organic interface can be treated as the ohmic contact according to computer simulation.[142,143] It has been shown that PEDOT:PSS coated on the ITO layer forms an ohmic contact with *m*-MTDATA and a quasi-ohmic contact with α-NPD from the analysis of $J-V$ and DI-SCLC characteristics.[144]

Numerous hole-transporting amorphous molecular materials that serve either as HTL1 or as HTL2 have been

Chart 8. Hole-Transporting Materials: TDAPB Family

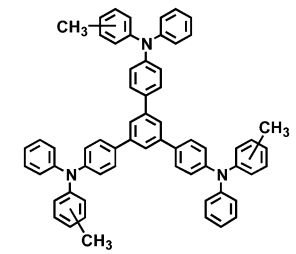

14~**16** (methyl-substituted TDAPB)

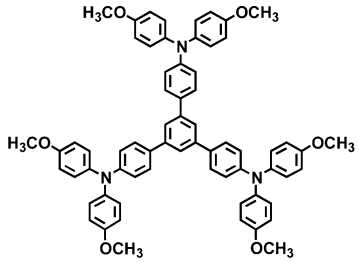

72

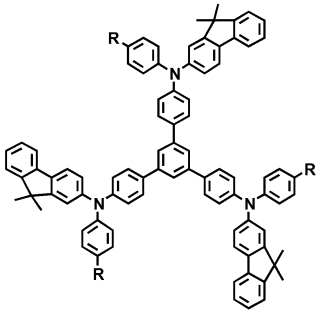

73 (TFAPB) : R=H
74 (MTFAPB) : R=CH_3

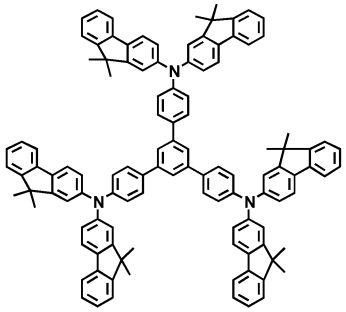

75 (TBFAPB)

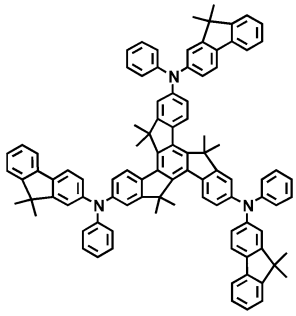

76 (TFATr)

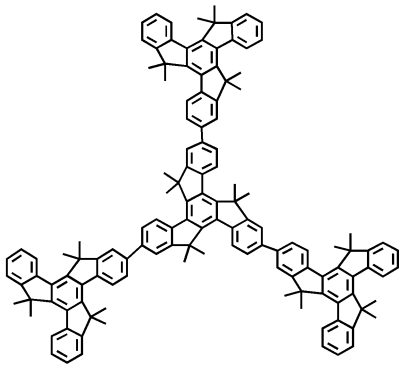

77 (TTrTr)

developed. They can be classified into the following categories on the basis of the structures of the central cores. Some charge-transporting materials function as host materials for phosphorescent emitters.

5.1.1.1. TDATA Family: Star-Shaped Compounds with a Triphenylamine Central Core. In addition to TDATA (**6**) and *m*-MTDATA (**8**) in Chart 2, their analogues with higher Tg's have been developed, which include *p*-PMTDATA (**32**),[122] 4,4′,4″-tris[1-naphthyl(phenyl)amino]triphenylamine (1-TNATA (**50**)),[133,145] and 4,4′,4″-tris[2-naphthyl(phenyl)amino]triphenylamine (2-TNATA (**51**)),[133] 4,4′,4″-tris[bis(4′-*tert*-butylbiphenyl-4-yl)amino]triphenylamine (*t*-Bu-TBATA (**52**)),[146] and 4,4′,4″-tris[9,9-dimethylfluoren-2-yl(phenyl)amino]triphenylamine (TFATA (**53**)).[147] These materials of the TDATA family are characterized by very low solid-state ionization potentials of ca. 5.1 eV,[111] good quality of amorphous films, and optical transparency in the visible light wavelength region. They are thermally more stable than *m*-MTDATA. Like *m*-MTDATA, these materials have also been proven to function as a thermally stable hole injection buffer layer (HTL1) in OLEDs.[133,145] The structures of these compounds are shown in Chart 5.

5.1.1.2. Structurally Modified TDATAs. The diphenylamino group in TDATA has been replaced by carbazolyl, phenothiazinyl, phenoxazinyl, and dibenzocarbazolyl groups to give TCTA (**33**)[107] and TPTTA (**34**)[92] in Chart 3, 4,4′,4″-tri(*N*-phenoxazinyl)triphenylamine (TPOTA (**54**)),[148] and TDCTA (**55**).[149] The replacement of the diphenylamino group in TDATA by a carbazolyl or a dibenzocarbazolyl group linked at its 9-position raises the ionization potential relative to the parent TDATA and significantly increases the Tg as a result of the rigid structure, as exemplifed by TCTA (**33**) and TDCTA (**55**). Other examples of modified TDATAs are given by **56**,[150] TPTE(S) (**57**),[151] **58**,[150] and **59**.[152] TPOTA functions as HTL1, and other compounds with higher ionization potentials serve as materials for HTL2. The structures of these compounds are shown in Chart 6.

TCTA (**33**) with a relatively large HOMO−LUMO energy gap has been shown to function not only as a hole-transporting material,[107,153] but also as a good host material for a green phosphorescent dopant.[154]

5.1.1.3. TDAB Family: Star-Shaped Compounds with Benzene as a Central Core. The TDAB family that functions as hole-transporting amorphous molecular materials include **60**,[155] **61**,[155] **62**,[155] 1,3,5-tri(*N*-carbazolyl)benzene (TCB (**63**)),[156] 1,3,5-tris[*N*-(4-diphenylaminophenyl)phenylamino]benzene (*p*-DPA-TDAB (**64**)),[104] 1,3,5-tris[*N*-(4′-methylbiphenyl-4-yl)-*N*-(4-diphenylaminophenyl)amino]benzene (MTDBB (**65**)),[106] **66**,[120] **67**,[120] **68**,[120] and 1,3,5-tris[2-(9-ethyl-3-carbazolyl)ethenyl]benzene (TECEB (**71**)).[157] TCB (**63**) has been further functionalized with the diarylamino group at the 3- and 6-positions of the carbazole ring to give

Chart 9. Hole-Transporting Materials: Tris(oligoarylenyl)amines

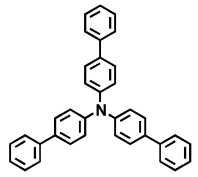

78 (TBA)

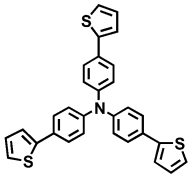

79 (TTPA)

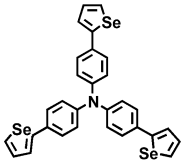

80 (TSePA)

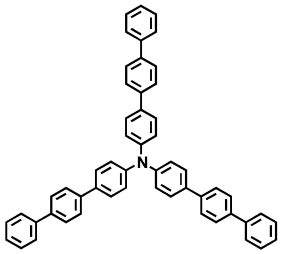

19 (*p*-TTA)

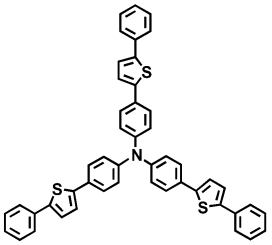

81 (TPTPA)

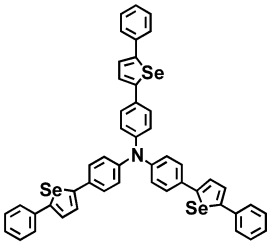

82 (TPSePA)

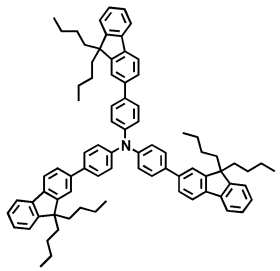

83

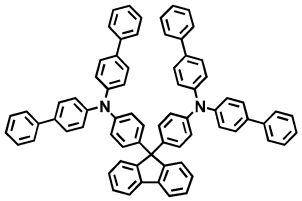

84 (BPAPF)

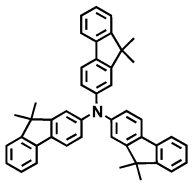

85 (TFlA)

69 and **70**.[158] Related to TCB (**63**), 1,3-di(*N*-carbazolyl)-benzene (mCB) has been used as a host material for blue phosphorescent dopant.[159] The structures of these compounds are shown in Chart 7.

5.1.1.4. TDAPB Family: Star-Shaped Compounds with a 1,3,5-Triphenylbenzene Central Core. Charge-transporting amorphous molecular materials of the TDAPB family include methyl-substituted TDAPB (**14**−**16**),[113] **72**,[160] 4,4′,4″-tris[9,9-dimethylfluoren-2-yl(phenyl)amino]triphenylbenzene (TFAPB (**73**)), 4,4′,4″-tris[9,9-dimethylfluoren-2-yl(4-methylphenyl)amino]triphenylbenzene (MTFAPB (**74**)), 4,4′,4″-tris[bis(9,9-dimethylfluoren-2-yl)amino]triphenylbenzene (TBFAPB (**75**)),[161] 2,7,12-tris[9,9-dimethylfluoren-2-yl(phenyl)amino]-5,5,10,10,15,15-hexamethyltruxene (TFATr (**76**)),[1d] and 2,7,12-tris(5,5,10,10,15,15-hexamethyltruxen-2-yl)-5,5,10,10,15,15-hexamethyltruxene (TTrTr (**77**)).[1d] The structurally rigid truxene-based hole-transporting amorphous molecular materials, TFATr (**76**) and TTrTr (**77**), exhibit very high Tg's above 200 °C.[1d,162] They are used as materials for HTL2.[1d] The compound **72** has been used as a host material for a phosphorescent dopant.[160] The structures of these compounds are shown in Chart 8.

5.1.1.5. Tris(oligoarylenyl)amines. A variety of tris(oligoarylenyl)amines have been developed (Chart 9).[108,109,129,163] The compounds BPAPF (**84**)[164] and tris(9,9-dimethylfluoren-2-yl)amine (TFlA (**85**))[165] are also included in this category for convenience. Among these, TBA (**78**), *p*-TTA (**19**), and their sulfur and selenium analogues, **79**−**82**, have been found to exhibit very high hole drift mobilities of $\sim 10^{-2}$ cm^2 V^{-1} s^{-1}.[163] Other tris(oligoarylenyl)amines have also been synthesized and used as materials for OPVs, which are described in section 5.2. *p*-TTA emits violet-blue to blue fluorescence.[166]

5.1.1.6. TPD Family: *N*,*N*,*N*′,*N*′-Tetraarylbenzidines. TPD (**86**)[167] dispersed in polycarbonate has been put into practical use as a CTL for photoreceptors in electrophotography. TPD has also been used as a hole transporter in Alq_3-based OLEDs.[168]

As TPD lacks thermal and morphological stability and tends to readily crystallize,[169] a variety of structural modifications of TPD have been made by replacing the phenyl group in the phenyl(3-methylphenyl)amino group in TPD by the naphthyl, biphenylyl, phenanthryl, fluorenyl, and carbazolyl groups. The developed materials include α-NPD (**87**),[136] *N*,*N*′-di(9-phenanthryl)-*N*,*N*′-diphenyl-[1,1′-biphenyl]-4,4′-diamine (PPD (**92**)),[170] 4,4′-di(*N*-carbazolyl)biphenyl (CBP (**91**)),[171] *N*,*N*′-di(biphenyl-2-yl)-*N*,*N*′-diphenyl-[1,1′-biphenyl]-4,4′-diamine (*o*-BPD (**88**)),[122] *N*,*N*′-di(biphenyl-3-yl)-*N*,*N*′-diphenyl-[1,1′-biphenyl]-4,4′-diamine (*m*-BPD (**89**)),[122] *N*,*N*′-di(biphenyl-4-yl)-*N*,*N*′-diphenyl-[1,1′-biphenyl]-4,4′-diamine (*p*-BPD (**90**)),[122] *N*,*N*,*N*′,*N*′-tetrakis(9,9-dimethylfluoren-2-yl)-[1,1′-biphenyl]-4,4′-diamine (FFD (**93**)),[147] and **97** and **98**.[158] The central biphenyl moiety is also replaced by a fluorenyl moiety to give TPF (**94**),[172] NPF (**95**),[172] and *N*,*N*′-bis(9,9-dimethylfluoren-2-yl)-*N*,*N*′-diphenyl-9,9-dimethylfluorene-2,7-diamine (PFFA (**96**)).[173] A dimeric compound of TPD, TPTE (**99**),[174] and a similar compound **100**[175] have also been developed. CBP has been widely employed as a host material for phosphorescent dopants.[29,154,176−180] TPD and α-NPD emit intense violet-blue and blue florescence with high quantum efficiencies. Chart 10 shows the structures of these compounds.

5.1.1.7. Oligothiophenes End-Capped with Triarylamines. Oligothiophenes are crystalline in nature; however, thiophene and oligothiophenes end-capped with triarylamine, for example, BMA-nT (**21**−**24**) in Chart 2,[60,61] 2,5-bis(2-

Chart 10. Hole-Transporting Materials: TPD Derivatives

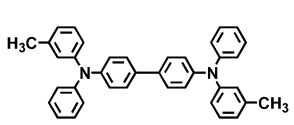

86 (TPD)

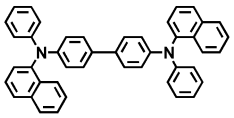

87 (α-NPD)

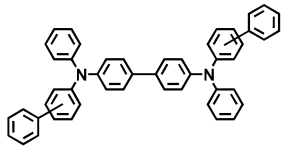

88 (*o*-BPD): *o*-Ph
89 (*m*-BPD): *m*-Ph
90 (*p*-BPD) : *p*-Ph

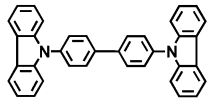

91 (CBP)

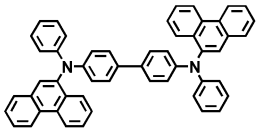

92 (PPD)

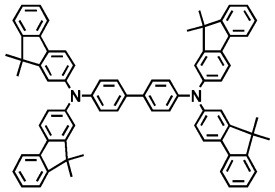

93 (FFD)

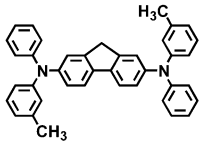

94 (TPF)

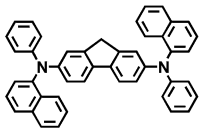

95 (NPF)

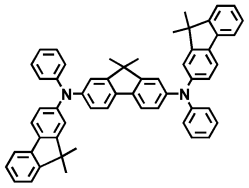

96 (PFFA)

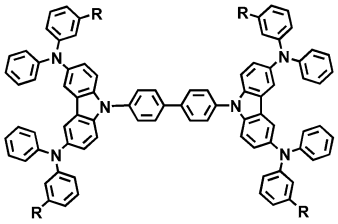

97 : R=H
98 : R=CH_3

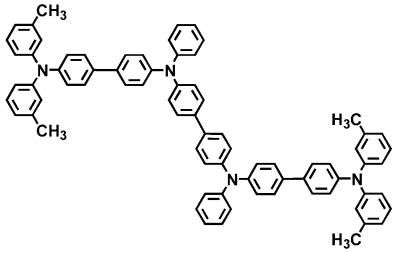

99 (TPTE)

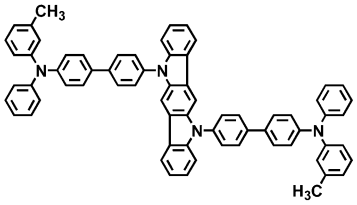

100

{4-[bis(4-methylphenyl)amino]phenyl}thiophen-5-yl)furan (BMA-TFT (**101**)),[181] and α,ω-bis{4-[*N*,*N*-bis(9,9-dimethylfluoren-2-yl)amino]phenyl}oligothiophenes (BFA-nT (**102**, **103**)),[182] readily form amorphous glasses. The compounds of the BMA-nT and BFA-nT families undergo reversible anodic oxidations and cathodic reductions. Noteworthy is that the oxidation and ionization potentials of BMA-nT are approximately the same regardless of the π-conjugation length of oligothiophenes.[61,115] They function as hole-transporting emitting materials, and the emission color can be tuned by varying the conjugation length of oligothiophenes.[62,182] These results indicate that the ionization potential is mainly governed by the triarylamine moiety, whereas the electron affinity is affected by the conjugation length of oligothiophenes. The structures of BMA-nT and BFA-nT are shown in Chart 11.

5.1.1.8. *N*,*N*,*N*′,*N*′-Tetraaryl Arylenediamines. Aromatic and heteroaromatic compounds such as benzene, naphthalene, anthracene, oligothiophenes, and so forth have been functionalized with bis(diarylamino) groups to give *N*-naphthyl-*N*,*N*′,*N*′-triphenyl-1,4-phenylenediamines ($DN_\alpha P$ (**104**), $TN_\beta P$ (**105**)), *N*,*N*′-dinaphthyl-*N*,*N*′-diphenyl-1,4-phenylenediamines ($N_\alpha N_\alpha P$ (**106**), $N_\beta N_\alpha P$ (**107**)), 1,5-bis(diarylamino)naphthalene derivatives (**115**),[183] 9,10-bis(diarylamino)anthracenes (PPA (**116**), TPA (**117**), α-NPA (**118**), β-NPA (**119**)),[184] and α,ω-diarylaminooligothiophenes (A-nT (**120**), **121**).[185−187] α-NPA was synthesized from 9,10-dibromoanthracene and *N*-phenyl-1-naphthylamine in *o*-xylene in the presence of palladium catalyst. The HOMO and LUMO energies of 9,10-bis(diarylamino)anthracene are ca. 5.5−5.6 and 3.1−3.3 eV, respectively. The diarylamino group has also been replaced by the carbazolyl group to give 1-(*N*-carbazolyl)-4-diarylaminobenzenes (DCP (**108**), TCP (**109**), $N_\alpha CP$ (**110**), $N_\beta CP$ (**111**)),[171] **112**,[188] **113** and **114**,[158,188] and **122** and **123**.[158] The compounds of this family possess relatively low ionization potentials. The structures of these compounds are shown in Chart 12.

5.1.1.9. Compounds with a Central Carbazole Core. The central core structure of triphenylamine in the TDATA family can be replaced by carbazole, which can be easily substituted with the aryl and diarylamino groups at its 3-, 6-, and 9-positions to make amorphous molecular materials. 3,6-Bis(*N*,*N*-diphenylamino)-9-phenylcarbazole (**124**) was synthesized by the Ullmann coupling reaction of 3,6-diiodo-9-phenylcarbazole with diphenylamine in the presence of anhydrous potassium carbonate, copper powder, and 18-crown-6 in *o*-dichlorobenzene.

The incorporation of the arylamino group attached to the 3- and 6-positions of the central carbazole ring enables glass formation and significantly reduces the ionization potential through π-conjugation, as exemplified by the compounds **124**−**127**.[189,190] The amorphous molecular materials with the

Chart 11. Hole-Transporting Materials: π-Electron Systems End-Capped with Triarylamines

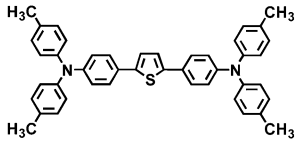

21 (BMA-1T)

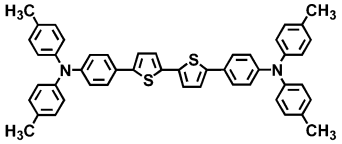

22 (BMA-2T)

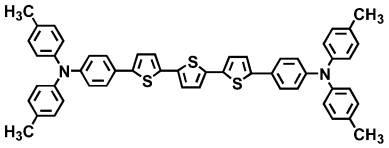

23 (BMA-3T)

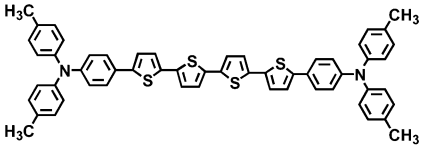

24 (BMA-4T)

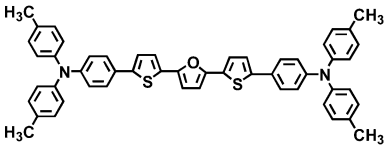

101 (BMA-TFT)

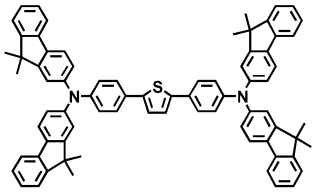

102 (BFA-1T)

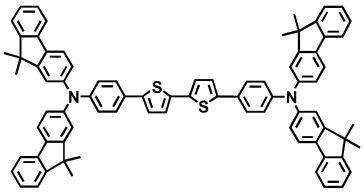

103 (BFA-2T)

central carbazole core, **126** and **127**, are characterized by high Tg's of ca. 180 °C. The structures of these compounds are shown in Chart 13.

5.1.1.10. Aryl Hydrazones. Arylaldehyde and arylketone hydrazones, for example, DPH (**20**), 4-diphenylaminoacetophenone diphenylhydrazone (M−DPH (**128**)), 4-diphenylaminobenzaldehyde methylphenylhydrazone (DPMH (**129**)), 9-ethylcarbazole-3-carbaldehyde diphenylhydrazone (ECH (**130**)), 3-acetyl-9-ethylcarbazole diphenylhydrazone (M-ECH (**131**)), and 9-ethylcarbazole-3-carbaldehyde methylphenylhydrazone (ECMH (**132**)), constitute one class of amorphous molecular materials which are capable of transporting holes.[114] The stability of the amorphous glassy state is greatly dependent on their molecular structures.[114] Other aryl hydrazone compounds include **133**−**136**[191] and **137**,[192] where arylhydrazone moieties are incorporated into the central triphenylamine core or 1,3-dicarbazolylcyclobutane core (Chart 14).

5.1.1.11. Spiro Compounds. Examples of spiro compounds that function as hole-transporting amorphous molecular materials are provided by **138**, **139**,[193] spiro-TAD (**140**),[194] spiro-*m*-TTB (**141**),[194] OMeTAD (**142**),[195,196] and spiro-CARB (**143**).[116] 9-Fluorene-type trispirocyclic compound (TX-F6S (**144**)) have also been synthesized and used as thermally stable hole-transporting materials in OLEDs[197] (Chart 15).

5.1.1.12. Other Hole-Transporting Materials. Compounds without the diarylamino or the carbazolyl group, for example, HPCzI (**145**),[198] **146**,[199] **147**,[199] and PF6 (**148**),[199,200] have also been shown to play a role in hole transport in OLEDs (Chart 16).

The Tg's, oxidation potentials, solid-state ionization potentials, and electron affinities of hole-transporting amorphous molecular materials shown in Charts 5−16 are summarized in Table 2.[201−211]

5.1.2. Electron-Transporting and Hole-Blocking Materials

Like the hole-transport layer, the electron-transport layer is used for attaining efficient electron injection from the metal cathode, which is usually low work-function metals such as calcium, magnesium, and aluminum. As was described in section 5.1, electron-transporting materials for use in the electron-transport layer in OLEDs should fulfill several requirements. They should have high electron drift mobilities to transport electrons. They should meet the energy level matching the electron injection from the cathode. The cathodic reduction processes of electron-transporting materials should be reversible to form stable anion radicals. In addition, they should form homogeneous thin films with morphological and thermal stability. The electron-transport layer in OLEDs plays a role in hole blocking as well as acceptance and transport of electrons.

In case electron-transporting materials lack effective hole-blocking ability, an independent hole-blocking material is used together with a suitable electron transporter that facilitates electron injection from the cathode. Hole-blocking materials should fulfill several requirements. They should have weak electron-accepting and -transporting properties. Their anion radicals should be stable. They should possess proper energy levels of HOMO and LUMO to be able to block holes from escaping from the emitting layer into the electron-transport layer but to pass on electrons from the electron-transport layer to the emitting layer. In other words, the difference in the HOMO energy levels between the emitting material and the hole-blocking material should be much larger than that in their LUMO energy levels. In

Chart 12. Hole-Transporting Materials: *N,N,N′,N′*-Tetraaryl Arylenediamine

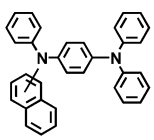

104 ($DN_\alpha P$)
105 : ($TN_\beta P$)

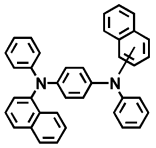

106 ($N_\alpha N_\alpha P$)
107 ($N_\beta N_\alpha P$)

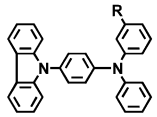

108 (DCP) : R =H
109 (TCP) : R = CH_3

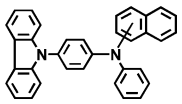

110 ($N_\alpha CP$)
111 ($N_\beta CP$)

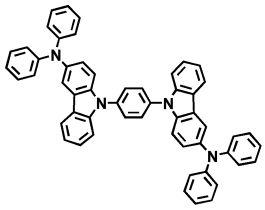

112

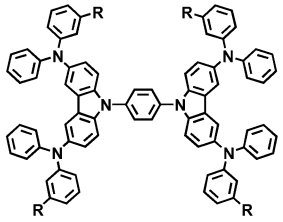

113 : R=H
114 : R=CH_3

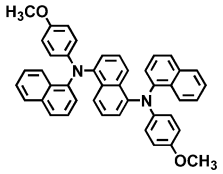

115

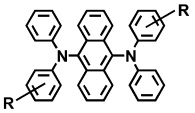

116 (PPA) : R=H
117 (TPA) : R=CH_3

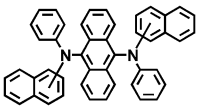

118 (α-NPA)
119 (β-NPA)

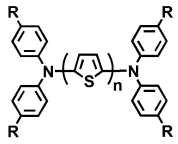

120 (A-nT) : R=H
121 : n=2, R=CH_3

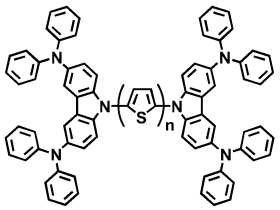

122 : n=1
123 : n=2

Chart 13. Hole-Transporting Materials: Compounds with a Central Carbazole Core

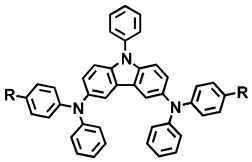

124 : R=H
125 : R=CH_3

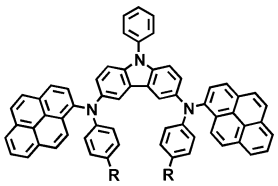

126 : R=H
127 : R=CH_3

addition, they should not form any exciplexes with emitting materials having electron-donating properties.

Electron-transporting materials contain electron-withdrawing moieties in the molecule. Heteroaromatic rings, for example, pyridine (**149**), triazine (**150**), 1,3,4-oxadiazole (**151**), triazole (**152**), and silacyclopentadiene (silole (**153**)), dimesitylboranes (**154**), and triarylboranes (**155**) comprise electron-withdrawing moieties in electron-transporting materials (Chart 17). Therefore, a definite concept for the molecular design of electron-transporting amorphous molecular materials is to incorporate these electron-withdrawing moieties at the 1,3,5-positions of the central benzene core or at the *o*-, *m*-, or *p*-position of the central 1,3,5-triphenylbenzene core to form nonplanar molecules. An electron-withdrawing dimesitylboryl group can be incorporated into other π-conjugated systems to create a different class of electron-transporting amorphous molecular materials.

Recent advances in electron-transporting materials have been reviewed.[212−214] Here, electron-transporting materials are classified into the following categories on the basis of the central structural units.

5.1.2.1. Tris(8-quinolinolato)aluminum (Alq_3) and Boron-Containing Complexes. Alq_3 (**156** in Chart 18), which is well-known as a green emitter, has been widely used as an excellent electron transporter and as a host material for green to red fluorescence-emissive dopants in OLEDs. It has been reported that Alq_3 takes up different polymorphs.[85] The vacuum-deposited Alq_3 thin films are of amorphous nature;[215] however, the initially amorphous thin film of Alq_3 readily crystallizes on exposure to solvent vapor.[85] Boron-containing complexes such as BPh_2q (**157**) and $B(2\text{-benzothienyl})_2q$ (**158**) have also been reported as candidates for electron transporters.[216,217] They emit fluorescence, but form exciplexes with α-NPD.[216,217]

5.1.2.2. Oxadiazole-Containing Oligo(arylene)s and Oligo(arylenevinylene)s. 2-(Biphenyl-4-yl)-5-(4-*tert*-butylphenyl)-1,3,4-oxadiazole (*t*-Bu−PBD (**159**)) has been widely used as an electron transporter in OLEDs;[168] however, this compound readily crystallizes. Other oxadiazole-contain-

Chart 14. Hole-Transporting Materials: Compounds with Aryl Hydrazone Moieties

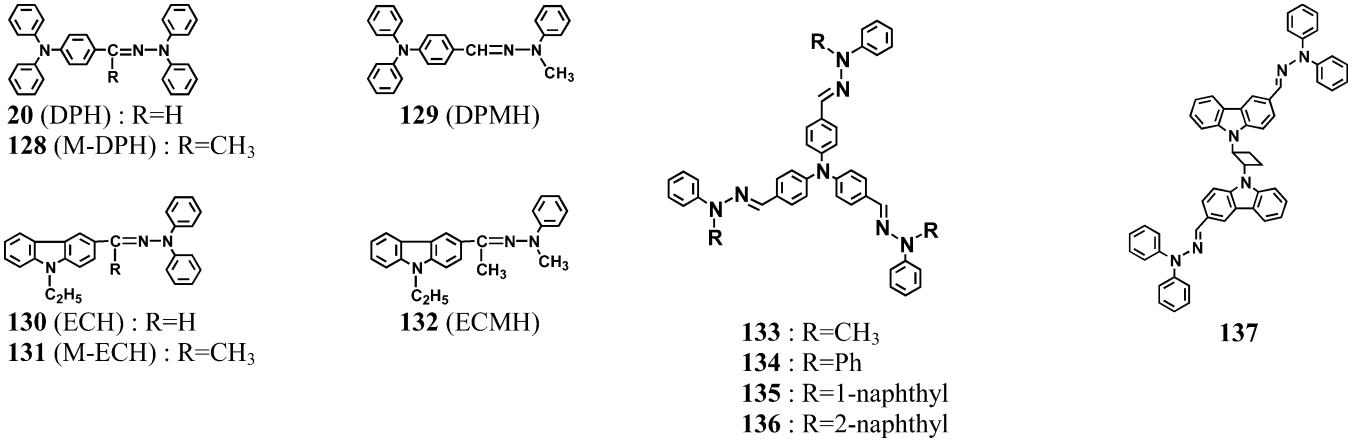

Chart 15. Hole-Transporting Materials: Spiro Compounds

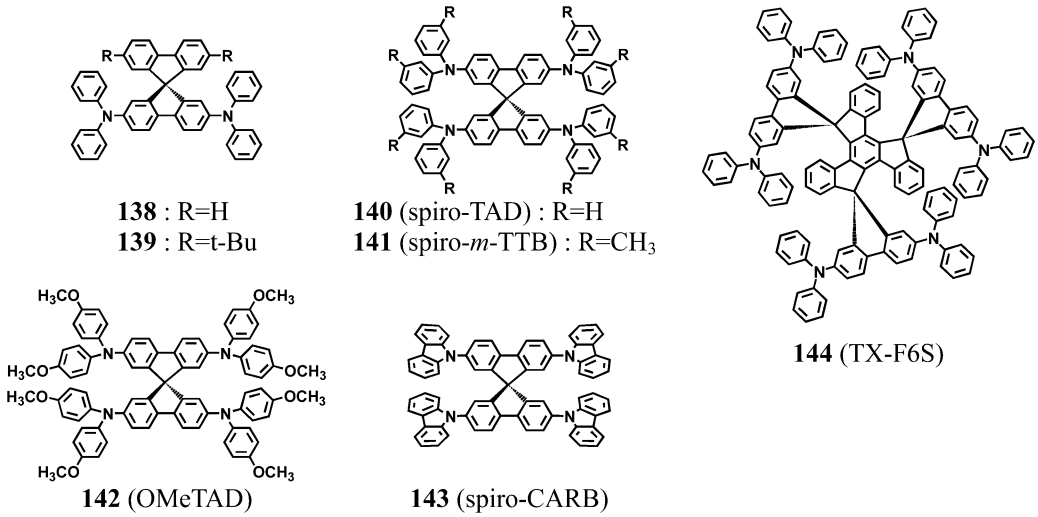

Chart 16. Hole-Transporting Materials without Diarylamino Groups

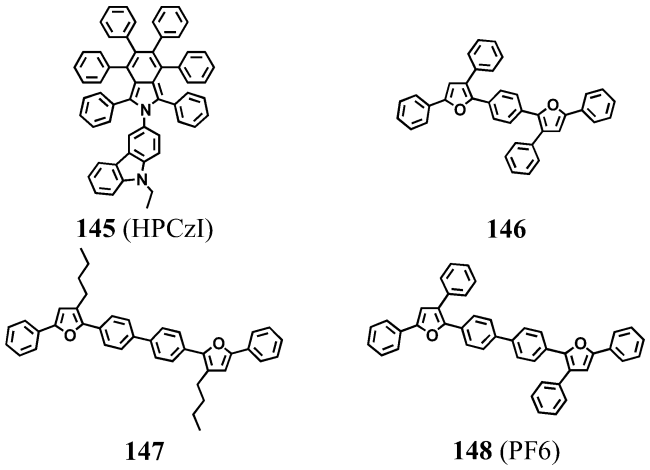

ing compounds include 3-bis[5-(4-*tert*-butylphenyl)-1,3,4-oxadiazol-2-yl]benzene (OXD-7 (**160**)),[31] **161**, and **162**.[218] A 2,5-diaryl-1,3,4-triazole derivative (TAZ (**163**)) has also been reported to serve as an electron transporter.[219] 4,7-Diphenyl-1,10-phenanthroline (BPhen (**164**)) doped with lithium has been reported to serve as an electron transporter[220−223] (Chart 18).

5.1.2.3. Compounds with a Benzene or Triazine Central Core. In accordance with the molecular design concept of the incorporation of electron-withdrawing pyridine, oxadiazole, quinoxaline, and benzimidazole at the 1,3,5-positions of the central benzene core, the following compounds have been synthesized and used as electron transporters in OLEDs. They include 1,3,5-tris(4-*tert*-butylphenyl-1,3,4-oxadizolyl)-benzene (TPOB (**165**)),[133,224,225] 1,3,5-tris(3-phenylquinoxalin-2-yl)benzene (TPQ (**166**)),[226] and a benzimidazole derivative (TPBI (**167**)).[227] 1,3,5-Tris(9,9-dimethylfluoren-2-yl)benzene (TFB (**168**)) acts as a hole-blocking material.[228] The central benzene core has also been replaced by a triazine central core to give 2,4,6-tris[di(2-pyridyl)amino]-1,3,5-triazine (**169**)[123] and TRZ2−4 (**170**−**172**)[229] (Chart 19).

5.1.2.4. Compounds with a 1,3,5-Triphenylbenzene or 2,4,6-Triphenyltriazine Central Core. Electron-transporting amorphous molecular materials with a central core of 1,3,5-triphenylbenzene or 2,4,6-triphenyltriazine have been developed. The examples are provided by 1,3,5-tris{4-[di(2-pyridyl)amino]phenyl}benzene (**44**),[123] 2,4,6-tris{4-[di(2-pyridyl)amino]phenyl}-1,3,5-triazine (**45**),[123] **173**,[230] 1,3,5-tris[5-(dimesitylboryl)thiophen-2-yl]benzene (TMB-TB (**174**)),[231] 1,3,5-tri(4-biphenylyl)benzene (TBB (**175**)), 1,3,5-tris(4-fluorobiphenyl-4′-yl)benzene (F-TBB (**176**)), 1,3,5-tris[4-(9,9-dimethylfluoren-2-yl)phenyl]benzene (TFPB (**177**)),[228,232] **178**,[233] and **179**[233] (Chart 20).

TMB-TB functions as an electron transporter with better hole-blocking character than that of Alq_3.[231] The materials of the 1,3,5-triarylbenzene family, TBB (**175**), F-TBB (**176**), TFPB (**177**), **178**, and **179**, act as hole-blocking materials in

Table 2. Glass-Transition Temperatures (Tg's), Oxidation Potentials, Ionization Potentials (IPs), and Electron Affinities (EAs) of Hole Transporting Amorphous Molecular Materials

compound	Tg (°C)	oxidation potential	IP (eV)	EA (eV)	ref
		Modified TDATA Derivatives			
50 (1-TNATA)	113	0.08 V vs Ag/Ag^+ (0.01 mol dm^{-3}) in CH_2Cl_2			1b
	113		5.1		133
51 (2-TNATA)	110	0.11 V vs Ag/Ag^+ (0.01 mol dm^{-3}) in CH_2Cl_2			1b
	110		5.1		133
52 (*t*-Bu-TBATA)	203	0.09 V vs Ag/Ag^+ (0.01 mol dm^{-3}) in CH_2Cl_2			146
53 (TFATA)	131	0.08 V vs Ag/Ag^+ (0.01 mol dm^{-3})			147
54 (TPOTA)	145	0.46 V vs Ag/Ag^+ (0.01 mol dm^{-3}) in CH_2Cl_2			148
55 (TDCTA)	212	0.92 V vs Ag/Ag^+ (0.01 mol dm^{-3}) (irreversible)			149
56	143	0.25 V vs Fc/Fc^+ in CH_2Cl_2			150
57 (TPTE(S))	106				151
58	160	0.34 V vs Fc/Fc^+ in CH_2Cl_2			150
59		1.2 V vs Ag/Ag^+			152
		Star-Shaped Compounds with Benzene as a Central Core			
60	54	0.27 V vs Fc/Fc^+	5.07		155
61	85	0.31 V vs Fc/Fc^+	5.11		155
62	123	0.36 V vs Fc/Fc^+	5.16		155
63 (TCB)	122	1.29 V vs Ag/Ag^+ (0.01 mol dm^{-3}) (irreversible)			156
64 (*p*-DPA-TDAB)	108	0.23 V vs Ag/Ag^+ (0.01 mol dm^{-3}) in CH_2Cl_2			104
65 (MTDBB)	128	0.23 V vs Ag/Ag^+ (0.01 mol dm^{-3}) in CH_2Cl_2			106
66	93	0.02 V vs Fc/Fc^+ in CH_3CN	4.82		120
67	141	0.14 V vs Fc/Fc^+ in CH_3CN	4.94		120
68	105				120
69	189	0.590 V vs Fc/Fc^+ in CH_2Cl_2	5.07	2.12	158
70	189	0.559 V vs Fc/Fc^+ in CH_2Cl_2	5.04	2.07	158
71 (TECEB)	130		5.2	2.8	157
73 (TFAPB)	150	0.61 V vs Ag/Ag^+			161
74 (MTFAPB)	154	0.54 V vs Ag/Ag^+			161
75 (TBFAPB)	189	0.53 V vs Ag/Ag^+			161
76 (TFATr)	208				1d
77 (TTrTr)	358				1d
		Tris(oligoarylenyl)amines			
78 (TBA)	76	0.61 V vs Ag/Ag^+ (0.01 mol dm^{-3}) in CH_2Cl_2			108
79 (TTPA)	70	0.57 V vs Ag/Ag^+ (0.01 mol dm^{-3}) in CH_2Cl_2			201
80 (TSePA)	80				163
81 (TPTPA)	83				163
82 (TPSePA)	106				163
83	96				129
84 (BPAPF)	167	0.95 V vs Ag/Ag^+			164
85 (TFlA)	125				165
		Tetraphenylbenzidines			
86 (TPD)			5.5	2.4	111
	60				151
	65		5.50	2.30	170
	60	0.733 V vs Ag/AgCl			171
			5.38		202
			5.2		203
87 (α-NPD)	95		5.1		136
	95		5.70	2.60	170
	100	0.767 V vs Ag/AgCl			171
			5.5	2.4	204
			5.2		205
			5.5	2.4	206
		0.38 V vs Fc/Fc^+ in DMF	5.3		48
88 (*o*-BPD)	75	0.48 V vs Ag/Ag^+ (0.01 mol dm^{-3}) in CH_2Cl_2			122, 207
89 (*m*-BPD)	81	0.51 V vs Ag/Ag^+ (0.01 mol dm^{-3}) in CH_2Cl_2			122, 207
90 (*p*-BPD)	102	0.50 V vs Ag/Ag^+ (0.01 mol dm^{-3}) in CH_2Cl_2			122, 207
91 (CBP)	—[a]	0.975 V vs Ag/AgCl			171
			6.3	3.2	204
			6.3	3.2	206
92 (PPD)	152				170
93 (FFD)	165	0.40 V vs Ag/Ag+ (0.01 mol dm^{-3})			147
94 (TPF)	78	0.626 V vs Ag/AgCl			172
95 (NPF)	118	0.658 V vs Ag/AgCl			172
96 (PFFA)	135	0.31 V vs Ag/Ag^+ (0.01 mol dm^{-3})			173
97	185	0.420 V vs Ag/Ag^+	5.00	1.73	158
98	154	0.401 V vs Ag/Ag^+	4.99	1.77	158
99 (TPTE)	130				174
100	163				175

Table 2 (Continued)

compound	Tg (°C)	oxidation potential	IP (eV)	EA (eV)	ref
		π-Electron Systems End-Capped with Triarylamines			
101 (BMA-TFT)	93	0.35 V vs $Ag/AgNO_3$ (0.01 mol dm^{-3})			181
102 (BFA-1T)[b]	158	0.39 V vs Ag/Ag^+ (0.01 mol dm^{-3})			182a
103 (BFA-2T)[b]	165	0.43 V vs $Ag/AgNO_3$ (0.01 mol dm^{-3}) in CH_2Cl_2			182b
		N,N,N′,N′-Tetraarylenyl Arylenediamines			
104 ($DN_\alpha P$)	62	0.611 V vs Ag/AgCl			171
105 ($TN_\alpha P$)	62	0.595 V vs Ag/AgCl			171
106 ($N_\alpha N_\alpha P$)	70	0.625 V vs Ag/AgCl			171
	66.5				208
107 ($N_\beta N_\alpha P$)	81	0.616 V vs Ag/AgCl			171
108 (DCP)	61	0.965 V vs Ag/AgCl			171
109 (TCP)	54	0.950 V vs Ag/AgCl			171
110 ($N_\alpha CP$)	88	0.945 V vs Ag/AgCl			171
111 ($N_\beta CP$)	83	0.947 V vs Ag/AgCl			171
112	141	0.796 V vs Ag/AgCl in CH_2Cl_2	5.15	1.64	188
113	157	0.744 V vs Ag/AgCl in CH_2Cl_2	5.10	1.74	188
114	146	0.428 V vs Ag/Ag^+ in CH_2Cl_2	5.01	2.08	158
115	131		5.14	2.11	183
116 (PPA)	—[a]		5.64	3.18	184
117 (TPA)	103		5.51	3.05	184
118 (α-NPA)	166		5.54	3.31	184
119 (*β*-NPA)	138		5.54	3.11	184
120 (A-2T)	—[a]	−0.01 V vs Fc/Fc^+ in benzonitrile			186
			5.07		187
120 (A-6T)	—[a]	0.13 V vs Fc/Fc+ in benzonitrile			186
121	−23	0.82 V vs SCE (irreversible)			185
122	158	0.569 V vs Fc/Fc^+ in CH_2Cl_2	5.01	2.07	158
123	188	0.560 V vs Fc/Fc^+ in CH_2Cl_2	5.04	2.10	158
		Compounds with Central Carbazole Core			
124	111		5.34		189
125	105		5.28		189
126	180	0.167 V vs Fc/Fc^+			190
127	184	0.111 V vs Fc/Fc^+			190
		Aryl Hydrazones			
128 (M-DPH)	35				114
129 (DPMH)	30				209
133	74	0.17 V vs Fc/Fc^+ in CH_2Cl_2			191
134	81	0.22 V vs Fc/Fc^+ in CH_2Cl_2			191
135	86	0.23 V vs Fc/Fc^+ in CH_2Cl_2			191
136	87	0.23 V vs Fc/Fc^+ in CH_2Cl_2			191
137	136		5.47		192
		Spiro Compounds			
138	111	0.62 V vs Ag/AgCl in CH_2Cl_2			193
139	122	0.60 V vs Ag/AgCl in CH_2Cl_2			193
140 (spiro-TAD)	133				116
	133				194
	133	0.230 V vs Fc/Fc^+ in CH_2Cl_2			210
	133	0.203 V vs Fc/Fc^+ in CH_2Cl_2			211
141 (spiro-*m*-TTB)	119				194
142 (OMeTAD)	120				195
144	170	0.42 V vs Ag/AgCl in CH_2Cl_2			197
		Others			
145 (HPCzI)			5.1	2.2	198
146	88	0.548 V vs Fc/Fc^+ in CH_2Cl_2	5.35	2.45	199
147	23	0.550 V vs Fc/Fc^+ in CH_2Cl_2	5.35	2.34	199
148 (PF6)	96	0.645 V vs Fc/Fc^+ in CH_2Cl_2	5.45	2.51	199
	96		5.3∼5.4	∼2.6	200

[a] These compounds do not form amorphous glasses. [b] Reduction potentials of these compounds are as follows: BFA-1T (−2.47 V vs $Ag/AgNO_3$ (0.01 mol dm^{-3}) in THF); BFA-2T (−2.26 V vs $Ag/AgNO_3$ (0.01 mol dm^{-3}) in THF).

Chart 17. Electron-Withdrawing Moieties in Electron-Transporting Materials

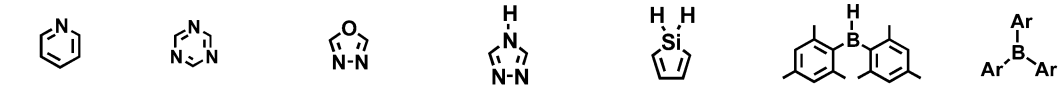

149 (pyridine) **150** (triazine) **151** (1,3,4-oxiadiazole) **152** (triazole) **153** (silacyclopentadiene, silole) **154**(dimesityl borane) **155** (triaryl-borane)

combination with other electron-transporting materials, for example, Alq_3, in OLEDs, permitting blue or blue-violet emission.[228,232] The compounds **44** and **45** with electron-transporting properties serve as blue-emitting materials.[123]

Chart 18. Electron-Transporting Materials: Alq_3, 2,5-Diaryl-1,3,4-oxadiazoles, and Triazoles

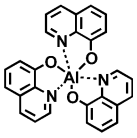

156 (Alq_3)

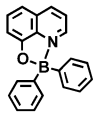

157 (BPh_2q)

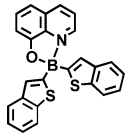

158 ($B(2\text{-benzothienyl})_2q$)

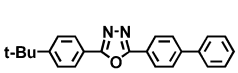

159 (t-Bu-PBD)

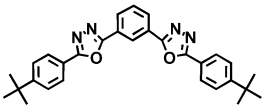

160 (OXD-7)

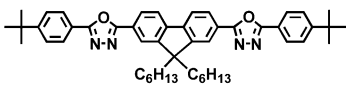

161

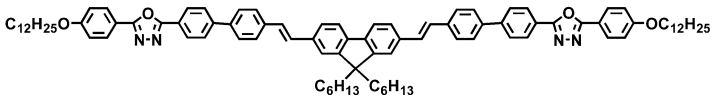

162

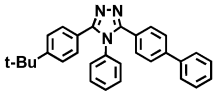

163 (TAZ)

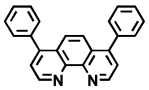

164 (BPhen)

Chart 19. Electron-Transporting Materials with a Benzene or Triazine Central Core

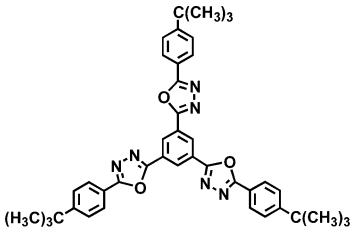

165 (TPOB)

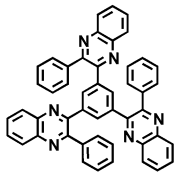

166 (TPQ)

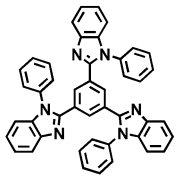

167 (TPBI)

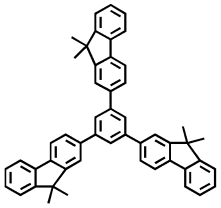

168 (TFB)

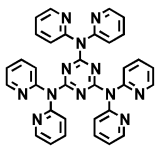

169

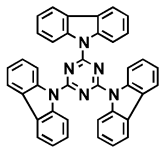

170 (TRZ2)

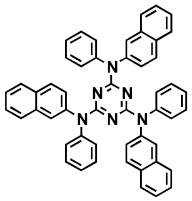

171 (TRZ3)

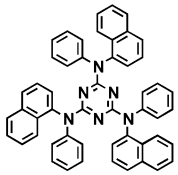

172 (TRZ4)

They have been prepared by the Ullmann coupling reation of 1,3,5-tris(4-bromophenyl)benzene or 2,4,6-tris(4-bromophenyl)-1,3,5-triazine with di(2-pyridyl)amine in the presence of potassium carbonate and copper sulfate.[123]

5.1.2.5. Compounds with a Tetraphenylmethane Central Core. Electron-transporting amorphous molecular materials with four 1,3,4-oxadiazolyl groups attached to the tetraphenylmethane central core, OMEOXD (**180**), CF_3OXD (**181**), and TBUOXD (**182**),[234] have been developed (Chart 21).

5.1.2.6. π-Electron Systems End-Capped with a Dimesitylboryl Group. Boron-containing oligothiophenes such as 2,5-bis(dimesitylboryl)thiophene (BMB-1T (**183**)), 5,5′-bis(dimesitylboryl)-2,2′-bithiophene (BMB-2T (**184**)), and 5,5″-bis(dimesitylboryl)-2,2′:5′,2″-terthiophene (BMB-3T (**185**)) have been synthesized. BMB-2T and -3T undergo reversible cathodic reductions, exhibiting two sequential cathodic and the corresponding anodic waves to generate the radical anion and dianion species.[63] They have also been characterized by UPS.[115,235] BMB-nT ($n = 1$, 2, and 3) have

Chart 20. Electron-Transporting Materials: Compounds with a 1,3,5-Triphenylbenzene or 2,4,6-Triphenyltriazine Central Core

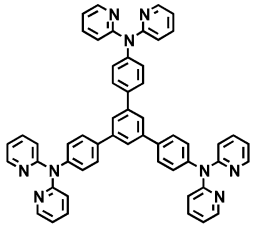

44

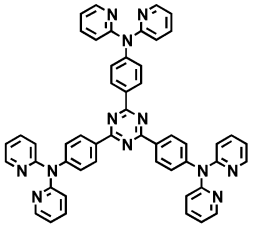

45

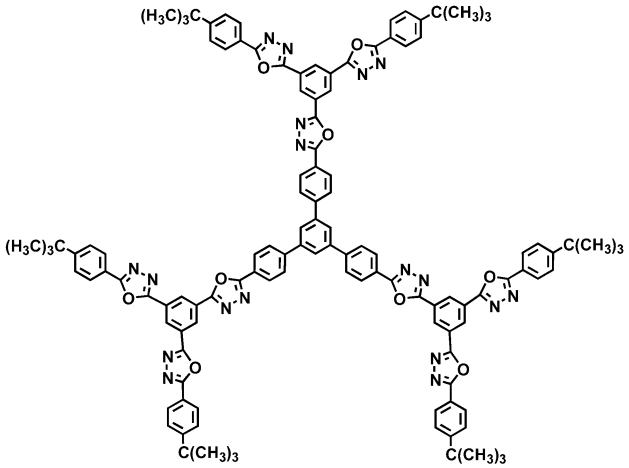

173

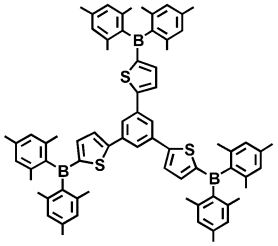

174 (TMB-TB)

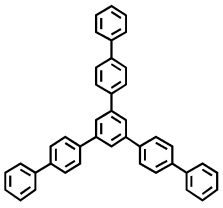

175 (TBB)

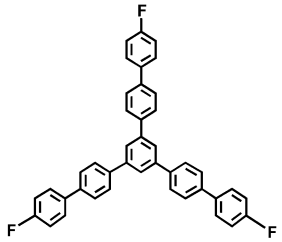

176 (F-TBB)

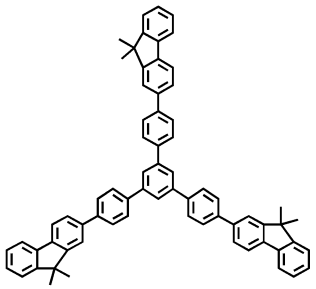

177 (TFPB)

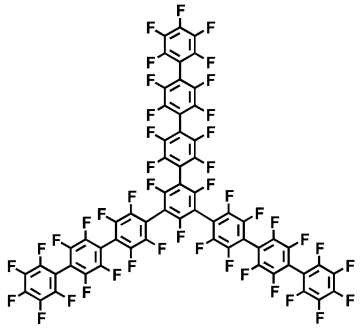

178 (CF-Y)

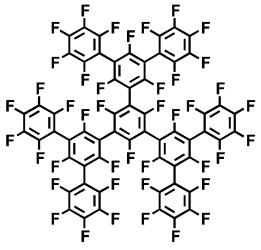

179

stronger electron-accepting properties than those of Alq_3.[63,115,235] Electron-transporting BMB-2T emits intense blue emission.[110] It also functions as a host matrix for emitters.[236] The compound **186** is also an electron-transporting emitter, and bright white light emission has been obtained from a single layer of its spin-coated film.[237] The structures of these compounds are shown in Chart 22.

5.1.2.7. Triarylboranes. The compounds of a triarylborane family, tris(2,3,5,6-tetramethylphenyl)borane (TPhB (**187**)), tris(2,3,5,6-tetramethylbiphenyl-4-yl)borane (TBPhB (**188**)), tris(2,3,5.6-tetramethyl-1,1′:4′,1″-terphenyl-4-yl)borane (TTPhB (**189**)), and tris[2,3,5,6-tetramethyl-4-(1,1′:3′,1″-terphenyl-5′-yl)phenyl]borane (TTPhPhB (**190**)), have been developed and used as hole-blocking materials in combination with Alq_3 as an electron transporter[238] (Chart 23).

5.1.2.8. Silole Derivatives. Silacyclopentadiene derivatives have constituted an important class of electron-transporting materials, which include 2,5-di(2-pyridyl)-1,1-dimethyl-3,4-diphenylsilacyclopentadiene (PySPy (**191**)),[239,240] 2,5-di-(biphenyl-3-yl)-1,1-dimethyl-3,4-diphenylsilacyclopentadiene (PPSPP (**192**)),[241,242] 2,5-bis(6-phenylpyridin-2-yl)-1,1-dimethyl-3,4-diphenylsilacyclopentadiene (PPySPyP (**193**)),[240]

Chart 21. Electron-Transporting Materials: Compounds with a Tetraphenylmethane Central Core

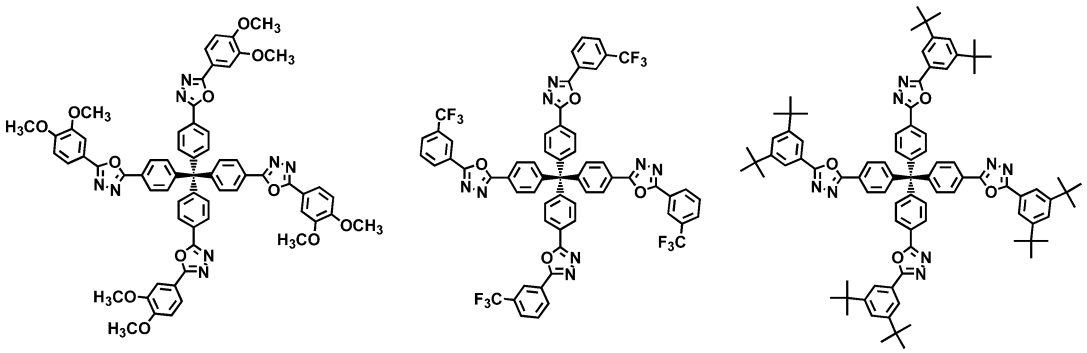

180 (OMEOXD) **181** (CF_3OXD) **182** (TBUOXD)

Chart 22. Electron-Transporting Materials: π-Electron Systems End-Capped with Two Dimesitylboryl Groups

183 (BMB-1T) : n=1
184 (BMB-2T) : n=2
185 (BMB-3T) : n=3

186

2,5-bis[3-(2-pyridyl)phenyl]-1,1-dimethyl-3,4-diphenylsilacyclopentadiene (PyPSPPy (**194**)),[240] 2,5-bis(2,2′-bipyridin-6-yl)-1,1-dimethyl-3,4-diphenylsilacyclopentadiene (PyPySPyPy (**195**)),[240−243] and 9-silafluorene-9-spiro-1′-(2′,3′,4′,5′-tetraphenyl)-1′*H*-silacyclopentadiene (ASP (**196**)).[242] They also function as good emitters. PyPySPyPy has been characterized by UPS.[244−246] Molecular orbital calculations has been performed on **191**, **192**, and **195**.[247] The structures of these compounds are shown in Chart 24.

5.1.2.9. X-Shaped Compounds with a 1,2,4,5-Tetraphenylbenzene Core. X-Branched oligophenylenes, **197**−**202**, have been synthesized by the palladium-catalyzed Suzuki cross-coupling reaction of 1,2,4,5-tetrakis(*p*-iodophenyl)benzene with the corresponding phenylboronic acid. The HOMO and LUMO energy levels of these X-branched oligophenylenes were estimated to be in the range of 5.9−6.5 and 2.4−3.3 eV, respectively.[248] These compounds have been used as hole-blocking materials for obtaining blue emission. Like BMB-nT, 2,3,5,6-tetra(2-pyridyl)pyrazine (TPP (**203**)) serves as an electron injection material in OLEDs.[249] The structures of these compounds are shown in Chart 25.

5.1.2.10. Spiro Compounds and Others. Electron-transporting amorphous molecular materials with a spiro center, **204**−**207**, have been reported (Chart 26).[210,218,250,251] TBPSF (**204**) functions as an emitter.

The Tg's, reduction potentials, solid-state ionization potentials, and electron affinities of electron-transporting amorphous molecular materials shown in Charts 18−26 are listed in Table 3.

5.1.3. Ambipolar Charge-Transporting Materials

As will be discussed in sections 5.3 and 6, charge-transporting materials are suggested to have the properties of ambipolar transport in nature so long as they accept both hole and electron carriers. Generally, hole- and electron-transporting materials readily accept holes and electrons, respectively, but do not readily accept electrons and holes, respectively. However, molecules containing both the electron-donating and -accepting moieties exhibit ambipolar character, readily accepting both holes and electrons. These materials usually function as materials for the emitting layer in OLEDs. Since the emitting layer in OLEDs acts as the recombination center for holes and electrons injected from the anode and cathode, respectively, materials for use in the emitting layer should accept both hole and electron carriers, and transport them. That is, the emitting materials should have bipolar character, permitting the formation of both stable cation and anion radicals. The emitting materials should have high luminescence quantum efficiencies. In addition to these requirements, they should be capable of forming smooth, uniform thin films with thermal and morphological stability. The use of emitting materials that fulfill these requirements is expected to lead to enhanced performance and improved durability of devices.

BMA-nT (**21**−**24**)[60−62,181,252] and BFA-nT (**102**, **103**)[182] in Chart 11 have ambipolar character and function as good emitters in OLEDs. These compounds undergo reversible anodic oxidations and cathodic reductions. The central oligothiophenes in BMA-nT are thought to play a role in electron acceptance. The HOMO energy levels of BMA-nT (n = 1∼4) were almost the same regardless of the conjugation length of oligothiophene, as determined by cyclic voltammetry and UPS.[115] The π-conjugation length of oligothiophenes mainly affected the LUMO energy levels, tuning the emission color from blue to green, yellow, and orange.

Chart 23. Electron-Transporting Materials: Triarylboranes

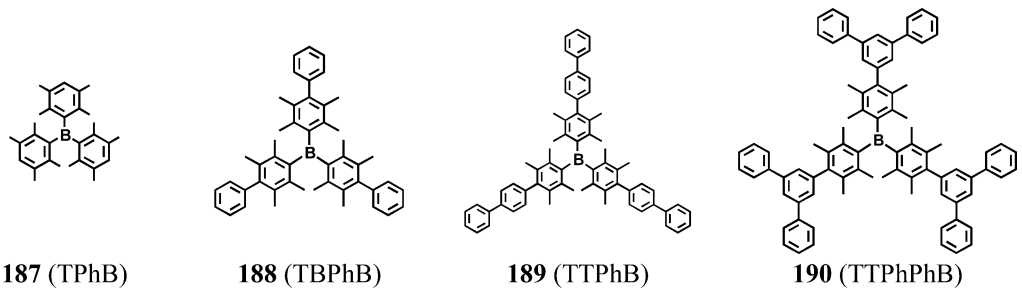

187 (TPhB) **188** (TBPhB) **189** (TTPhB) **190** (TTPhPhB)

Chart 24. Electron-Transporting Materials: Silole Derivatives

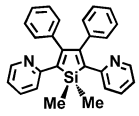

191 (PySPy)

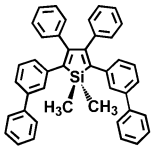

192 (PPSPP)

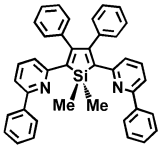

193 (PPySPyP)

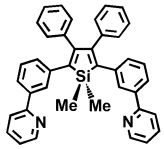

194 (PyPSPPy)

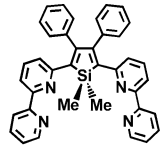

195 (PyPySPyPy)

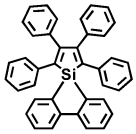

196 (ASP)

2,6-Bis{4-[*N*,*N*-bis(9,9-dimethylfluoren-2-yl)amino]-phenyl}pyridine (BFA-Py (**208**)),[253] 4,7-bis{4-[bis(9,9-dimethylfluoren-2-yl)amino]phenyl}-2,1,3-benzothiadiazole (BFA-BT (**209**)),[1d,253] 9,10-bis{4-[*N*,*N*-bis(9,9-dimethylfluoren-2-yl)amino]phenyl}anthracene (BFA-An (**210**)),[1d,253] and α-{4-[bis(9,9-dimethylfluoren-2-yl)amino]phenyl}-*ω*-(dimesitylboryl)oligothiophenes (FlAMB-nT (**211**−**214**))[254,255] have also provided definite examples of ambipolar emitting materials that meet all the requirements described above. All these compounds were found to readily form stable amorphous glasses with well-defined Tg's, as characterized by DSC, XRD, and IR and Raman spectroscopy.[256,257] They exhibited intense fluorescence with relatively high fluorescence quantum yields. They undergo both reversible anodic oxidations and cathodic reductions to permit the formation of stable cation and anion radicals. The results of cyclic voltammetry of the FlAMB-nT ($n = 0 \sim 3$) family showed that the oxidation potentials gradually decreased and the reduction potentials became increasingly more positive with the increasing conjugation length of the central thiophene unit. The π-conjugation length of the central oligothiophenes finely control the HOMO and LUMO energy gap and hence the emission color. The HOMO and LUMO energy levels of the BFA family greatly depended on the kinds of the central π-electron system. The emission color of the materials of the BFA family changed from blue to red, depending upon the kind of the central π-electron system.

The compounds, AODF (**216**)[258] and CzOxa (**217**),[259] are examples of materials containing an electron-withdrawing 1,3,4-oxadiazole group and an electron-donating dimethylamino or *N*-phenylcarbazolyl group. Bis(4-(*N*-(1-naphthyl)-phenylamino)phenyl)fumaronitrile (NPAFN (**218**))[260] and *N*-methyl-bis{4-[*N*-(1-naphthyl)-*N*-phenylamino]phenyl}-maleimide (NPAMLMe (**219**))[261] with electron donor−acceptor moieties provide the examples of red-emitting amorphous molecular materials. Emissive donor−acceptor molecules based on phenoxazine and quinoline as donor and acceptor moieties, 10-methyl-3,7-bis(4-phenylquinolin-2-yl)-

Chart 25. Electron-Transporting Materials: Compounds with a 1,2,4,5-Tetraphenylbenzene Core

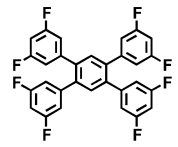

197 (X-OPP(3)-F_2)

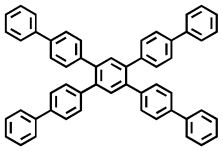

198 (X-OPP(5)-H)

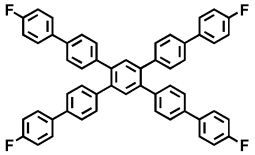

199 (X-OPP(5)-F_1)

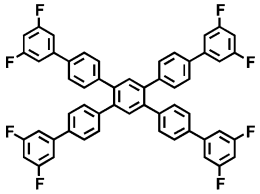

200 (X-OPP(5)-F_2)

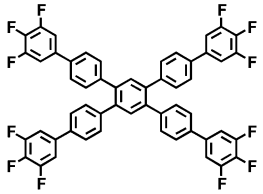

201 (X-OPP(5)-F_3)

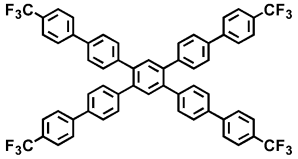

202 (X-OPP(5)-CF_3)

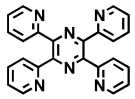

203

Chart 26. Electron-Transporting Materials: Spiro Compounds

204 (spiro-PBD)

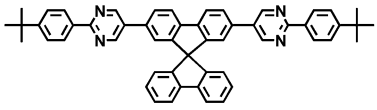

205 (TBPSF)

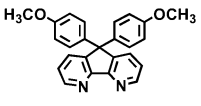

206

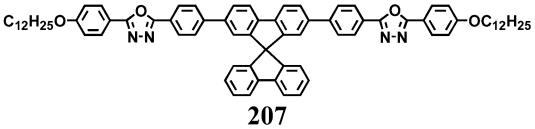

207

Table 3. Glass-Transition Temperatures (Tg's), Reduction Potentials, Ionization Potentials (IPs), and Electron Affinities (EAs) of Electron-Transporting Amorphous Molecular Materials

compound	Tg (°C)	reduction potential	IP (eV)	EA (eV)	ref
		Alq_3, 2,5-Diaryl-1,3,4-oxadiazoles, and Triazoles			
156 (Alq_3)[a,c]			5.8	3.1	111
			5.93		202
			6.1	3.4	204
			5.7		205
			5.8	3.1	206
			5.65		48
159 (*t*-Bu-PBD)[a]			6.3	2.4	47
160 (OXD-7)[a]			~6.5	~2.8	31
		Electron-Transporting Materials with a Central Benzene Core			
40	80		5.09	1.64	123
165 (TPOB)	142				224
	137				133
166 (TPQ)	151				226
167 (TPBI)			6.2	2.7	227
168 (TFB)[c]	133				228
169[a]			5.07	1.35	123
170 (TRZ2)			6.0	2.6	229
171 (TRZ3)			5.8	2.3	229
172 (TRZ4)	113		5.8	2.2	229
		Compounds with a 1,3,5-Triphenylbenzene Central Core			
173	248				230
174 (TMB-TB)	160	−1.98 V vs Ag/Ag^+ (0.01 mol dm^{-3}) in THF			231
175 (TBB)[c]	88				228
176 (F-TBB)[c]	87				228
177 (TFPB)[c]	149				228
178 (CF-Y)	135	−2.24 V vs Fc/Fc^+			233
179	125	−2.56 V vs Fc/Fc^+			233
		Compounds with a Tetraphenylmethane Central Core			
180 (OMEOXD)	97	~ −2.50 V vs Fc/Fc^+			234
181 (CF_3OXD)	125	−2.30 V vs Fc/Fc^+			234
182 (TBUOXD)	175	−2.40 ~ −2.45 V vs Fc/Fc^+			234
		π-Electron Systems End-Capped with Dimesitylboryl Groups			
183 (BMB-1T)	71		6.81	3.61	115
184 (BMB-2T)	107	−1.76 V vs Ag/Ag^+ (0.01 mol dm^{-3}) in THF			63
	107		6.25	3.45	115
185 (BMB-3T)	115	−1.76 V vs Ag/Ag^+ (0.01mol dm^{-3}) in THF			63
	115		5.85	3.25	115
		Compounds with a Triarylborane Central Core			
187 (TPhB)	63	−2.5 V vs Ag/Ag^+ (0.01 mol dm^{-3}) in THF	6.1	2.6	238
188 (TBPhB)	127	−2.5 V vs Ag/Ag^+ (0.01 mol dm^{-3}) in THF	6.1	2.6	238
189 (TTBPhB)	163	−2.5 V vs Ag/Ag^+ (0.01 mol dm^{-3}) in THF	6.1	2.6	238
190 (TTPhPhB)	183	−2.5 V vs Ag/Ag^+ (0.01 mol dm^{-3}) in THF	6.1	2.6	238
		Silole Derivatives			
191 (PySPy)[a]					240
192 (PPSPP)			~5.9	~3.1	241, 242
193 (PPySPyP)	81				240
194 (PyPSPPy)	81				240
195 (PyPySPyPy)	77				240
			~5.9	~3.2	242
		X-Shaped Compounds with a 1,2,4,5-Tetraphenylbenzene Core			
197 (X-OPP(3)-F_2)	—[b]		6.20	3.27	248
198 (X-OPP(5)-H)	—[b]		5.90	2.40	248
199 (X-OPP(5)-F_1)	—[b]		6.48	2.87	248
200 (X-OPP(5)-F_2)	—[b]		6.47	2.93	248
201 (X-OPP(5)-F_3)	—[b]		6.50	2.96	248
202 (X-OPP(5)-CF_3)	—[b]		6.40	2.87	248
203 (TPP)			>6.8		249
		Spiro Compounds and Others			
204 (spiro-PBD)	163	−2.46 V vs Fc/Fc^+ in THF			210
205 (TBPSF)	195		~ 6.1	~ 3	250
206		−2.48 V vs Fc/Fc^+ in DMF			251
207			5.64	2.04	218

[a] These compounds do not form amorphous glasses. [b] These compounds do not show glass transition phenomena, but form smooth films. [c] Oxidation potentials of these compounds are as follows: Alq_3 (0.75 V vs Fc/Fc^+ in DMF),[48] TFB (1.25 V vs Ag/Ag^+ (0.01 mol dm^{-3}) in CH_2Cl_2),[228] TBB (1.32 V vs Ag/Ag^+ (0.01 mol dm^{-3}) in CH_2Cl_2),[228] F-TBB (1.29 V vs Ag/Ag^+ (0.01 mol dm^{-3}) in CH_2Cl_2),[228] and TFPB (1.25 V vs Ag/Ag^+ (0.01 mol dm^{-3}) in CH_2Cl_2).[228]

10*H*-phenoxazine (BPQ-MPO (**220**)) and 10-phenyl-3,7-bis-(4-phenylquinolin-2-yl)-10*H*-phenoxazine (BPQ-PPO (**221**)), have also been synthesized.[262] Single-layer OLEDs have been developed using ambipolar materials, such as a dibenzothiophene *S*,*S*-dioxide derivative containing a diphenylaminophenyl group (**222**)[263] and a boron-containing com-

Chart 27. Compounds Containing Electron-Donating and Electron-Accepting Moieties

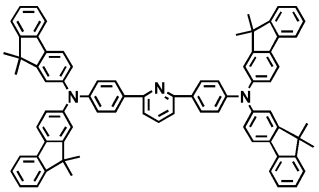

208 (BFA-Py)

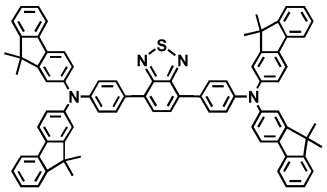

209 (BFA-BT)

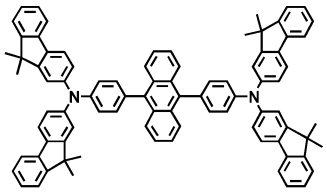

210 (BFA-An)

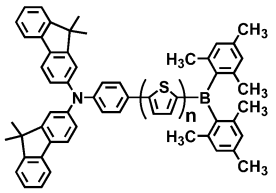

211 (FlAMB-0T) : n=0
212 (FlAMB-1T) : n=1
213 (FlAMB-2T) : n=2
214 (FlAMB-3T) : n=3

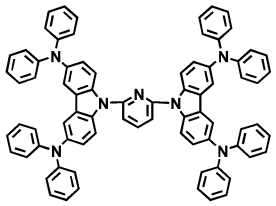

215

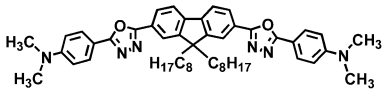

216 (AODF)

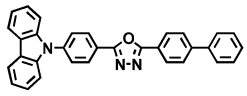

217 (CzOxa)

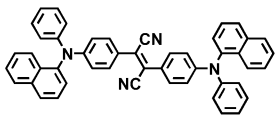

218 (NPAFN)

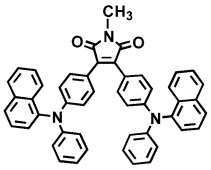

219 (NPAMLMe)

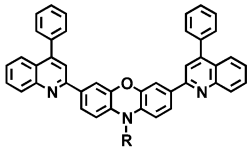

220 (BPQ-MPO) : R = CH_3
221 (BPQ-PPO) : R = Ph

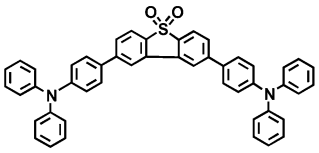

222

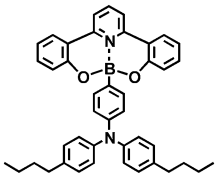

223 ((dppy)BTPA)

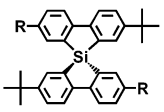

224 : R = Ph
225 : R = 2-pyridyl
226 : R = biphenyl-4-yl
227 : R = 2,2'-pyridin-6-yl

pound containing hole-transporting, electron-transporting, and emitting components ((dppy)BTPA (**223**)).[264] A novel class of amorphous molecular materials, spirosilabifluorenes, **224**−**227**, forms transparent and stable amorphous glasses with high Tg's above 200 °C. The electronic absorption spectra of these compounds show a significant bathochromic shift relative to those of the corresponding carbon analogues as a result of $\sigma^*-\pi^*$ conjugation. They exhibit violet-blue emission peaking at 398∼415 nm.[265]

In phosphorescence-based OLEDs, charge-transporting materials with large optical band gaps, such as CBP (**91**),[29,154,176−180] TCTA (**33**),[154] and compound **72**,[160] have been used as host materials for phosphorescent dopants. The host material in the emitting layer serves as a recombination center for holes and electrons to generate the electronically excited states, followed by both singlet−singlet and triplet−triplet excitation energy transfer from the host to the dopant, and hence, host materials possess ambipolar transport properties.

The molecular structures of ambipolar charge-transporting materials are shown in Chart 27, and the Tg's, oxidation and reduction potentials, solid-state ionization potentials, and

Table 4. Glass-Transition Temperatures (Tg's), Oxidation and Reduction Potentials, Ionization Potentials (IPs), and Electron Affinities (EAs) of Ambipolar Charge-Transporting Amorphous Molecular Materials

compound	Tg (°C)	oxidation potential	reduction potential	IP (eV)	EA (eV)	ref
Compounds Containing Electron-Donating and Electron-Accepting Moieties						
208 (BFA-Py)	173	0.57 V vs $Ag/AgNO_3$ (0.01 mol dm^{-3}) in CH_2Cl_2	−2.61 V vs $Ag/AgNO_3$ (0.01 mol dm^{-3}) in THF			253
209 (BFA-BT)	145	0.56 V vs $Ag/AgNO_3$ (0.01 mol dm^{-3}) in THF	−1.72 V vs $Ag/AgNO_3$ (0.01 mol dm^{-3}) in THF			253
210 (BFA-An)	185	0.56 V vs $Ag/AgNO_3$ (0.01 mol dm^{-3}) in CH_2Cl_2	−2.26 V vs $Ag/AgNO_3$ (0.01 mol dm^{-3}) in THF			253
211 (FlAMB-0T)	129	0.36 V vs Fc/Fc^+ in CH_2Cl_2	−2.51 V vs Fc/Fc^+ in THF			255
212 (FlAMB-1T)	124	0.31 V vs Fc/Fc^+ in CH_2Cl_2	−2.17 V vs Fc/Fc^+ in THF			255
213 (FlAMB-2T)	127	0.28 V vs Fc/Fc^+ in CH_2Cl_2	−2.11 V vs Fc/Fc^+ in THF			255
214 (FlAMB-3T)	131	0.27 V vs Fc/Fc^+ in CH_2Cl_2	−2.03 V vs Fc/Fc^+ in THF			255
215	157	0.592 V vs Fc/Fc^+ in CH_2Cl_2		5.07	2.18	158
217 (CzOxa)				6.22	3.13	259
218 (NPAFN)	109					260
219 (NPAMLMe)	120			5.8	3.7 ∼ 3.8	261
220 (BPQ-MPO)	137	0.71 V vs SCE in C_6H_6/CH_3CN	−2.02 V vs SCE in C_6H_6/CH_3CN	5.1	2.4	262
221 (BPQ-PPO)	149	0.79 V vs SCE in C_6H_6/CH_3CN	−2.00 V vs SCE in C_6H_6/CH_3CN	5.2	2.4	262
222	123	0.553 V vs Fc/Fc+ in CH_2Cl_2/DMF	−1.935 V vs Fc/Fc+ in CH_2Cl_2/DMF	5.35	2.61	263
223 ((dppy)BTPA)				5.3	2.9	264
224	203	1.09 V vs Ag/AgCl (0.01 mol dm^{-3}) in CH_3CN:THF		5.79		265
225	203	1.17 V vs Ag/AgCl (0.01 mol dm^{-3}) in CH_3CN:THF	−2.24 V vs Ag/AgCl (0.01 mol dm^{-3}) in CH_3CN:THF	5.87	2.46	265
226	228	1.11 V vs Ag/AgCl (0.01 mol dm^{-3}) in CH_3CN:THF	−2.42 V vs Ag/AgCl (0.01 mol dm^{-3}) in CH_3CN:THF	5.81	2.28	265

electron affinities of ambipolar charge-transporting amorphous molecular materials are summarized in Table 4.

5.1.4. Interactions at the Interface between the Hole-Transport Layer and the Electron-Transport Layer

Electron donor−acceptor interactions between hole- and electron-transporting layers in multilayer OLEDs sometimes lead to the formation of exciplexes at the solid interface between organic/organic layers. Since amorphous molecular materials form homogeneous thin films without any grain boundaries, they are suitable for studying solid-state exciplex formation.

The direct contact between the hole-transporting materials of the TDATA family and electron-transporting emitter Alq_3 results in the formation of exciplexes at the interface.[266,267] OLEDs consisting of the two layers of *m*-MTDATA or 2-TNATA and Alq_3 emit yellow light at low drive voltages and green light at high drive voltages. While the green emission originates from Alq_3, the yellow emission results from the contribution of the exciplex emission. Thus, the two emission colors can be reversibly switched by varying the drive voltage.[266] Exciplex formation in OLEDs has been observed for a number of combinations of hole- and electron-transporting amorphous molecular materials.[225,241,259,268−270]

The intensity of the exciplex emission is usually lower than that of the single component emission. From the viewpoint of the EL efficiency, formation of exciplexes should be avoided, and hence, attention has been directed to avoid exciplex formation in organic EL devices. The exciplex formation can be prevented by the insertion of a thin layer of a suitable material between the two layers that form an exciplex.[110,270] The other way is to use the material as a dopant.[271]

On the other hand, the utilization of intense exciplex emission is one approach for obtaining desired emission color.[259,269] Highly efficient exciplex emission has been observed from OLEDs based on hole-transporting α-NPD or TPD and electron-transporting silole derivatives, PPSPP or PyPySPyPy.[241] A luminance of 100 cd m^{-2} has been obtained at a drive voltage of 4.5 V, and an EL quantum efficiency of 3.4% has been achieved at 100 A m^{-2} for the combination of PPSPP and α-NPD.[241] Exciplexes have also been exploited to tune the emission color[225,266,268] and to obtain white light.[272−276]

Chart 28. Emitting Materials Described in Section 5.1.5.

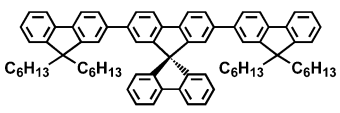

228 (THPF)

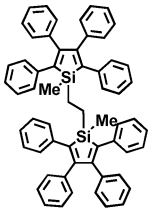

229 (2PSP)

5.1.5. Device Structures and Performance

Multilayer OLEDs using Alq_3 with or without emissive dopants as an emitting layer and various kinds of charge-transporting materials as charge-transport layers have been fabricated, and their performance has been examined. Typical device structures are as follows: ITO/HTL/Alq_3/metal and ITO/HTL1/HTL2/Alq_3/metal. An alloy of magnesium and silver or aluminum is often employed as the cathode. When aluminum is used as the cathode, a very thin layer (<1 nm) of lithium fluoride (LiF) is inserted between the cathode and the electron-transport layer to facilitate electron injection from the Al cathode.[277]

Multilayer OLEDs consisting of an emitting layer of Alq_3, a hole-injection layer (HTL1) of *m*-MTDATA, and a hole-transport layer (HTL2) of TPD or α-NPD exhibited higher luminous efficiency and significantly enhanced operational stability than those of the corresponding double-layer devices without the hole-injection layer (HTL1).[111,133−135] The increase in the electrical conductivity of a hole-injection buffer layer material *m*-MTDATA by doping with iodine or 2,3,5,6-tetrafluoro-7,7,8,8-tetracyanoquinodimethane (F_4TCNQ) has been shown to lead to significant reductions of drive voltage and the enhancement of external quantum efficiency for Alq_3-based OLEDs relative to the corresponding device using the

Table 5. Examples of Performance of OLEDs

device	color wavelength chromaticity	turn-on voltage (V)	maximum luminance (cd m^{-2})	power efficiency (lm W^{-1})	current efficiency (cd A^{-1})	external quantum efficiency (%)	ref
			Non-Doped Systems				
ITO/*m*-MTDATA (40 nm)/ TPD (20 nm)/TTPhPhB (10 nm)/Alq_3 (30 nm)/LiF (0.5 nm)/Al	blue-violet 404 nm -	3.4	2600 (11 V)	0.33 (300 cd m^{-2})	0.71 (300 cd m^{-2})	1.5 (300 cd m^{-2})	238
ITO/TCTA (40 nm)/THPF (40 nm)/BCP (10 nm)/Alq_3 (20 nm)/ LiF/Al	blue 404, 424 nm (0.18, 0.09)				1.27	1.8	282
ITO/spiro-TAD (40 nm)/ spiro-PBD (40 nm)/Al:Mg	blue - -	2.7	500 (5 V)				116
ITO/PEDOT:PSS (30 nm)/ PF6 (40 nm)/BCP (10 nm)/ Alq_3 (50 nm)/LiF (0.5 nm)/Al (150 nm)	blue - -	∼2.4	18500 (13.5 V)	0.75	1.4	0.9	200
ITO/PEDOT:PSS/TCTA (40 nm)/T3 (30 nm)/TPBI (30 nm)/LiF/Al	blue - (0.158, 0.041)	∼2.5	∼14000		1.53	5.3	153
ITO/*m*-MTDATA (40 nm)/ α-NPD (20 nm)/TTPhPhB (10 nm)/Alq_3 (30 nm)/LiF (0.5 nm)/Al	blue 444 nm -	3.2	9100 (11 V)	1.0 (300 cd m^{-2})	2.0 (300 cd m^{-2})	2.5 (300 cd m^{-2})	238
ITO/α-NPD (50 nm)/PPSPP (50 nm) /PyPySPyPy (10 nm)/MgAg (100 nm)	- 495 nm -		7325 (12 V)			3.4 (100 A m^{-2} 1000 cd m^{-2})	241
ITO/TPD (50 nm)/2PSP (20 nm)/PyPySPyPy (30 nm)/ MgAg (100 nm)	blue-green 500 nm -	2.5	1400 (6.5 V, 15 mA cm^{-2})	12 (10 cd m^{-2}, 3.25 V)		4.8 (0.01∼1mA cm^{-2})	289
ITO/**222** (80 nm)/LiF (1 nm)/ Al (150 nm)	- 496 nm (0.16, 0.44)	2.2	37699 (at 12.5 V)	7.2 (maximum)	7.7 (maximum)	3.1 (maximum)	263
ITO/TAPC (75 nm)/Alq_3 (60 nm)/MgAg	green 550 nm -	2.5	>1000 (less than 10 V)				25
ITO/*m*-MTDATA (60 nm)/ TPD (10 nm)/Alq_3 (50 nm)/ MgAg	green - -		24000 (at 15V)	2.3			111
ITO/2-TNATA (46 nm)/TPD (7 nm)/Alq_3 (57 nm)/MgAg	green - -	5.5	22200 (14 V)	2.5 (300 cd m^{-2})			133
ITO/TECEB (70 nm)/Alq_3 (60 nm)/MgAg	green 530 nm -	3.5	9680 (20 V)		3.27 (230 mA cm^{-2})		157
ITO/TX-F6S (60 nm)/Alq_3 (60 nm)/LiF (0.5 nm)/Al (150 nm)	green 530 nm -	3	37000 (14 V)		3.4		197
ITO/HPCzI (70 nm)/Alq_3 (70 nm)/MgAg	green 532 nm -	3.8		1.25 (20 mA cm^{-2}, 8.8 V)	3.5 (20 mA cm^{-2}, 8.8 V)		198
ITO/**113** (40 nm)/Alq_3 (60 nm)/LiF/Al	green - -	3.2	15739 (16 V)	2.56	4.79		188
ITO/**113** (40 nm)/Alq_3 (40 nm)/MgAg (50 nm)	green 524 nm (0.31, 0.56)	3.4	27,341	1.8 (100 mA cm^{-2})		1.3 (100 mA cm^{-2})	158
ITO/**97** (40 nm)/Alq_3 (40 nm)/MgAg (50 nm)	green 518 nm (0.30, 0.55)	3.3	26,567	1.7 (100 mA cm^{-2})		1.0 (100 mA cm^{-2})	158
ITO/TDCTA (14 nm)/Alq_3 (60 nm)/LiF−Al alloy (12 nm)/Al (150 nm)	green - -				2.9∼3.4	0.6∼0.7	149
ITO/TPTE(S) (70 nm)/Alq_3 (70 nm)/MgAg (180 nm)	green 530 nm -	3.0 (0.1 cd m^{-2})	10000 (<1 A cm^{-2})	1.0 (100 cd m^{-2})		0.87 (100 cd m^{-2})	151
ITO/**62** (100 nm)/Alq_3 (40 nm)/Al	green - -	5.0					155
ITO/TPTE (70 nm)/Alq_3 (70 nm)/MgAg (180 nm)	- - -	3.1	11000 (14 V)				174
ITO/PEDOT:PSS/**146**/Alq_3/ LiF/Al	- 535 nm -	2.0	30400	3.6		1.5	199
ITO/TPD (50 nm)/Alq_3 (15 nm)/PySPy (35 nm)/MgAg	green 520 nm -		820 (5 V)	1.9 (100 cd m^{-2})			239
ITO/α-NPD (40 nm)/Alq_3 (5 nm)/CF_3OXD (40 nm)/MgAg	green 515 nm -	7∼8				0.75∼1 (8 V)	234
ITO/*m*-MTDATA (50 nm)/ FlAMB-1T (20 nm)/BMB-2T (20 nm)/Alq_3 (10 nm)/LiF (0.5 nm)/Al	green 509 nm (0.24, 0.61)		26900 (12.0 V)	3.1 (300 cd m^{-2})		2.0 (300 cd m^{-2})	255

Table 5 (Continued)

device	color wavelength chromaticity	turn-on voltage (V)	maximum luminance (cd m^{-2})	power efficiency (lm W^{-1})	current efficiency (cd A^{-1})	external quantum efficiency (%)	ref
			Non-Doped Systems				
ITO/PEDOT:PSS/TAPC (35 nm)/BPQ-PPO (45 nm)/LiF/Al	green 504 nm (0.20, 0.58)	3.0	9,510		3.42	1.10 at 6580 cd m^{-2}	262
ITO/*m*-MTDATA (20 nm)/PPA (40 nm)/TPBI (50 nm)/MgAg	green 518 nm (0.33, 0.59)	4.4	42915 (15.5 V)	5.54 (4.5 V)	10.60 (8.0 V)	2.93 (8.0 V)	184
ITO/*m*-MTDATA (20 nm)/α-NPA (40 nm)/TPBI (50 nm)/MgAg	green 522 nm (0.24, 0.69)	4.6	65129 (13.5 V)	5.12 (7.0 V)	12.05 (7.5 V)	3.07 (7.5 V)	184
ITO/**126** (40 nm)/TPBI (40 nm)/MgAg (50 nm)/Ag (100 nm)	green 530 nm -	5	38000 (13.5 V)	2.5 (5 V)		1.5 (5 V)	190
ITO/α-NPB (50 nm)/ASP (40∼50 nm)/PyPySPyPy (10∼20 nm)/MgAg	- 525 nm -		7000∼10000 (12 V)	5.2 (100 cd m^{-2})		3.8 (100 cd m^{-2})	242
ITO/(dppy)BTPA (100 nm)/LiF (1 nm)/Al (200 nm)	yellow - -	3.8	2,654	3.6 (maximum)	5.2 (maximum)		264
ITO/PEDOT:PSS/**186**/LiF/Al	white - (0.31, 0.42)		3,800			0.35	237
			Doped Systems (Fluorescence)				
ITO/1-TNATA (40 nm)/NPB (10 nm)/Alq_3+quinacridone (35 nm) /Alq_3 (35 nm)/MgAg	- - -			7.6 (100 mA cm^{-2}, 90 °C)		2.2 (10 mA cm^{-2})	145
ITO/BPAPF (60 nm)/Alq_3+quinacridone (0.5%) (20 nm)/Alq_3 (30 nm)/Al	- - -		140000 (15 V)	10.0 (3.5 V)	13.7 (5.5 V)	4.1 (5.5 V)	164
ITO/PEDOT:PSS/2a (40 nm)/Alq_3+quinacridone (0.5%) (20 nm)/Alq_3 (40 nm)/LiF (0.5 nm)/Al (150 nm)	- 542, 578 nm -	2.0	182800 (20 mA cm^{-2}, 18V)	10.1		2.8 (20 mA cm^{-2}, 18V)	199
			Doped Systems (Phosphorescence)				
ITO/α-NPD (40 nm)/CBP + 6% $Ir(ppy)_3$ (20 nm)/BCP (6 nm)/Alq3 (20 nm)/MgAg	green 510 nm (0.27, 0.63)		100,000	31	28	8	29
ITO/α-NPD (40 nm)/TCTA + 6.2 mol % $Ir(ppy)_3$ (20 nm)/CF-Y (20 nm)/Alq_3 (30 nm)/LiF (0.5 nm)/Al (150 nm)	- 511 nm -	2.4	6000∼12000 (10∼20 mA cm^{-2})	71.8 (2.8 V)	64.1 (2.8 V)	> 15	154
ITO/PEDOT:PSS (40 nm)/α-NPD (30 nm)/CBP + FIrpic (6 wt %) (20 nm)/BCP (3 nm)/CBP + $Btp_2Ir(acac)$ (10 nm)/BCP (40 nm)/LiF/Al	white - (0.35, 0.36)		30000 (13.4 V)	3.6	6.1	3.8	179

undoped hole-injection buffer layer.[278−280] The results show that the hole current dominates in these devices and that the use of doped *m*-MTDATA facilitates not only hole injection from the ITO electrode, but also electron injection from the cathode into Alq_3 probably due to the formation of a steeper electric field in the Alq_3 layer.[280]

Likewise, BMB-nT (**183**−**185**), TPP (**203**), and PySPy (**191**) function as an electron-injection layer that facilitates electron injection from the MgAg cathode into the Alq_3 layer. Multilayer OLEDs using BMB-2T or BMB-3T as an electron-transporting material, Alq_3 as an electron-transporting emissive material, and *m*-MTDATA and α-NPD as hole-transporting materials, ITO/*m*-MTDATA (30 nm)/α-NPD (20 nm)/Alq_3 (30 nm)/BMB-nT (n = 2 and 3) (20 nm)/MgAg, emitted bright green light originating from Alq_3, exhibiting approximately 1.1−1.2 times higher luminous and quantum efficiencies and 1.6−1.8 times higher maximum luminance than those of the corresponding OLED without the BMB-nT layer, ITO/*m*-MTDATA (30 nm)/α-NPD (20 nm)/Alq_3 (50 nm)/MgAg.[63] The comparison of the performance between two devices, ITO/TPD (50 nm)/Alq_3 (15 nm)/PySPy (**191**) (30 nm)/MgAg and ITO/TPD (50 nm)/Alq_3 (50 nm)/MgAg, showed that the use of PySPy (**191**) as the electron-injection layer resulted in ca. 1.3 times higher luminous efficiency.[239] A high current density of 100 mA cm^{-2} at less than 10 V and the external quantum efficiency of 1.0% have been obtained for a device using α-NPD as a hole-transport layer, Alq_3 as an electron-transporting emitting layer, and a thin layer (10 nm) of TPP (**203**) as an electron-injection layer sandwiched between ITO and MgAg electrodes, ITO/α-NPD (50 nm)/Alq_3 (50 nm)/TPP (10 nm)/MgAg.[249]

As was described earlier, various kinds of thermally stable charge-transporting amorphous molecular materials have been developed. In the 1990s, charge-transporting materials with Tg's over 130 °C have been created. The examples are provided by TCTA (**33**),[107] TPTTA (**34**),[92] Spiro-8Φ (**26**),[116] *t*-Bu-TBATA (**52**),[146] TPOTA (**54**),[148] **173**,[230] and so forth. In the 2000s, materials with Tg's above 200 °C have been created, as exemplified by B3 (**46**),[125] T3 (**47**),[125] **48**,[127] TDCTA (**55**),[149] TFATr (**76**),[1d] TTrTr (**77**),[1d] **224**∼**226**,[265] and so forth. The use of charge-transporting materials with high Tg's permitted the fabrication of thermally stable, Alq_3-based OLEDs.[107,133,145,146,281]

When materials other than Alq_3 have been used as an emitting layer, Alq_3 (**156**) and TPBI (**167**) have been used frequently as an electron-transport layer. OLEDs using BMA-

Chart 29. Representative Materials for OPVs

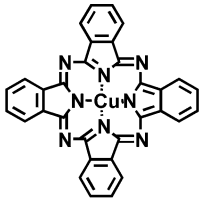

2 (CuPc)

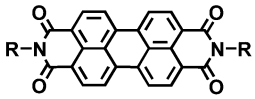

5

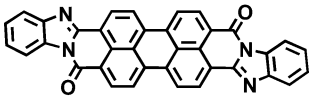

230 (PTCBI)

231

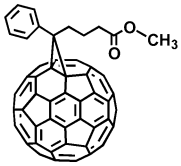

232 ([6,6]-PCBM)

nT and FlAMB-nT as emitters and Alq_3 as an electron transporter gave multicolor emission depending on the conjugation length of the central oligothiophene.[61,255] The compounds T3 (**47**) and THPF (**228**) emit intense blue fluorescence. An OLED, ITO/TCTA (**33**) (40 nm)/THPF (**228**) (40 nm)/BCP (10 nm)/Alq_3 (20 nm)/LiF/Al, has been reported to emit pure blue EL with chromaticity coordinates at (0.18, 0.09) and a maximum efficiency of 1.27 cd A^{-1}.[282] Some devices exhibit external EL quantum efficiencies close to or over the theoretical limit (5%) for a fluorescent emitter with a PL quantum yield close to unity. High-performance blue EL (external quantum efficiency of 5.3%, luminance of ~14 000 cd m^{-2}) has been reported for a device ITO/PEDOT:PSS/TCTA (**33**) (40 nm)/T3 (**47**) (30 nm)/TPBI (30 nm)/LiF/Al.[153] An OLED using β-NPA (**119**) as an emitter; ITO/*m*-MTDATA (20 nm)/β-NPA (40 nm)/TPBI (50 nm)/MgAg, has been reported to emit green light at 530 nm and exhibit high performance with a maximum external quantum efficiency of 3.68%, a current efficiency of 14.79 cd A^{-1}, a power efficiency of 7.76 lm W^{-1}, and a maximum brightness of 64 991 cd m^{-2}.[184] A double-layer device using hole-transporting emitter **126** and TPBI as an electron-transport layer emitted green light with a turn-on voltage of 5 V, and an external quantum efficiency of 1.5% at 5 V and a luminous efficiency of 2.5 lm W^{-1} at 5 V.[190]

An electron-transporting material with better hole-blocking ability than that of Alq_3, TPOB (**165**), enabled blue emission from BMA-1T in OLEDs.[62] The use of electron transporter with a better hole-blocking ability, TMB-TB (**174**), also permitted blue emission from *p*-TTA in OLEDs.[231] In case electron transporters do not function well as hole blockers, hole-blocking materials are inserted between the electron-transport layer and the emitting layer. Bathocuproine (BCP) has been reported to function as a hole-blocking material.[283] BCP has also been used as an exciton-blocking layer in OLEDs.[284] However, it forms exciplexes with a number of hole-transporting materials to give new emissions at longer wavelength regions.[285]

The compounds of the triarylbenzene family,[228,232] triarylboranes,[238] fluoro-substituted phenylene compounds, and X-shaped compounds with a 1,2,4,5-tetraphenylbenzene core,[248] have been shown to serve as effective hole-blocking materials. High-performance blue- and blue-violet-emitting organic EL devices have been developed by the use of these hole-blocking materials and TPD, *N*,*N*-bis(9,9-dimethylfluoren-2-yl)aniline (F_2PA), *p*-TTA, and α-NPD as blue-violet and blue emitters.[228,232,238] For example, a device, ITO/*m*-MTDATA (50 nm)/TPD (20 nm)/F-TBB (10 nm)/Alq_3 (20 nm)/MgAg, exhibited blue violet emission with a turn-on voltage of 4.0 V and an external quantum efficiency of 1.40%.[232] BMB-2T (**184**) with a larger ionization potential than that of Alq_3 has also been used as an effective hole-blocking material.[63] Tetraarylsilanes have been reported to function as effective hole-blocking materials or host materials for phosphorescent dopants.[286−288] 9,9′-Diaryl-4,5-diazafluorene has also been reported to act as a hole-blocking electron-transporting material.[251]

Some electron-transporting materials, for example, BMB-2T (**184**),[63] compound **186**,[237] silole derivatives,[242,289] and so forth, exhibit intense photoluminescence, serving also as emitting materials in OLEDs. It has been reported that a device, ITO/TPD (50 nm)/2PSP (20 nm)/PyPySPyPy (30 nm)/MgAg (100 nm), exhibits blue-green emission with an external EL quantum efficiency of 4.8%.[289]

Host materials for phosphorescent dopants in phosphorescence-based OLEDs usually function as the recombination center for holes and electrons. In some systems, phosphorescent dopants directly accept holes and electrons from the adjacent organic layer. A device using *m*-MTDATA as a hole injection buffer layer and CBP doped with *fac*-tris(2-phenylpyridine)iridium ($Ir(ppy_3)$) has been reported to exhibit peak external quantum and power efficiencies of 12.0 ± 0.6% and 45 ± 2 lm W^{-1}, respectively. It is shown that $Ir(ppy)_3$ directly accept holes from the *m*-MTDATA layer and that electrons are injected into and transported by the CBP layer. Thus, the $Ir(ppy)_3$:CBP layer exhibits ambipolar transport.[290]

There are a few reports stating that high performance of OLEDs stems from high charge carrier drift mobilities. A device using 2PSP (**229**) as an emitting layer, TPD (**86**) as a hole-transport layer, and PyPySPyPy (**195**) as an electron-transport layer emits blue-green light originating from 2PSP, exhibiting very high performance, as described above. A significant reduction of drive voltage for this device relative to the corresponding device using Alq_3 in place of PyPySPyPy, ITO/TPD/2PSP/Alq_3/MgAg, has been attributed to a higher mobility of PyPySPyPy relative to Alq_3.[289] An OLED consisting of α-NPD (**87**) as a hole-transport layer, PPSPP (**192**) as an emissive layer, and PyPySPyPy (**195**) as an electron-transport layer, ITO/α-NPD/PPSPP/PyPySPyPy/MgAg, exhibits efficient exciplex emission formed between α-NPD and PPSPP. A higher performance of this device than that of a device without the PyPySPyPy layer, ITO/α-NPD/PPSPP/MgAg, is attributed to a higher electron mobility of PyPySPyPy compared to that of PPSPP.[241] It has been

reported that doping of C_{60} in a hole-transport layer using TDAPB derivative (**72**) resulted in efficient hole injection and low drive voltage at high luminance for a phosphorescence-based OLED using CBP as a host material. The increase in the hole mobility from 1.0×10^{-4} cm^2 V^{-1} s^{-1} for the undoped TDAPB derivative to 5.1×10^{-4} cm^2 V^{-1} s^{-1} for the TDAPB derivative:C_{60} is responsible for the enhancement of performance.[291]

The performance of OLEDs depends on the combination of materials. Combinatorial fabrication of OLEDs has been

Chart 30. Reported Materials for OPVs

p-Type Organic Semiconductors

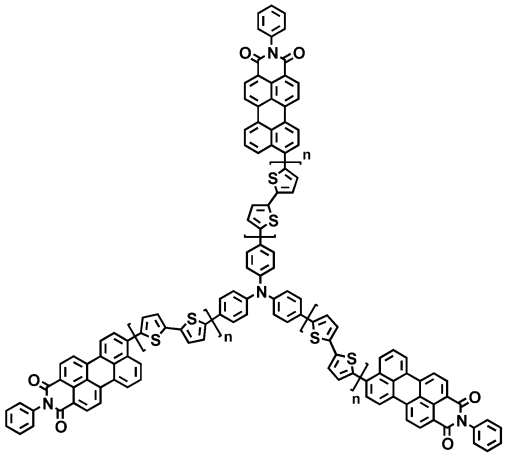

233

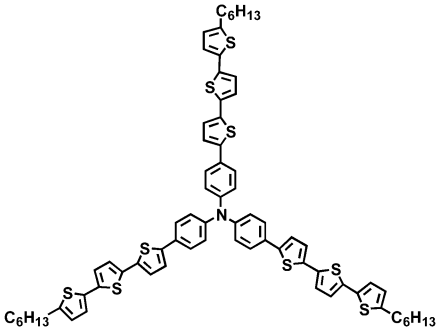

234

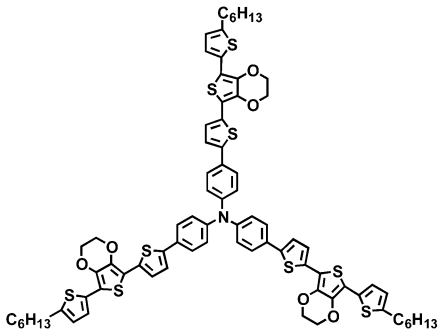

235

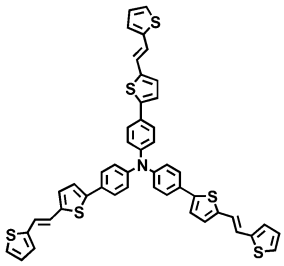

236

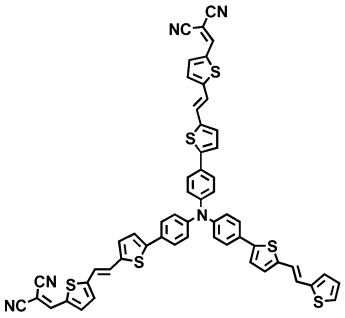

237

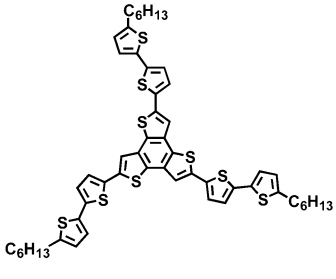

238

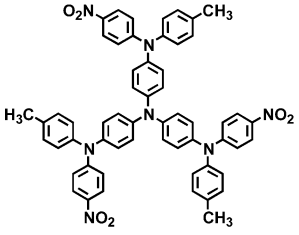

239 (MNTDATA)

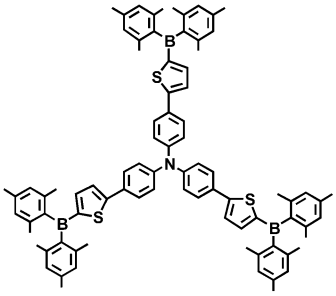

240 (MB-TTPA)

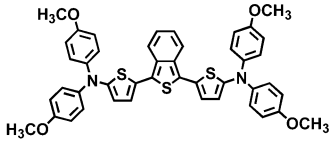

241

Chart 30. (Continued)

n-Type Organic Semiconductors

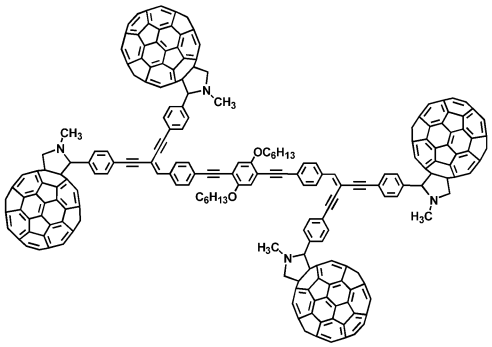

242

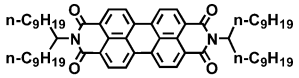

243 (PDI-C9)

Ambipolar Organic Semiconductor

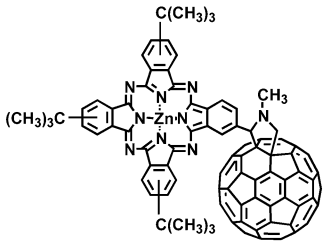

244

shown to be a powerful tool for screening materials and configurations, and for studying their basic properties.[292]

The molecular structures of emitting materials used for the fabrication of OLEDs described above, THPF (**228**)[282] and 2PSP (**229**),[242,289] are shown in Chart 28. Table 5 lists the performance of OLEDs.

5.2. Molecular Materials for Organic Photovoltaic Devices (OPVs)

OPVs have been a focus of considerable research in the last two decades because of their light weight, large-area, flexible device fabrication, potentially low cost, and the ease of materials design based on the molecular level. To develop high-performance OPVs, it is necessary to overcome several problems encountered with organic materials, such as small exciton diffusion lengths, low quantum yields for photogeneration of charge carriers, low charge carrier drift mobilities, and high bulk resistance. Early studies on OPVs afforded poor power conversion efficiencies, but significant improvements in the power conversion efficiency of OPVs have been achieved in the last several years by the use of suitable materials and the implementation of new device structures.[293] One is a *pn*-heterojunction structure consisting of the double layers of *p*-type and *n*-type organic semiconductors, that is, electron-donating and -accepting organic materials, sandwiched between two electrodes.[35] This device structure favors photogeneration of charge carriers by electron donor−acceptor interactions at the interface between *p*-type and *n*-type organic semiconductors. This concept has been extended to bulk *pn*-heterojunction structures, namely, the incorporation of a mixed layer of either electron-donating polymer and electron-accepting small molecule[294−296] or electron-donating and -accepting small molecules.[297−301] The enhancements of donor−acceptor interactions that result in the increase in charge carrier generation efficiencies and the formation of the transport paths for holes and electrons are important requirements for the attainment of high power conversion efficiencies. Therefore, morphology control to permit hole and electron transport is of essential importance in bulk *pn*-heterojunction devices.[302,303] Other strategies for increasing power conversion efficiencies include the insertion of an exciton-blocking layer to prevent exciton quenching at the metal cathode and at the same time to prevent damages of the photoactive layer caused by the evaporation of metal cathodes,[304,305] doping for reducing the bulk resistivities of materials,[306,307] and the introduction of tandem cell structures.[307−309] A tandem structure with a thin layer of silver inserted between the two *pn*-heterojunction cells, electrode/donor/acceptor/Ag/donor/acceptor/electrode, exhibits a doubled V_{OC} relative to the corresponding single *pn*-heterojunction cell.[308]

Both small organic molecules and polymers have been studied for use as photoactive materials in OPVs. As for small organic molecules, polycrystalline materials have been preferentially used in OPVs. Among small molecules, phthalocyanines, for example, CuPc (**2**), as *p*-type organic semiconductors, fullerenes, C_{60} (**231**) and [6,6]-PCBM (**232**),[294,310] and perylene tetracarboxylic diimides, for example, **5** and PTCBI (**230**), as *n*-type organic semiconductors, have been found to be most promising candidates for molecular materials for the fabrication of high-performance *pn*-heterojunction photovoltaic cells (Chart 29). BCP has been used as an exciton blocker in OPVs.[304,305]

Table 6. Glass-Transition Temperatures (Tg's), Oxidation and Reduction Potentials, Ionization Potentials (IPs), and Electron Affinities (EAs) of Crystalline and Amorphous Molecular Materials for OPVs

compound		Tg (°C)	oxidation potential	reduction potential	IP (eV)	EA (eV)	ref
2 (CuPc)			0.98 V vs SCE				325
			1.22 V vs NHE	−0.6 V vs NHE			326
					4.7		136
					5.0	3.3	204
					4.8		205
					5.2	3.6	206
					5.3	3.6	315
5 ($R = CH_3$)					6.8	4.6	327
					6.1		328
230 (PTCBI)					6.2	4.2	206
					6.2	4.5	308
231 (C_{60})					6.2	4.5	324
					6.2	4.5	315
					6.2	4.5	321
					6.38	3.78	329
					6.1	4.5	330
232 ([6,6]-PCBM)					6.1	3.7	331
239 (MNTDATA)		134	0.31 V vs Ag/Ag^+ (0.01 mol dm^{-3})				319
240 (MB-TTPA)		161	0.66 V vs Ag/Ag^+ (0.01 mol dm^{-3})				319
233	$n = 1$		0.29 V vs Fc/Fc^+ in CH_2Cl_2	−1.43 V vs Fc/Fc^+ in CH_2Cl_2			311
	$n = 2$		0.24 V vs Fc/Fc^+ in CH_2Cl_2	−1.44 V vs Fc/Fc^+ in CH_2Cl_2			
	$n = 3$		0.22 V vs Fc/Fc^+ in CH_2Cl_2	−1.43 V vs Fc/Fc^+ in CH_2Cl_2			
234			0.53 V vs Ag/AgCl in CH_2Cl_2				312
235			0.47 V vs Ag/AgCl in CH_2Cl_2				312
236			0.62 V vs Ag/AgCl in CH_2Cl_2				313
237			0.87 V vs Ag/AgCl in CH_2Cl_2	−1.25 V vs Ag/AgCl in CH_2Cl_2			313
238			0.93 V vs Ag/AgCl in CH_2Cl_2				314
242				−0.88 V vs Ag/Ag^+ in CH_3CN			332
243 (PDI-C9)		76		−1.11 V vs Fc/Fc^+ in CH_2Cl_2	5.82	3.69	333

Many other compounds have been developed for use in OPVs (Chart 30). One family of photoactive organic materials is *p*-TTA derivatives, for example, **233**−**237**.[311−313] A new π-conjugated system in which three linear oligothiophene chains are connected to a central planar and rigid trithienobenzene core (**238**) has also been synthesized (Chart 30).[314] The search for new materials that respond to near-IR wavelength light remains to be a subject of challenge.[315] A photovoltaic cell using amorphous TiOPc and a perylene pigment (PTCBI) as photoactive materials, ITO/PTCBI/TiOPc/Au, exhibited lower performance than that of the corresponding device using polycrystalline CuPc;[316] however, the cell using α-crystalline TiOPc obtained from the amorphous phase upon exposure to solvent vapor responded to near-IR light.[316]

Amorphous molecular materials have also been studied for materials in OPVs. A Schottkey-type device using *m*-MTDATA (**8**) sandwiched between the ITO and aluminum electrodes has been reported.[91] A bilayer device using *m*-MTDATA (**8**) as an electron donor and Alq_3 (**156**) as an electron acceptor showed both PV and EL properties.[317] It was found that PV performance was significantly enhanced for a trilayer device with a thin layer of a mixture of *m*-MTDATA and Alq_3 inserted between the two layers. It is shown that strong exciplex emission in an OLED is a good indicator of efficient charge transfer at the organic interface. *m*-MTDATA doped with F_4TCNQ has been used as a hole-transport layer in bulk heterojunction OPVs based on CuPc and ZnPc and C_{60} as *p*-type and *n*-type organic semiconductors.[309,318] As *m*-MTDATA responds only to near-UV light, photosensitivity is extended to visible light by the introduction of intramolecular charge transfer. 4,4′,4″-Tris[4-nitrophenyl(4-methylphenyl)amino]triphenylamine (MNTDATA (**239**)) and 4,4′,4″-tris[5-(dimesitylboryl)thiophen-2-yl]triphenylamine (MB-TTPA (**240**)) show electronic absorption bands extending to the wavelength of visible light.[319] The structural modification of BMA-nT (**21**−**24**) gives **241**, where the thiophene unit is replaced by an benzothiophene group.[320] The electronic absorption of this compound is expanded to the visible wavelength region. A high-performance *pn*-heterojunction device using α-NPD (**87**) and C_{60} (**231**), ITO/PEDOT:PSS (30 nm)/α-NPD (10 nm)/C_{60} (48 nm)/MgAg (170 nm), has recently been reported to exhibit a conversion efficiency of 1% under AM1.5 illumination at 97 mW cm^{-2}.[321]

At present, high-conversion efficiencies of 2.5∼5.0% under AM1.5 illumination have been attained for the cells using CuPc and C_{60}.[304,305,322] A power conversion efficiency of 5.0% has been reported for the device, ITO/CuPc (15 nm)/CuPc:C_{60} (10 nm) mixture/C_{60} (35 nm)/BCP (10 nm)/Ag (100 nm).[322] Polycyclic aromatic compounds such as tetracene and pentacene have also been reported to serve as *p*-type organic semiconductors for OPVs. *pn*-Heterojunction devices using tetracene and pentacene (**1**) as *p*-type semiconductors and C_{60} (**231**) as an *n*-type semiconductor, ITO/PEDOT:PSS/tetracene (80 nm)/C_{60} (30 nm)/BCP (8 nm)/Al (100 nm) and ITO/pentacene (45 nm)/C_{60} (50 nm)/BCP (10 nm)/Al, have been reported to exhibit power conversion efficiencies of 2.3 and 2.7% under AM1.5 illumination at 100 mW cm^{-2}, respectively.[323,324]

The Tg's, oxidation and reduction potentials, ionization potentials and electron affinities of materials for OPVs are listed in Table 6.[325−333] The performance of OPVs with various cell structures and molecular materials is summarized in Table 7.[334,335]

Hole-transporting amorphous molecular materials have been used in dye-sensitized, organic solar cells using nanocrystalline TiO_2 to transport hole carriers from the dye cation radical to the counter electrode instead of using the I^{3-}/I^- redox species.[195,336]

Table 7. Examples of Performance of OPVs[a]

device	light source	intensity of incident light (mW cm^{-2})	J_{sc} (mA cm^{-2})	V_{oc} (V)	FF	η (%)	ref
Planar *pn* Heterojunction Devices							
ITO/CuPc (30 nm)/PV (50 nm)/Ag	AM2	75	2.3	0.45	0.65	0.95	35
ITO/PEDOT:PSS/**238** (20 nm)/Perylene dye (20 nm)/LiF/Al	W	77	1.35	0.86	0.51	0.77	314
ITO/**239** (MNTDATA)/PV/Ag	Xe	100				0.1	319
ITO/**240** (MB-TTPA)/PV/Ag	Xe	100				0.07	319
ITO/PEDOT:PSS (60 nm)/**237**/C_{60}/Al (60 nm)	AM1.5	100	3.65	0.89	0.36	1.17	313
ITO/CuPc (15 nm)/PTCBI (6 nm)/ BCP:PTCBI (80 nm)/Ag	AM1.5	100				1	304
ITO (150 nm)/CuPc (20 nm)/C_{60} (40 nm)/ BCP (10 nm)/Ag (100 nm)	AM1.5	>440			0.61	4.2	305
ITO /PEDOT:PSS/tetracene (80 nm)/C_{60} (30 nm)/BCP (8 nm)/Al (100 nm)	AM1.5	100	7.0	0.58	0.57	2.3	323
ITO /pentacene (45 nm)/C_{60} (50 nm)/BCP (10 nm)/Al	AM1.5	100	15	0.363	0.50	2.7	324
ITO /PEDOT:PSS (30 nm)/α-NPD (10 nm)/ C_{60} (48 nm)/MgAg (170 nm)	AM1.5	97		0.85		1	321
Bulk *pn* Heterojunction Devices							
ITO/PEDOT:PSS/**233**:[6,6]-PCBM (1:4)/Al	AM1.5	100	1.4	0.60	0.29	0.25	311
ITO/PEDOT:PSS/**234**:C_{60} (spin coated)/ C_{60}/Al	AM1.5	100	1.7	0.67	0.3	0.32	312
ITO/PEDOT:PSS/**235**:C_{60} (spin coated)/ C_{60}/Al	AM1.5	100	1.5	0.32	0.3	0.14	312
ITO/PEDOT:PSS (60 nm)/**236**:PCBM (1:3)/Al (60 nm)	AM1.5	100	2.43	0.60	0.28	0.41	313
ITO/CuPc:C_{60} (1:1) (33 nm)/C_{60} (10 nm)/ BCP (7.5 nm)/Ag	AM1.5	100	15.4	0.50	0.46	3.5	298
ITO/CuPc (15 nm)/CuPc:C_{60} (1:1, 10 nm)/ C_{60} (35 nm)/ BCP (10 nm)/Ag (100 nm)	AM1.5					5.0	322
ITO/PEDOT:PSS/**242**:P3HT/LiF/Al	Halogen	75	1.2	0.65	0.17		332
ITO/PEDOT:PSS (40 nm)/ P3HT:[6,6]-PCBM (1:0.8)/Al (100 nm) (annealed at 150 °C)	AM1.5	80	9.5	0.63	0.68	5	334
ITO/P3HT:**243** (1:4, 70 nm)/LiF/Al	AM1.5	100	1.32	0.36	0.38	0.182	333
ITO/*m*-MTDATA (50 nm)/*m*-MTDATA:Alq_3 (5 nm)/Alq_3 (60 nm)/MgAg	365 nm	1.27				0.40	317
Tandem Devices							
ITO/CuPc (10 nm)/CuPc:C_{60} (18 nm)/C_{60} (2 nm)/PTCBI (5 nm)/Ag (0.5 nm)/ *m*-MTDATA:F_4-TCNQ (5mol%, 5 nm)/CuPc (2 nm)/CuPc:C_{60} (13 nm)/C_{60} (25 nm)/BCP (7.5 nm)/Ag	AM1.5			1.2 (10suns)		5.4 (0.34suns)	309
ITO/*p*-doped TPD (30 nm)/ZnPc:C_{60} (1:2) (60 nm)/*n*-doped C_{60} (20 nm)/Au (0.5 nm)/ *p*-doped TPD (125 nm)/ZnPc:C_{60} (1:2) (50 nm)/*n*-doped C_{60} (20 nm)/Al (100 nm)	AM1.5	130	10.8	0.99	0.47	3.80	307
Single Component Device							
ITO/PEDOT:PSS/**244** (100∼150 nm)/LiF/Al	White	80	0.2	0.32	0.26	0.02	335

[a] P3HT: poly(3-hexylthiophene).

5.3. Molecular Materials for Organic Field-Effect Transistors (OFETs)

5.3.1. Molecular Materials for OFETs and Device Performance

OFETs using a variety of organic semiconductors have been fabricated, and their performance has been examined. The target performance for practical applications should be similar to or over the performance of amorphous silicon-based FETs. That is, field-effect mobilities (μ_{FET}) should be greater than ∼1 cm^2 V^{-1} s^{-1}, and the on/off ratio should be larger than 10^6. Since organic semiconductors are essentially electronic insulators as already described in section 1, holes and electrons are generally injected from the source electrode into the *p*- and *n*-type organic semiconductors and transported toward the drain electrode. Organic materials with electron-donating and -accepting properties, that is, *p*- and *n*-type organic semiconductors, form *p*- and *n*-channels, respectively, in OFETs. In cases where materials can allow efficient injection of both holes and electrons from the source electrode, they exhibit ambipolar character.

Crystalline materials, single crystals and polycrystals, have been used mostly for OFETs. The representative materials recently studied for the fabrication of OFETs are CuPc (**2**) and pentacene (**1**). Transistor performance is highly dependent on the morphology of CuPc.[337] The μ_{FET} values of polycrystalline CuPc have been determined to be ∼10^{-2} cm^2 V^{-1} s^{-1}.[337,338] The μ_{FET} values determined for single crystals of CuPc are 10^{-1}∼1 cm^2 V^{-1} s^{-1}.[339−341] On the other hand, the μ_{FET} value of a nonplanar metal phthalocyanine, for example, TiOPc, has been reported to be 10^{-5} cm^2 V^{-1} s^{-1},[342] which is 3∼5 orders of magnitude smaller than those of planar CuPc. Notably, TiOPc acts as an *n*-channel material in vacuo and as a *p*-channel material in the air ($\mu_{FET} = 9 \times 10^{-6}$ cm^2 V^{-1} s^{-1} for electrons; $\mu_{FET} = 1 \times 10^{-5}$ cm^2 V^{-1}

Chart 31. Reported Materials for OFETs

a. Oligothiophenes and their analogues

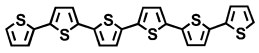

245 (α-6T)

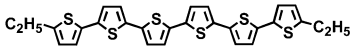

246 (DEt-α-6T)

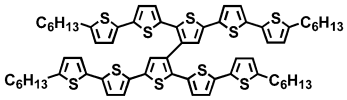

247

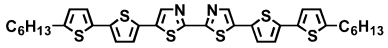

248

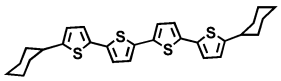

249

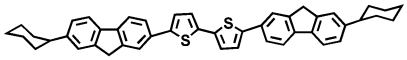

250

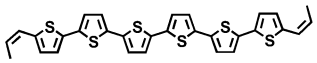

251

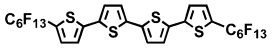

252

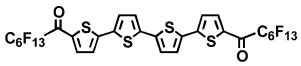

253

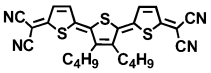

254

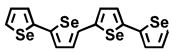

255

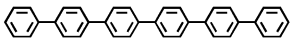

256

b. Phenylene-thienylene oligomers

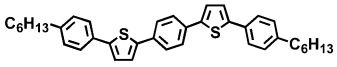

257

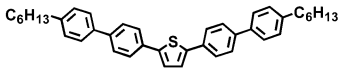

258

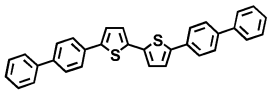

259

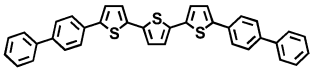

260

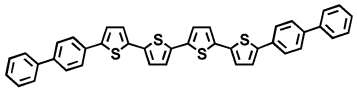

261

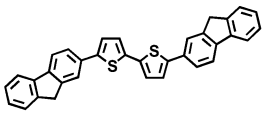

262

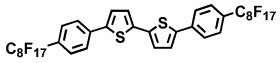

263

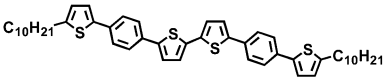

264

c. Oligoarylenevinylenes

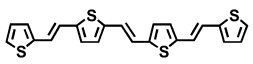

265

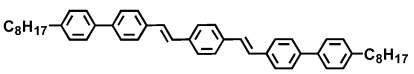

266

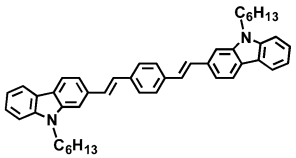

267

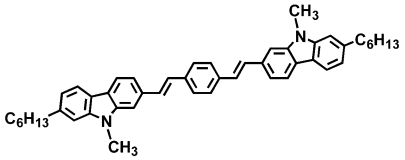

268

Chart 31. (Continued)

d. Oligofluorenes

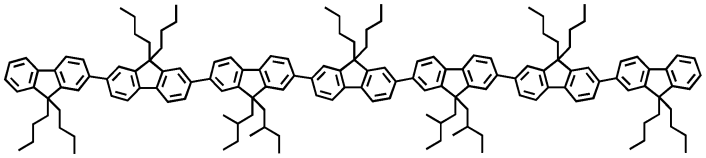

269

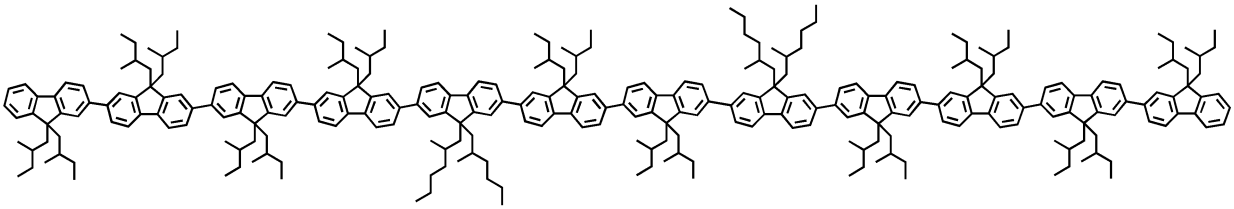

270

e. Polycyclic aromatic compounds

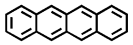

271

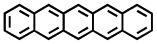

1

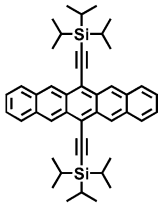

272

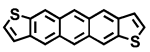

273

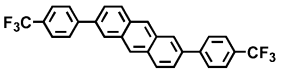

274

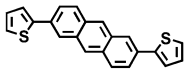

275

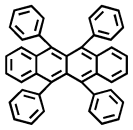

276

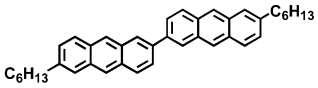

277

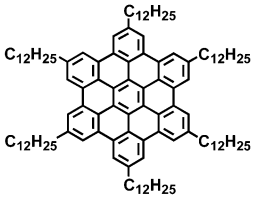

278

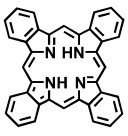

279 (H_2Pc)

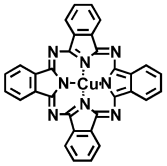

2 (CuPc)

280 (FePc)

Chart 31. (Continued)

f. Macrocycles

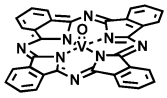

281 (VOPc)

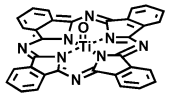

282 (TiOPc)

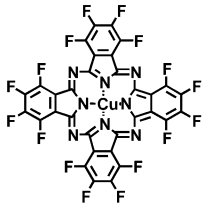

283 (F_{16}CuPc)

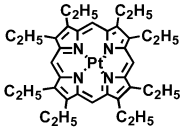

284 (PtOEP)

g. Fullerenes

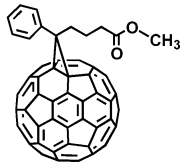

232 ([6,6]-PCBM)

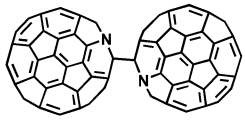

285

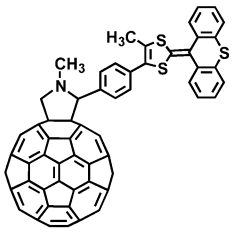

286

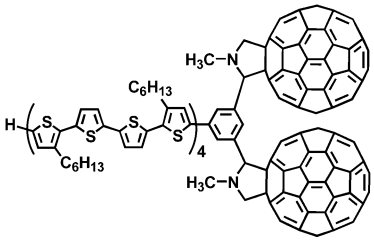

287

h. Perylenes dyes

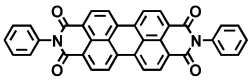

288

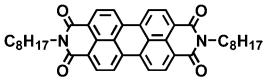

289

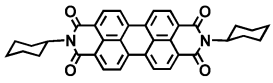

290

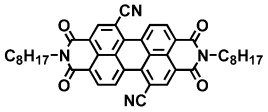

291

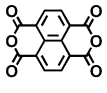

292

i. Fused heterocyclic aromatic compounds

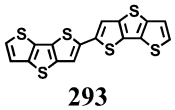

293

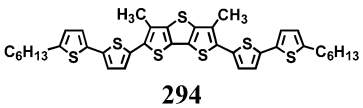

294

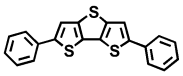

295

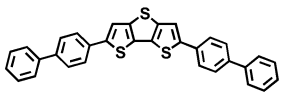

296

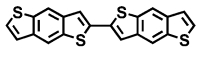

297

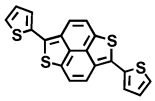

298

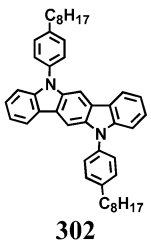

302

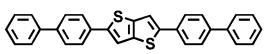

299

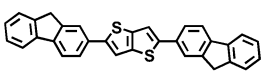

300

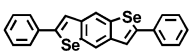

301

Chart 31. (Continued)

j. Tetrathiafulvalene derivatives

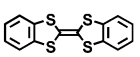

303

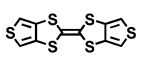

304

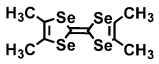

305

k. Thiadiazole derivatives

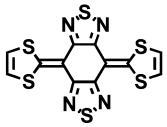

306

l. Tris(oligoarylenyl)amines

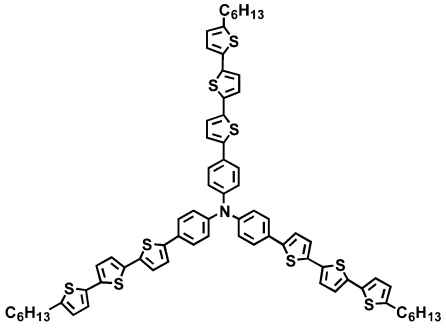

234

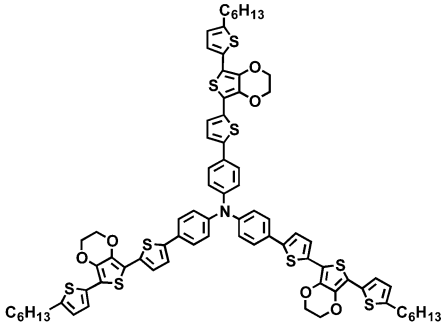

235

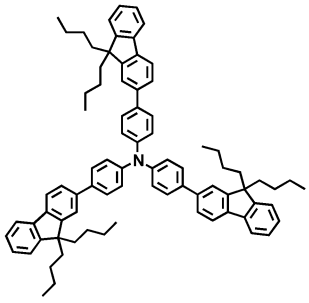

83

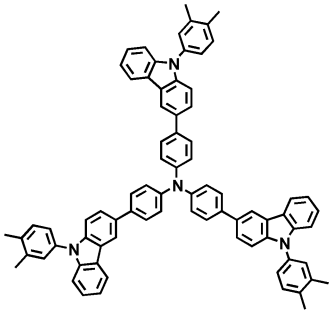

307

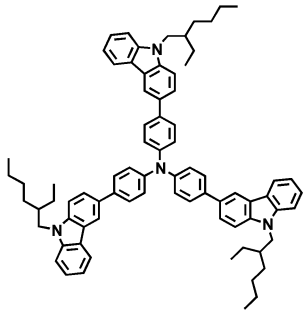

308

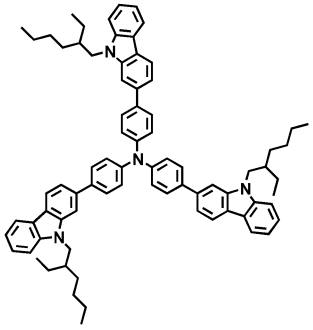

309

m. Compounds with a 1,3,5-triarylbenzene central core

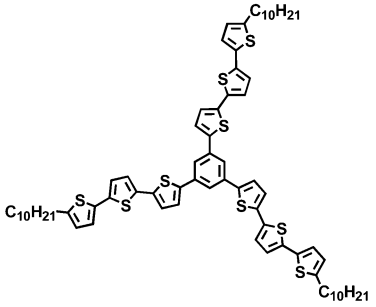

310

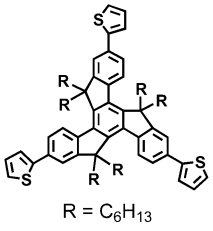

311

Chart 31. (Continued)

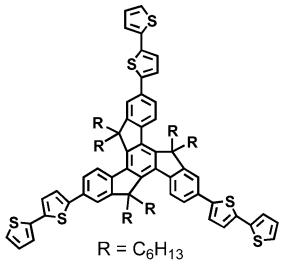

312

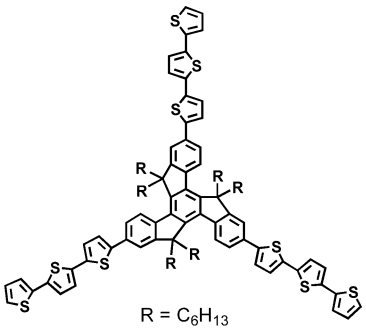

313

n. N,N,N',N'-Tetraarylbenzidines

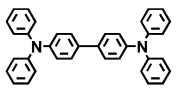

314 (DDB)

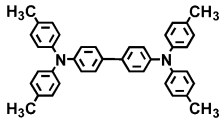

315 (TTB)

o. Spiro compounds

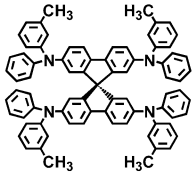

316 (spiro-TPD)

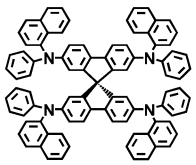

317 (spiro-α-NPD)

s^{-1} for holes).[342] The μ_{FET} of laterally grown nonplanar vanadyl phthalocyanoine (VOPc) has been reported to be ca. 5×10^{-3} cm^2 V^{-1} s^{-1}.[343] OFETs using crystalline pentacene have been reported to exhibit very high mobilities of $\sim$1.0 cm^2 V^{-1} s^{-1} and high on/off ratios of ca. 10^8.[51] A μ_{FET} value of 20 cm^2 V^{-1} s^{-1} has been obtained for an OFET using a single crystal of rubrene.[344]

A number of organic compounds have been studied for use in OFETs. They are classified into oligothiophenes and their analogues,[40,345−359] phenylene−thienylene oligomers,[360−364] oligoarylenevinylenes,[365−367] oligofluorenes,[368] polycyclic aromatic compounds,[51,344,369−385] macrocycles,[38,337−343,386−390] fullerenes,[391−402] perylene dyes,[403−406] fused heterocyclic aromatic compounds,[407−414] tetrathiafulvalene derivatives,[415−417] a thiadiazole derivative,[418] tris(oligoarylenyl)amines,[129,312] compounds with a 1,3,5-triarylbenzene central core,[419,420] *N,N,N′,N′*-tetraarylbenzidines,[211] and spiro compounds.[211] Most of these compounds act as *p*-channel materials. The introduction of electron-withdrawing fluorine atom into *p*-channel materials, for example, CuPc, converts the original *p*-channel to an *n*-channel material. Generally, OFETs using *p*-type organic semiconductors are much more stable than those using *n*-type organic semiconductors.

The structures of compounds for OFETs are shown in Chart 31. The performance of OFETs using these materials are summarized in Tables 8−10.

5.3.2. Organic Light-Emitting Field-Effect Transistors (OLETs)

Very recently, OLETs have been developed. OLETs are a novel class of bifunctional organic optoelectronic devices which combine the switching function of OFETs and the light-emission function of OLEDs in a single device. The progress in OLETs has been reviewed.[421] Both holes and electrons are injected from the source and drain electrodes, respectively, into the organic semiconductor plane at the interface with the dielectric to generate an exciton through the recombination of injected holes and electrons. Light emission from an OFET was demonstrated for a device using vacuum-evaporated tetracene polycrystalline film as an organic semiconductor, gold as the source and drain electrodes, and SiO_2 as a dielectric. The light emission was localized near the drain electrode due to unipolar character of tetracene, namely, better hole-transporting properties.[422] Ambipolar OLETs have been developed by the use of a bulk heterojunction layer consisting of the coevaporated thin films of α-quinquethiophene (α-5T) as a hole-transporting material and *N,N′*-ditridecylperylene-3,4,9,10-teytracarboxylic diimide (P13) as an electron-transporting material.[423] OLETs based on two-component layered structures have also been realized, which consist of a 5,5‴-dihexyl-α-quaterthiophene (DH4T) layer in contact with the dielectric and a P13 layer on the DH4T layer. Balanced

Table 8. Examples of Performance of OFETs Using *p*-Type Organic Semiconductors[a]

compound	morphology	configuration	gate dielectric	electrode metal	preparation of sample	μ ($cm^2 V^{-1} s^{-1}$)	on/off ratio	threshold voltage (V)	ref
				Oligothiophenes and Their Analogues					
245 (α-6T)	crystal	bottom	SiO_2	Au	vap.depo.	0.01∼0.03	$>10^6$		348
	single crystal	top	PMMA	Au	sublimation	0.075	$>10^4$	6.4	40
246 (DEt-α-6T)	crystal	top	PVP	Au	vap.depo.	1.1	10^4	3.9	353
247	crystal	top	HMDS-treated SiO_2	Au	vap.depo.	0.012	$>10^5$	∼0	359
248	polycrystal	top	SiO_2	Au	vap.depo. T_{sub} = 55 °C	0.011	$>10^4$		352
249	polycrystal	top	SiO_2	Au	vap.depo. T_{sub} = 80 °C	0.03	2×10^6		357
250	polycrystal	top	SiO_2	Au	vap.depo. T_{sub} = 130 °C	0.17	8×10^5		357
251	polycrystal	top	SiO_2	Au	precursor	0.03	$>10^5$		356
255	polycrystal	top	SiO_2	Au	vap.depo. T_{sub} = 60 °C	3.6×10^{-3}			59
256	crystal	top	SiO_2	Au	vap.depo. T_{sub} = 200 °C	0.07	$>10^6$	−45	350
				Phenylene-thienylene Oligomers					
257	polycrystal	top	HMDS-treated SiO_2	Au	vap.depo. T_{sub} = 50 °C	0.054	6×10^4		360
258	polycrystal	top	HMDS-treated SiO_2	Au	vap.depo. T_{sub} = 50 °C	0.018	1.5×10^4		360
259	polycrystal	top	SiO_2	Au	vap.depo. T_{sub} = 150 °C	7.7×10^{-3}			361
260	polycrystal	top	SiO_2	Au	vap.depo. T_{sub} = 200 °C	1.7×10^{-1}			361
261	polycrystal	top	SiO_2	Au	vap.depo. T_{sub} = 150 °C	5.5×10^{-2}			361
262	polycrystal	top	HMDS-treated SiO_2	Au	vap.depo. T_{sub} = 150 °C	0.05∼0.06	6.3×10^4	−19	363
264	crystal	bottom	SiO_2	Au	vap.depo.	0.4	10^5	−13	364
				Oligoarylenevinylenes					
265	crystal	top	PMMA	Au	vap.depo. T_{sub} = 25 °C	$(1.2∼1.4) \times 10^{-3}$			365
266	crystal	top	HMDS-treated SiO_2	Au	vap.depo.	0.066	$>10^6$	−22	366
267	polycrystal	top	OTS-treated SiO_2	Au	vap.depo. T_{sub} = 150 °C	0.093	10^7	−24	367
268	polycrystal	top	OTS-treated SiO_2	Au	vap.depo. T_{sub} = 125 °C	0.024	10^6	−20	367
				Oligofluorenes					
269	glassy nematic liquid crystal	top	parylene	Au	spin coating	1.7×10^{-3}			368
270	glassy nematic liquid crystal	top	parylene	Au	spin coating	0.012	10^4	−43	368
				Polycyclic Aromatic Compounds					
271	single crystal	bottom	SiO_2	Au	sublimation	0.4		10	374
1	polycrystal	top	SiO_2	Au	vap.depo. T_{sub} = 50∼120 °C	0.7	$>10^8$		51
	crystal	top	SiO_2	Au	vap.depo. T_{sub} = 60∼90 °C	1.3			369
	crystal	bottom	HMDS-treated SiO_2	Au	precursor	0.42	2×10^7		371
	polycrystal	top	OTS-treated SiO_2	Au	vap.depo. T_{sub} = 40 °C	1.6	10^6		372
	polycrystal	bottom	SiO_2/PS	FDT-treated Au	vap.depo.	0.440		−1.3	385
	crystal	top	cross-linked PVP	Au	vap.depo.	3.0	10^5	−5	373
	polycrystal	top	AlO_x	NiO_x	vap.depo.	0.9	5×10^5	−7	379
	polycrystal	top	SiO_2/PMMA	Au	vap.depo.	1.4	10^6	−12	380
272	polycrystal	top	OTS-treated SiO_2	Au	vap.depo. T_{sub} = 90 °C	0.4	10^6		375
273	polycrystal	bottom	SiO_2	Au	vap.depo. T_{sub} = 85 °C	0.09			370
275	polycrystal	top	SiO_2	Au	vap.depo. T_{sub} = 20 °C	4.5×10^{-3}	10^3	−40	382
276	single crystal	top	parylene	Ag	sublimation	8			376
	single crystal	bottom	free-space	Au	sublimation	10.7		3.6	377
	single crystal	bottom	free-space	Au	sublimation	20			344
277	polycrystal	top	Ta_2O_5	Au	vap.depo. T_{sub} = 70 °C	0.22	10^6	−6	378
278	columnar alignment	top	HMDS-treated SiO_2	Au	drop casting	5×10^{-3}	10^4	−15	383
				Macrocycles					
2 (CuPc)	polycrystal	bottom	SiO_2	Au	vap.depo. T_{sub} = 125∼175 °C	0.01∼0.02	4×10^5	−10	337, 338
	polycrystal	bottom	SiO_2	Au	vap.depo.	$(0.94∼1.3) \times 10^{-3}$			388
	single crystal	bottom	parylene	colloidal graphite	sublimation	1	$>10^4$	−6	340
	single crystal	top	SiO_2	Au	sublimation	0.1∼0.2		−2.4∼ −2.9	341
281 (VOPc)	crystal	bottom	$(Sc_{0.7}Y_{0.3})_2O_3$	ITO	MBE	$\sim 5 \times 10^{-3}$	$\sim 10^3$	−3	343

Table 8 (Continued)

compound	morphology	configuration	gate dielectric	electrode metal	preparation of sample	μ ($cm^2 V^{-1} s^{-1}$)	on/off ratio	threshold voltage (V)	ref
				Macrocycles					
279 (H_2Pc)	crystal	bottom	SiO_2	Au	precursor	0.017	1×10^5	−3.4	389
284 (PtOEP)	crystal	top	SiO_2	Au	MBE $T_{sub} = 50$ °C	2.2×10^{-4}	10^4∼10^5		387
				Fused Heterocyclic Aromatic Compounds					
293	crystal	bottom	SiO_2	Au	vap.depo. $T_{sub} = 100$ °C	0.02∼0.05	10^8	<5	407
294	polycrystal	bottom	MPTMS-treated SiO_2	Au	vap.depo.	∼0.02	∼10^6	∼ −10	412
295	crystal	top	OTS-treated SiO_2	Au	vap.depo. $T_{sub} = 70$ °C	0.42	5×10^6	−23.4	413
296	crystal	top	OTS-treated SiO_2	Au	vap.depo. $T_{sub} = 70$ °C	0.12	5×10^5	−20.2	413
	polycrystal	top	PVA	Au	vap.deop.	0.4	5×10^4	−0.36	414
297	polycrystal	bottom	SiO_2	Au	vap.depo. $T_{sub} = 100$ °C	0.04		−24	408
298	polycrystal	top	SiO_2	Au	vap.depo.	$(2∼3) \times 10^{-4}$			409
299	polycrystal	top	HMDS-treated SiO_2	Au	vap.depo. $T_{sub} = 150$ °C	0.08∼0.09	7.3×10^4	−22	363
300	polycrystal	top	HMDS-treated SiO_2	Au	vap.depo. $T_{sub} = 150$ °C	0.05∼0.06	7×10^4	−24	363
301	crystal	top	SiO_2	Au	vap.depo. $T_{sub} = 60$ °C	0.17	10^5		410
302	polycrystal	top	OTS-treated SiO_2	Au	vap.depo.	0.07∼0.12	10^6∼10^7		411
				Tetrathiafulvalene Derivatives					
303	single crystal	bottom	SiO_2	Au	solvent cast	0.1∼1	10^6		417
304	single crystal	bottom	SiO_2	Au	solvent cast	1.4	7×10^5	0.4	416
305	single crystal	bottom	PET	Au	sublimation	0.027			415
				A Thiadiazole Derivative					
306	polycrystal	top	OTS-coated SNx	Au	OMBD	0.044	10^3		418
				Tris(oligoarylenyl)amines					
234	crystal	top	SiO_2	Au	vap.depo.	0.011	170∼200	−18∼−20	312
235	amorphous solid	top	SiO_2	Au	spin coating	10^{-5}			312
83	amorphous solid	bottom	SiO_2	Au	drop casting	1×10^{-4}	10^5	−1	129
307	amorphous solid	bottom	SiO_2	Au	drop casting	1×10^{-4}	10^3	−3	129
308	amorphous solid	bottom	SiO_2	Au	drop casting	1×10^{-4}	10^4	−2	129
309	amorphous solid	bottom	SiO_2	Au	drop casting	3×10^{-4}	10^4	−5	129
				Compounds with a 1,3,5-Triarylbenzene Central Core					
310	polycrystal	bottom	SiO_2	Au	spin coating	2×10^{-4}			419
311	polycrystal	top	SiO_2	Au	spin coating	1.03×10^{-3}	$<10^3$		420
312	semicrystalline	top	SiO_2	Au	spin coating	6.5×10^{-4}	10^2		420
313	amorphous solid	top	SiO_2	Au	spin coating	2.2×10^{-4}	$<10^2$		420
				N,N,N,N-Tetraarylbenzidines					
314 (DDB)	amorphous solid	bottom	HMDS-treated SiO_2	Au	vap.depo.	6.7×10^{-5}			211
86 (TPD)	amorphous solid	bottom	HMDS-treated SiO_2	Au	vap.depo.	8.7×10^{-5}			211
315 (TTB)	amorphous solid	bottom	HMDS-treated SiO_2	Au	vap.depo.	1.8×10^{-5}			211
87 (α-NPD)	amorphous solid	bottom	HMDS-treated SiO_2	Au	vap.depo.	6.1×10^{-5}			211
				Spiro Compounds					
140 (spiro-TAD)	amorphous solid	bottom	HMDS-treated SiO_2	Au	vap.depo.	6.7×10^{-5}			211
316 (spiro-TPD)	amorphous solid	bottom	HMDS-treated SiO_2	Au	vap.depo.	6.9×10^{-5}			211
141 (spiro-*m*-TTB)	amorphous solid	bottom	HMDS-treated SiO_2	Au	vap.depo.	5.7×10^{-5}			211
317 (spiro-α-NPD)	amorphous solid	bottom	HMDS-treated SiO_2	Au	vap.depo.	4.4×10^{-5}			211

[a] PMMA, poly(methylmethacylate); PVP, poly(vinylphenol); HMDS, hexamethyldisilazane; OTS, octadecyltrichlorosilane; PS, poly(α-methylstylene); MPTMS, (3-mercaptopropyl)trimethoxysilane; PVA, poly(vinylalcohol); PET, poly(ethylene terephthalate); FDT, 3,3,4,4,5,5,-6,6,7,7,8,8,9,9,10,10,10-heptadecafluoro-1-decanethiol; MBE, molecular beam epitaxial growth; OMBD, organic molecular beam deposition; precursor, a method for preparing thin films via precursor films.

ambipolar transport and mobility values as large as 3×10^{-2} $cm^2 V^{-1} s^{-1}$ have been achieved for the latter device.[424]

6. Charge Transport in Molecular Materials

6.1. General Aspects

Charge transport is greatly affected by the organization state of molecular materials. The charge carrier drift mobilities of organic single crystals, for example, anthracene, are in the range from 10^{-2} to 1 $cm^2 V^{-1} s^{-1}$, depending on the transport direction in a single crystal.[425] The mobilities of a C_{60} single crystal have been reported to be 1.7 $cm^2 V^{-1} s^{-1}$ for holes and 0.5 $cm^2 V^{-1} s^{-1}$ for electrons, as determined by the TOF method.[426] The mobility values tend to increase with increasing purity of materials. Very high mobilities of 400 and 20 $cm^2 V^{-1} s^{-1}$ for holes and electrons, respectively, as determined by the TOF method, have been reported for a highly purified naphthalene single crystal.[427]

Charge carrier drift mobilites of a number of polycrystalline molecular materials have been determined from the performance of OFETs, as listed in Tables 8−10. They are

Table 9. Examples of Performance of OFETs Using *n*-Type Organic Semiconductors[a]

compound	morphology	configuration	gate dielectric	electrode metal	preparation of sample	μ ($cm^2\ V^{-1}\ s^{-1}$)	on/off ratio	threshold voltage (V)	ref
				Oligothiophenes and Their Analogues					
252	polycrystal	top	HMDS-treated SiO_2	Au	vap.depo. $T_{sub} = 70$ °C	0.048	10^5	25∼30	354
254	polycrystal	bottom	SiO_2	Au	vap.depo. $T_{sub} = 130$ °C	0.2	$>10^6$	11	355
				Phenylene-thienylene Oligomers					
263	crystal	top	HMDS-treated SiO_2	Au	vap.depo. $T_{sub} = 110$ °C	0.074	6×10^6	55	362
				Polycyclic Aromatic Compounds					
274	polycrystal	top	SiO_2	Au	vap.depo. $T_{sub} = 20$ °C	3.4×10^{-3}	10^4	75	382
				Macrocycles					
283 (F_{16}CuPc)	polycrystal	bottom	SiO_2	Au	vap.depo. $T_{sub} = 125$ °C	0.03	3×10^5		386
	polycrystal	bottom	OTS-treated SiO_2	Au	vap.depo.	0.01		50	390
				Fullerenes					
C_{60}		bottom	SiO_2	Au	vap.depo. $T_{sub} =$ r.t.	4×10^{-5}			391
		bottom	SiO_2	Au	vap.depo.	2×10^{-3}			393
		bottom	SiO_2	Au	vap.depo.	0.08	10^6	15	392
	nanowire	bottom	SiO_2	Au	LLIP	0.02			402
	crystal	bottom	SiO_2	Au	vap.depo. $T_{sub} = 80$ °C	0.5			400
C_{84}		bottom	SiO_2	Au	vap.depo.	1.1×10^{-3}		−42	395
C_{88}	crystal	bottom	HMDS-treated SiO_2	Au	vap.depo.	2.5×10^{-3}	∼ 7	−142	401
232 ([6,6]-PCBM)		top	organic resin	Ca	spin coating	4.5×10^{-3}		41	394
		top	PVA	Cr	spin coating	0.09	10^4		397
		top	cross-linked PVP	Ca	spin coating	0.1			331
285	crystal	bottom	SiO_2	Au	vap.depo.	3.8×10^{-4}	10^3	13.2	398
				Perylene Pigments					
288		bottom	PMMA	Au	vap.depo.	1.5×10^{-5}			403
289	crystal	bottom	SiO_2	Au	vap.depo.	0.6	$>10^5$	75	405
290	polycrystal	top	SiO_2	Au	vap.depo. $T_{sub} = 125$ °C	1.9×10^{-4}	10^2		357
291		bottom	HMDS-treated SiO_2	ODT-treated Au	vap.depo.	0.14	1.2×10^3	1.6	406
292	polycrystal	bottom	SiO_2	Au	vap.depo. $T_{sub} = 55$ °C	$(1∼3) \times 10^{-3}$			404

[a] HMDS, hexamethyldisilazane; OTS, octadecyltrichlorosilane; PVA, poly(vinylalcohol); PVP, poly(vinylphenol); ODT, 1-octadodecanethiol; LLIP, liquid-liquid interfacial precipitation method.

in the range from 10^{-4} to 1 $cm^2\ V^{-1}\ s^{-1}$. Studies of charge transport in liquid crystalline materials have recently advanced, and drift mobilities up to ∼1 $cm^2\ V^{-1}\ s^{-1}$ have been attained.[7,428−430] As will be described in section 6.2.−6.5., charge carrier drift mobilities of amorphous molecular materials, which have been determined mainly by the TOF method, are in the range from 10^{-6} to 10^{-2} $cm^2\ V^{-1}\ s^{-1}$.

6.2. Comparison of Mobilities Measured by Different Methods

As is described in section 2.2., several methods are available for the measurement of carrier drift mobilities. The thickness of samples for the measurement is different depending upon the method. The question is whether these different methods give almost the same mobility values. It has been reported that mobility values are different depending on the thickness of samples especially for low-mobility dispersive materials.[196,431] Comparative studies of charge transport using different techniques have been made for certain classes of materials, for example, *m*-MTDATA,[138,144,432] OMeTAD,[196] α-NPD,[144,211] Alq_3,[433] CuPc,[388] and so forth.

The hole mobilities of *m*-MTDATA and α-NPD determined by the DI-SCLC method have been shown to be in excellent agreement with those determined by the TOF method.[144] Room-temperature mobilities of OMeTAD (**142**) measured by three independent methods, TOF, DI-SCLC, and steady-state TF-SCLC methods, have been shown to agree well over a range of sample thicknesses from 4 μm to 135 nm.[196] The plots of the logarithm of electron mobilities of Alq_3 measured by the transient EL and TOF methods as a function of the square root of the electric field have been shown to be on the same line, and hence, the results measured by the two methods are in good agreement with each other.[433] Comparison of the hole mobility data of CuPc by the TOF and FET methods shows that they gave almost the same results; $\mu_{FET} = (0.94−1.3) \times 10^{-3}$ $cm^2\ V^{-1}\ s^{-1}$ and $\mu_{TOF} = (1.5−2.0) \times 10^{-3}$ $cm^2\ V^{-1}\ s^{-1}$.[388] Likewise, mobility data for *m*-MTDATA determined by the TOF and FET methods were almost the same.[432] On the other hand, μ_{FET} values of TPTPA (**81**), TTB (**315**), TPD, and α-NPD were approximately 2 orders of magnitude smaller than those determined by the TOF method.[211,432]

6.3. Hole Transport in Amorphous Molecular Materials

Drift mobilities of a number of hole-transporting amorphous molecular materials have been determined by the TOF technique.[1b,1d,432,434,435] Amorphous molecular glasses have

Table 10. Examples of Performance of OFETs Using Ambipolar Materials[a]

compound	morphology	configuration	gate dielectric	electrode metal	preparation of sample	μ ($cm^2 V^{-1} s^{-1}$)	on/off ratio	threshold voltage (V)	ref
				Oligothiophenes and Their Analogues					
253	crystal	top	HMDS-treated SiO_2	Au	vap.depo. T_{sub} = 25∼90 °C	0.6 (e)	$>10^7$		358
					vap.depo. T_{sub} = 70∼90 °C	$\sim10^{-3}$ (h)			
				Polycyclic Aromatic Compounds					
1	polycrystal	top	PVA	Au	vap.depo. T_{sub} = 50 °C	0.5 (h) 0.2 (e)		−27.57 (h, e)	381
276	amorphous solid	bottom	SiO_2	Au	vap.depo.	8.0×10^{-6} (h) 2.2×10^{-6} (e)		−36 (h) −30 (e)	384
				Macrocycles					
2 (CuPc)	single crystal	bottom	SiO_2	Au	sublimation	0.3 (h) $<10^{-3}$ (e)			339
280 (FePc)	single crystal	bottom	SiO_2	Au	sublimation	10^{-3}∼0.3 (h) 5×10^{-4}∼0.03 (e)			339
282 (TiOPc)	crystal	bottom	SiO_2	Au	vap.depo.	1×10^{-5} (h) (in air) 9×10^{-6} (e) (in vacuum)			342
				Fullerenes					
286	polycrystal	top	SiO_2	Au	spin coating	10^{-6} (h) 4×10^{-5} (e)	10^2 (h, e)		399
287	crystal	bottom	SiO_2	Au	spin coating	1.1×10^{-5} (h) 4.3×10^{-5} (e)	10^2 (h, e)		396

[a] HMDS, hexamethyldisilazane; PVA, poly(vinylalcohol).

been found to exhibit mostly nondispersive transient photocurrents. Their hole drift mobilities greatly vary from 10^{-6} to 10^{-2} cm^2 V^{-1} s^{-1} depending upon molecular structures. It should also be noted that charge carrier drift mobilities depend upon the purity of samples, generally increasing with increasing purity.

Materials of the family of arylhydrazones, for example, DPH (**20**), M-DPH (**128**), DPMH (**129**), ECH (**130**), M-ECH (**131**), and ECMH (**132**), have been reported to exhibit room-temperature hole drift mobilities in the range from 10^{-6} to 10^{-4} cm^2 V^{-1} s^{-1} at an electric field of ca. 10^5 V cm^{-1}.[114,209,434,436,437] One order of magnitude difference in the hole drift mobility has been observed between DPH (2.2×10^{-4} cm^2 V^{-1} s^{-1}) and ECH (3.7×10^{-5} cm^2 V^{-1} s^{-1}).[434]

Materials of the TDATA family, which have been proven to serve as good hole-injection buffer layer in multilayer OLEDs, for example, *m*-MTDATA,[91,111,133] 1-TNATA,[133] *p*-PMTDATA (**32**),[122] and TFATA,[147] exhibit relatively low hole drift mobilities of the order of 10^{-5} cm^2 V^{-1} s^{-1}.[122,138,147]

The drift mobilities of TPD (**86**) and α-NPD (**87**), which have been widely used as good hole-transporting materials in OLEDs, have been reported to be 1.0×10^{-3} and 8.8×10^{-4} cm^2 V^{-1} s^{-1}.[167,438] The TPD analogues with higher Tg's above 100 °C, for example, *p*-BPD (**90**),[207] PFFA (**96**),[173] and FFD (**93**),[147,173] also exhibit high mobilities of 1.0×10^{-3} cm^2 V^{-1} s^{-1} or greater.[147,173,207]

A new class of hole-transporting amorphous molecular materials, *N*,*N*-bis(9,9-dimethylfluoren-2-yl)aniline (F_2PA),[228] 4-[bis(9,9-dimethylfluoren-2-yl)amino]biphenyl (F_2BPA),[165] and TFlA (**85**),[165] functions as good hole-transporting materials. F_2PA also functions as a good host material for a phosphorescent iridium complex in OLEDs.[228] These materials of the triarylamine family exhibit high mobilities exceeding 5.0×10^{-3} cm^2 V^{-1} s^{-1}.[432]

Among amorphous molecular materials, thiophene- and selenophene-containing tris(oligoarylenylamine)s, TTPA (**79**), TSePA (**80**), TPTPA (**81**), and TPSePA (**82**), exhibit the highest mobilities of 1.0×10^{-2} cm^2 V^{-1} s^{-1} at an electric field of 1.0×10^5 V cm^{-1} at room temperature.[163]

The hole mobility of the TDAPB family, 1,3,5-tris[*N*,*N*′-bis(4,5-methoxyphenyl)aminophenyl]benzene, has been shown to increase when C_{60} was doped.[439] The hole mobility of C_{60}-doped TDAPB was 9.0×10^{-4} cm^2 V^{-1} s^{-1} compared with 1.0×10^{-4} cm^2 V^{-1} s^{-1} for nondoped TDAPB. A furan-containing oligoarylene (PF6 (**148**) in Chart 16) has been reported to exhibit a room-temperature hole mobility over 10^{-3} cm^2 V^{-1} s^{-1} under high electric field.[200]

Table 11 lists charge carrier mobilities of hole-transporting amorphous molecular materials.[440−443]

6.4. Electron Transport in Amorphous Molecular Materials

As compared with extensive studies on hole transport, there have been fewer studies on electron transport. While hole-transporting amorphous molecular materials show μ_{TOF} values up to 10^{-2} cm^2 V^{-1} s^{-1}, the mobilities of electron-transporting amorphous molecular materials are usually orders of magnitude lower. The electron-transporting materials often exhibit dispersive transient photocurrents due to extrinsic carrier trapping.

Electron transport in amorphous films of Alq_3 have been studied in detail by the TOF method.[444−446] Nondispersive photocurrent transients have been observed for carefully prepared Alq_3 films; however, exposure of the films to an ambient atmosphere or oxygen resulted in highly dispersive transport.[444−446] It was concluded that oxygen acts as an extrinsic dopant and induces electron traps in Alq_3.[445] Transient photocurrents became dispersive when Alq_3 was exposed to H_2O vapor, but when the H_2O-treated sample was annealed, a nondispersive TOF signal was recovered.[445] The mobility has been found to obey the Poole−Frenkel model.[444] The reported electron drift mobilities are in the range from 1.2×10^{-6} to 6.7×10^{-5} cm^2 V^{-1} s^{-1}. The hole mobilities of Alq_3 has been shown to be at least 2 orders of

Table 11. Examples of Charge Carrier Mobilities of Hole-Transporting Amorphous Molecular Materials

compound	mobility ($cm^2 V^{-1} s^{-1}$)	temp. (K)	electric field ($V cm^{-1}$)	method	ref
		TDATA Derivatives			
8 (*m*-MTDATA)	3×10^{-5}		10^5	TOF	138
	$(2\sim5) \times 10^{-5}$ [a]	rt	$(2.5\sim6) \times 10^5$	DI-SCLC	440
	2.7×10^{-5}	293	1.0×10^5	TOF	432
50 (1-TNATA)	1.9×10^{-5}	293	1.0×10^5	TOF	432
51 (2-TNATA)	$(3\sim8) \times 10^{-5}$ (h)[a]	290	$(0.4\sim8) \times 10^5$	TOF	442
	$(1\sim3) \times 10^{-4}$ (e)				
53 (TFATA)	1.7×10^{-5}			TOF	147
		TDAB Derivatives			
10 (*o*-MTDAB)	3.0×10^{-3}	293	2.0×10^5	TOF	1b
30 (MTBDAB)	2.5×10^{-5}	293	2.0×10^5	TOF	1b
64 (*p*-DPA-TDAB)	1.4×10^{-4}	293	2.0×10^5	TOF	1b
71 (TECEB)	$\sim10^{-4}$			EL	157
		TDAPB Derivatives			
73 (TFAPB)	6.4×10^{-3}			TOF	161
		Tris(oligoarylenyl)amines			
78 (TBA)	8.6×10^{-3}	293	1.0×10^5	TOF	163
79 (TTPA)	1.1×10^{-2}	293	1.0×10^5	TOF	163
80 (TSePA)	1.5×10^{-2}	293	1.0×10^5	TOF	163
17 (*o*-TTA)	7.9×10^{-4}	293	1.0×10^5	TOF	432, 441
18 (*m*-TTA)	2.3×10^{-5}	293	1.0×10^5	TOF	432
19 (*p*-TTA)	6.9×10^{-3}	293	1.0×10^5	TOF	432
81 (TPTPA)	1.0×10^{-2}	293	1.0×10^5	TOF	163
82 (TPSePA)	1.1×10^{-2}	293	1.0×10^5	TOF	163
85 (TFlA)	8.1×10^{-3}	293	1.0×10^5	TOF	432
		Tetraphenylbenzidines			
86 (TPD)	$(0.7\sim2) \times 10^{-3}$ [a]	295	$(0.4\sim4) \times 10^5$	TOF	167
	$(0.7\sim2) \times 10^{-3}$ [a]	297	$(0.4\sim1.6) \times 10^5$	TOF	443
	1.1×10^{-3}	293	1.0×10^5	TOF	173
87 (α-NPD)	$(7.8\sim9.9) \times 10^{-4}$		$(0.76\sim1.4) \times 10^6$	EL	198
	8.8×10^{-4}	rt	2.3×10^5	TOF	438
	$(3\sim5) \times 10^{-4}$ (h)[a]	290	$(0.4\sim8) \times 10^5$	TOF	442
	$(6\sim9) \times 10^{-4}$ (e)				
88 (*o*-BPD)	6.5×10^{-4}	293	1.0×10^5	TOF	122, 207
89 (*m*-BPD)	5.3×10^{-5}	293	1.0×10^5	TOF	122, 207
90 (*p*-BPD)	1.0×10^{-3}	293	1.0×10^5	TOF	122, 207
93 (FFD)	4.1×10^{-3}	293	1.0×10^5	TOF	147
96 (PFFA)	1.1×10^{-3}	293	1.0×10^5	TOF	173
		Arylhydrazones			
20 (DPH)	2.2×10^{-4}	293	2.0×10^5	TOF	114
129 (DPMH)	4.9×10^{-5}	293	2.0×10^5	TOF	437
130 (ECH)	3.7×10^{-5}	rt	$\sim10^5$	TOF	434
131 (M-ECH)	4.4×10^{-6}	rt	$\sim10^5$	TOF	434
132 (ECMH)	2.6×10^{-6}	rt	$\sim10^5$	TOF	434
137	1×10^{-3}		1×10^6	TOF	192
		π-Electron Systems End-Capped with Triarylamines			
23 (BMA-3T)	2.8×10^{-5}	295	1.0×10^5	TOF	60, 61
24 (BMA-4T)	1.0×10^{-5}	295	1.0×10^5	TOF	60, 61
102 (BFA-1T)	1.1×10^{-3}	293	1.0×10^5	TOF	182
		N,N,N′,N′-Tetraarylenyl Arylenediamines			
106 ($N_\alpha N_\alpha P$)	1.6×10^{-4}	296	5.0×10^5	TOF	208
112	1.74×10^{-6}			TOF	188
113	2.47×10^{-6}			TOF	188
124	4.5×10^{-4}	rt	3.6×10^5	TOF	189
125	8.5×10^{-4}	rt	3.6×10^5	TOF	189
		Spiro Compounds			
46 (B3)	$(2\sim4) \times 10^{-3}$ (h)[a]	rt	$(0.7\sim4) \times 10^5$	TOF	125
	$(4\sim6) \times 10^{-4}$ (e)[a]	rt	$(4\sim7) \times 10^5$	TOF	125
140 (spiro-TAD)	$(2\sim4) \times 10^{-4}$ [a]	295	$(0.6\sim3) \times 10^5$	TOF	194
141 (spiro-*m*-TTB)	$(3\sim4) \times 10^{-4}$ [a]	295	$(0.9\sim3) \times 10^5$	TOF	194
142 (OMeTAD)	2×10^{-4}	300	2.6×10^5	TOF	196
		Others			
145 (HPCzI)	$(4.3\sim6.0) \times 10^{-5}$		$(0.76\sim1.4) \times 10^6$	EL	198
148 (PF6)	3.36×10^{-4}	300	2×10^5	TOF	200

[a] Estimated from the figures.

Table 12. Examples of Charge Carrier Mobilites of Electron-Transporting Amorphous Molecular Materials

compound	mobility ($cm^2 V^{-1} s^{-1}$)	temp. (K)	electric field ($V cm^{-1}$)	method	ref
		Alq_3, 2,5-Diaryl-1,3,4-oxadiazoles, and Triazoles			
156 (Alq_3)	5×10^{-5}		1×10^6	EL	9
	2×10^{-8} (h)	293	4×10^5	TOF	448
	1.4×10^{-6}				
	$(0.3\sim2) \times 10^{-4}$ [a]		$(2.5\sim5) \times 10^5$	TOF	449
	$(0.04\sim1) \times 10^{-5}$ [a]	294	$(0.5\sim 1.4) \times 10^6$	TOF	444
	6.7×10^{-5}	rt	2.3×10^5	TOF	438
	$(0.5\sim1) \times 10^{-5}$ [a]		$(0.4\sim1.2) \times 10^6$	EL	12
	1.2×10^{-6}		5.5×10^5	TOF	243
	4.7×10^{-6}		1×10^6	SCLC	450
159 (*t*-Bu-PBD)	1.9×10^{-5}		1×10^6	SCLC	450
	1.9×10^{-6}	rt	7.5×10^5	TOF	451
	(50 wt % in PC)				
	$2\sim4 \times 10^{-5}$ [a]		$(1\sim1.7) \times 10^6$	EL	452
160 (OXD-7)	2.1×10^{-5}		1×10^6	SCLC	450
		Electron-Transporting Materials with a Central Benzene Core			
165 (TPOB)	1.2×10^{-6}	273	7×10^5	TOF	453
	(50 wt % in PC)				
167 (TPBI)	$(0.25\sim1.7) \times 10^{-5}$ [a]		$(0.5\sim1.2) \times 10^6$	EL	12
		Silole Derivatives			
195 (PyPySPyPy)	2.0×10^{-4}		6.4×10^5	TOF	243
		Fullerene			
232 ([6,6]-PCBM)	2.0×10^{-7}	rt		SCLC	454

[a] Estimated from the figures.

Chart 32. Phosphorescent Emitters with Ambipolar Transport

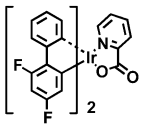

318

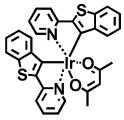

319

magnitude less than electron mobility under identical preparation and measurement conditions.[447] BPhen (**164**) shows an electron mobility of 2.4×10^{-4} $cm^2 V^{-1} s^{-1}$ at an electric filed of 3×10^5 $V cm^{-1}$.[221] A silole derivative, PyPySPyPy (**195**), has been reported to exhibit nondispersive and air-stable electron transport with a high mobility of 2.0×10^{-4} $cm^2 V^{-1} s^{-1}$.[243]

Charge carrier mobilities of electron-transporting materials[9,12,243,438,444,448−454] are listed in Table 12.

6.5. Ambipolar Transport in Amorphous Molecular Materials

Charge-transporting materials are thought to possess ambipolar transport character if they can readily accept both holes and electrons. Usually, unipolar transport, namely, either hole or electron transport, has been observed for a number of charge-transporting materials in the measurement of carrier drift mobilities.

Both hole and electron mobilities have been determined for some materials. Phosphorescent emitters such as **318** and **319** (Chart 32) have been reported to show ambipolar transport with higher hole mobilities than electron mobilities.[455] The compounds B3 (**46**) and T3 (**47**) exhibit hole and electron transport. These materials show nondispersive transients even in air for both hole and electron transport and a high electron mobility of over 10^{-3} $cm^2 V^{-1} s^{-1}$ for T3 (**47**) and a high hole mobility of 4×10^{-3} $cm^2 V^{-1} s^{-1}$ for B3 (**46**).[125,126]

6.6. Relationship between Charge Carrier Mobilities and Molecular Structures

Although many papers on charge transport have appeared in recent years, there have been few reports that discuss the correlation between molecular structures and carrier drift mobilities.

It is useful to discuss charge-transport parameters, which have been obtained by the analysis of the electric-field and temperature dependencies of charge carrier drift mobilities in terms of the disorder formalism. The charge transport parameters based on the disorder formalism are summarized in Table 13. With regard to the materials of the TDATA family, which exhibit mobilities of 10^{-5} $cm^2 V^{-1} s^{-1}$, μ_0 is of the order of 10^{-3} $cm^2 V^{-1} s^{-1}$, and σ is in the range from 0.097 to 0.092 eV. For DPH with a mobility of 10^{-4} $cm^2 V^{-1} s^{-1}$, μ_0 was still of the order of 10^{-3} $cm^2 V^{-1} s^{-1}$, but σ decreased to 0.079 eV. For the materials of the triarylamine and tris(oligoarylenyl)amine families with mobilities greater than 5.0×10^{-3} $cm^2 V^{-1} s^{-1}$, μ_0 was found to be of the order of 10^{-1} $cm^2 V^{-1} s^{-1}$, and σ was in the range from 0.075 to 0.063 eV. These results clearly show that the significant increase in μ_0 accompanied by the decrease in σ is responsible for high mobilities.

The substitution position of a phenyl group in tri(terphenyl-4-yl)amine (*o*-, *m*-, and *p*-TTA (**17**, **18**, **19**)) and *N*,*N*′-di-(biphenylyl)-*N*,*N*′-diphenyl-[1,1′-biphenyl]-4,4′-diamines (*o*-, *m*-, and *p*-BPD (**88**, **89**, **90**)) has been found to exert a significant influence on the hole drift mobility.[207] The mobilities of *p*-substituted molecules (*p*-TTA and *p*-BPD) are more than 1 order of magnitude higher than those of the *m*-substituted molecules (*m*-TTA and *m*-BPD). Charge-transport parameters reveal that the energetic disorder σ for the *p*-isomers is smaller than that for the *m*-isomers. It is thought that a smaller conformational change due to bond rotation for the *p*-isomers results in a smaller energetic disorder. These results suggest that reducing the conformational change resulting from bond rotation serves as a

Table 13. Examples of Charge-Transport Parameters Based on the Disorder Formalism

material	μ_0 ($cm^2 V^{-1} s^{-1}$)	σ (eV)	Σ	C ($(cm V^{-1})^{1/2}$)	ref
Hole-Transporting Materials					
TDATA Family: Star-Shaped Compounds with a Triphenylamine Central Core					
8 (*m*-MTDATA)	1.74×10^{-2}	0.111	3.23	4.23×10^{-4}	440
	5.3×10^{-3}	0.092	2.0	2.3×10^{-4}	432
50 (1-TNATA)	6.1×10^{-3}	0.097	1.5	2.0×10^{-4}	432
53 (TFATA)	7.4×10^{-3}	0.096	1.9	2.2×10^{-4}	432
32 (*p*-PMTDATA)	7.9×10^{-3}	0.097	2.0	2.8×10^{-4}	432
Tris(oligoarylenyl)amines					
79 (TTPA)	1.1×10^{-1}	0.064	1.1	3.3×10^{-4}	163
80 (TSePA)	1.6×10^{-1}	0.063	1.8	3.6×10^{-4}	163
17 (*o*-TTA)	9.7×10^{-3}	0.059	2.4	4.4×10^{-4}	441
18 (*m*-TTA)	5.3×10^{-3}	0.093	2.6	3.0×10^{-4}	432
19 (*p*-TTA)	1.3×10^{-1}	0.071	1.5	1.1×10^{-4}	432
81 (TPTPA)	1.8×10^{-1}	0.075	1.3	4.1×10^{-4}	163
82 (TPSePA)	1.1×10^{-1}	0.067	1.0	3.7×10^{-4}	163
85 (TFlA)	1.5×10^{-1}	0.069	1.8	1.2×10^{-4}	432
TPD Family: *N*,*N*,*N*′,*N*′-Tetraarylbenzidines					
86 (TPD)	3.5×10^{-2}	0.074	1.2		456
	3.2×10^{-2}	0.077	1.6	2.6×10^{-4}	443
	3.9×10^{-2}	0.078	1.9	2.8×10^{-4}	173
87 (α-NPD)	3.5×10^{-1}	0.073	2.0		457
88 (*o*-BPD)	1.4×10^{-2}	0.071	1.5	2.6×10^{-4}	207
89 (*m*-BPD)	5.4×10^{-2}	0.105	2.7	2.6×10^{-4}	207
90 (*p*-BPD)	2.9×10^{-2}	0.075	1.8	2.4×10^{-4}	207
93 (FFD)	8.7×10^{-2}	0.073	1.6	3.3×10^{-4}	173
96 (PFFA)	4.5×10^{-2}	0.078	1.5	2.3×10^{-4}	173
N,*N*,*N*′,*N*′-Tetraarylenyl Arylenediamines					
106 ($N_\alpha N_\alpha P$)	2.8×10^{-2}	0.098			208
Arylhydrazones					
20 (DPH)	3.3×10^{-3}	0.079	1.8	3.9×10^{-4}	432
Spiro Compounds					
140 (spiro-TAD)	1.6×10^{-2}	0.08	2.3		194
141 (spiro-*m*-TTB)	1.0×10^{-2}	0.08	1.2		194
142 (OMeTAD)	4.7×10^{-2}	0.101	2.3	3.4×10^{-4}	196
Other Materials					
148 (PF6)	2.86×10^{-1}	0.0943	2.6	4.56×10^{-4}	200
Electron-Transporting Materials					
232 ([6,6]-PCBM)		0.073			454

molecular design concept for higher mobility. A significant difference in the hole drift mobility between triphenylamine and *N*-ethylcarbazole moieties has been found for DPH and ECH.[22]

7. Outlook

Organic electronics and optoelectronics are newly emerging fields of science and technology that cover chemistry, physics, and materials science. Electronic and optoelectronic devices using organic materials are attractive because of the materials characteristics of light weight, potentially low cost, and capability of large-area, flexible device fabrication. Such devices as OLEDs, OPVs, and OFETs involve charge transport as a main process in their operation processes, and therefore, require high-performance charge-transporting materials.

This review article focuses on charge-transporting molecular materials for use in OLEDs, OPVs, and OFETs. We have tried to arrange a vast number of charge-transporting materials in order by classifying them on the basis of their molecular structures. Molecular design concepts for charge-transporting molecular materials and their charge-transport properties are discussed. Both the basic aspects of charge transport and the operation processes of the above-mentioned devices are also described.

Control of materials morphology is of essential importance in materials science and practical applications. Like crystals and liquid crystals, amorphous molecular glasses have recently constituted an important class of organic functional materials. The relation between materials morphologies and properties and device performance is a subject of interest for further studies. A significant progress has been made on charge transport in amorphous molecular materials, but the relationship between molecular structures and charge carrier drift mobilities remains to be investigated. The materials which have been put to practical applications are few in number. For practical applications in devices, not only the performance, but also other factors, for example, facile synthesis, purifications, low cost, stability, toxicity, device durability, and so forth, have to be solved.

A future progress will be directed toward a deeper understanding of materials chemistry and device physics, development of new devices including memories and sensors, fabrication of flexible devices, and integration of mulifunctions in a single device.

8. References

(1) (a) Friend, R. H.; Gymer, R. W.; Holmes, A. B.; Burroughes, J. H.; Marks, R. N.; Taliani, C.; Bradley, D. D. C.; Dos Santos, D. A.; Brédas, J. L.; Lögdlund, M.; Salaneck, W. R. *Nature* **1999**, *397*, 121. (b) Shirota, Y. *J. Mater. Chem.* **2000**, *10*, 1. (c) Forrest, S. R. *Nature* **2004**, *428*, 911. (d) Shirota, Y. *J. Mater. Chem.* **2005**, *15*, 75.

(2) (a) *Organic Electroluminescent Materials and Devices*; Miyata, S., Nalwa, H. S., Eds.; Gordon and Breach: New York, 1997. (b) Kraft, A.; Grimsdale, A. C.; Holmes, A. B. *Angew. Chem., Int. Ed. Engl.* **1998**, *37*, 402. (c) Mitschke, U.; Bäuerle, P. *J. Mater. Chem.* **2000**, *10*, 1471. (d) *Organic Electroluminescence*; Kafafi, Z. H., Ed; Taylor & Francis: New York, 2005. (e) *Organic Light-Emitting Devices, Synthesis, Properties, and Applications*; Müllen, K, Scherf, U., Eds.; Wiley-VCH: Weinheim, Germany, 2006.

(3) (a) Spanggaard, H.; Krebs, F. C. *Solar Energy Mater. Solar Cells* **2004**, *83*, 125. (b) *Organic Photovoltaics, Mechanisms, Materials and Devices*; Sun, S. S., Sariciftci, N. S., Eds.; CRC Press: New York, 2005.

(4) (a) Horowitz, G. *Adv. Mater.* **1998**, *10*, 365. (b) Katz, H. E.; Bao, Z.; Gilat, S. L. *Acc. Chem. Res.* **2001**, *34*, 359. (c) Dimitrakopoulos, C. D.; Malenfant, P. R. L. *Adv. Mater.* **2002**, *14*, 99. (d) Katz, H. E. *Chem. Mater.* **2004**, *16*, 4748. (e) Sun, Y., Liu, Y., Zhu, D. *J. Mater. Chem.* **2005**, *15*, 53. (f) Mas-Torrent, M.; Rovira, C. *J. Mater. Chem.* **2006**, *16*, 433.

(5) Lampert, M. A.; Mark, P. *Current Injection in Solids*; Academic Press: New York, 1970.

(6) *Photoconductivity and Related Phenomena*; Mort, J., Pai, D. M., Eds; Elsevier: New York, 1976.

(7) An, Z.; Yu, J.; Jones, S. C.; Barlow, S.; Yoo, S.; Domercq, B.; Prins, P.; Siebbeles, L. D. A.; Kippelen, B.; Marder, S. R. *Adv. Mater.* **2005**, *17*, 2580.

(8) Sze, S. M. *Physics of Semiconductor Devices*, 2nd ed.: Wiley; New York, 1981.

(9) Hosokawa, C.; Tokailin, H.; Higashi, H.; Kusumoto, T. *Appl. Phys. Lett.* **1992**, *60*, 1220.

(10) Hosokawa, C.; Tokailin, H.; Higashi, H.; Kusumoto, T. *Appl. Phys. Lett.* **1993**, *63*, 1322.

(11) Redecker, M.; Bässler, H.; Hörhold, H. H. *J. Phys. Chem. B* **1997**, *101*, 7398.

(12) Wong, T. C.; Kovac, J.; Lee, C. S.; Hung, L. S.; Lee, S. T. *Chem. Phys. Lett.* **2001**, *334*, 61.

(13) Schouten, P. G.; Warman, J. M.; de Haas, M. P. *J. Phys. Chem.* **1993**, *97*, 9863.

(14) Scher, H.; Montroll, E. W. *Phys. Rev. B* **1975**, *12*, 2455.

(15) Murgatroyd, P. N. *J. Phys. D* **1971**, *3*, 151.

(16) Schein, L. B. *Phys. Rev. B* **1997**, *15*, 1024.

(17) Gill, W. D. *J. Appl. Phys.* **1972**, *43*, 5033.

(18) Frenkel, J. *Phys. Rev.* **1938**, *54*, 647.

(19) Schein, L. B.; Mack, J. X. *Chem. Phys. Lett.* **1988**, *149*, 109.

(20) (a) Bässler, H. *Phys. Status Solidi B* **1981**, *107*, 9. (b) Bässler, H. *Phys. Status Solidi B* **1993**, *175*, 15.

(21) Peled, A.; Schein, L. B.; Glatz, D. *Phys. Rev. B* **1990**, *41*, 10835.

(22) Nomura, S.; Shirota, Y. *Chem. Phys. Lett.* **1997**, *268*, 461.

(23) Pope, M.; Kallmann, H. P.; Magnante, P. *J. Chem. Phys.* **1963**, *38*, 2042.

(24) Vincett, P. S.; Barlow, W. A.; Hann, R. A.; Roberts, G. G. *Thin Solid Films* **1982**, *94*, 171.

(25) Tang, C. W.; VanSlyke, S. A. *Appl. Phys. Lett.* **1987**, *51*, 913.

(26) Tang, C. W.; VanSlyke, S. A.; Chen, C. H. *J. Appl. Phys.* **1989**, *65*, 3610.

(27) Burroughes, J. H.; Bradley, D. D. C.; Brown, A. R.; Marks, R. N.; Mackay, K.; Friend, R. H.; Burns, P. L.; Holmes, A. B. *Nature* **1990**, *347*, 539.

(28) Baldo, M. A.; O'Brien, D. F.; You, Y.; Shoustikov, A.; Sibley, S.; Thompson, M. E.; Forrest, S. R. *Nature* **1998**, *395*, 151.

(29) Baldo, M. A.; Lamansky, S.; Thompson, P. E.; Forrest, S. R. *Appl. Phys. Lett.* **1999**, *75*, 4.

(30) Lamansky, S.; Djurovich, P.; Murphy, D.; Abdel-Razzaq, F.; Lee, H.-E.; Adachi, C.; Burrows, P. E.; Forrest, S. R.; Thompson, M. E. *J. Am. Chem. Soc.* **2001**, *123*, 4304.

(31) O'Brien, D.; Bleyer, A.; Lidzey, D. G.; Bradley, D. D. C.; Tsutsui, T. *J. Appl. Phys.* **1997**, *82*, 2662.

(32) Cleave, V.; Yahioglu, G.; Le Barny, P.; Friend, R. H.; Tessler, N. *Adv. Mater.* **1999**, *11*, 285.

(33) O'Regan, B.; Grätzel, M. *Nature* **1991**, *353*, 737.

(34) Nazeeruddin, M. K.; Kay, A.; Rodicio, I.; Humphry-Baker, R.; Müller, E.; Liska, P.; Vlachopoulos, N.; Grätzel, M. *J. Am. Chem. Soc.* **1993**, *115*, 6382.

(35) Tang, C. W. *Appl. Phys. Lett.* **1986**, *48*, 183.

(36) Chabinyc, M. L.; Salleo, A. *Chem. Mater.* **2004**, *16*, 4509.

(37) Tsumura, A.; Koezuka, H.; Ando, T. *Appl. Phys. Lett.* **1986**, *49*, 1210.

(38) Madru, R.; Guillaud, G.; Al Sadoun, M.; Maitrot, M.; André, J.-J.; Simon, J.; Even, R. *Chem. Phys. Lett.* **1988**, *145*, 343.

(39) Veres, J.; Ogier, S.; Lloyd, G.; de Leeuw, D. *Chem. Mater.* **2004**, *16*, 4543.

(40) Horowitz, G.; Garnier, F.; Yassar, A.; Hajlaoui, R.; Kouki, F. *Adv. Mater.* **1996**, *8*, 52.

(41) Podzorov, V.; Pudalov, V. M.; Gershenson, M. E. *Appl. Phys. Lett.* **2003**, *82*, 1739.

(42) Mochizuki, H.; Hasui, T.; Shiono, T.; Ikeda, T.; Adachi, C.; Taniguchi, Y.; Shirota, Y. *Appl. Phys. Lett.* **2000**, *77*, 1587.

(43) Mochizuki, H.; Hasui, T.; Kawamoto, M.; Shiono, T.; Ikeda, T.; Adachi, C.; Taniguchi, Y.; Shirota, Y. *Chem. Commun.* **2000**, 1923.

(44) Mochizuki, H.; Hasui, T.; Kawamoto, M.; Ikeda, T.; Adachi, C.; Taniguchi, Y.; Shirota, Y. *Macromolecules* **2003**, *36*, 3457.

(45) Kawamoto, M.; Mochizuki, H.; Shishido, A.; Tsutsumi, O.; Ikeda, T.; Lee, B.; Shirota, Y. *J. Phys. Chem. B* **2003**, *107*, 4887.

(46) Kawamoto, M.; Mochizuki, H.; Ikeda, T.; Lee, B.; Shirota, Y. *J. Appl. Phys.* **2003**, *94*, 6442.

(47) Pommerehne, J.; Vestweber, H.; Guss, W.; Mahrt, R. F.; Bässler, H.; Porsch, M.; Daub, J. *Adv. Mater.* **1995**, *7*, 551.

(48) D'Andrade, B. W.; Datta, S.; Forrest, S. R.; Djurovich, P.; Polikarpov, E.; Thompson, M. E. *Org. Electron.* **2005**, *6*, 11.

(49) Inokuchi, H. *Org. Electron.* **2006**, *7*, 62 and references cited therein.

(50) Akamatu, H.; Inokuchi, H.; Matsunaga, Y. *Nature* **1954**, *173*, 168.

(51) Gundlach, D. J.; Lin, Y. Y.; Jackson, T. N.; Nelson, S. F.; Schlom, D. G. *IEEE Electron Device Lett.* **1997**, *18*, 87.

(52) Iwatsu, F.; Kobayashi, T.; Uyeda, N. *J. Phys. Chem.* **1980**, *84*, 3223.

(53) Hor, A. M.; Loutfy, R. O. *Thin Solid Films* **1983**, *106*, 291.

(54) Nakayama, J.; Konishi, T.; Hoshino, M. *Heterocycles* **1988**, *27*, 1731.

(55) Bäuerle, P.; Fischer, T.; Bidlingmeier, B.; Stabel, A.; Rabe, J. P. *Angew. Chem., Int. Ed. Engl.* **1995**, *34*, 303.

(56) Nakanishi, H.; Sumi, N.; Aso, Y.; Otsubo, T. *J. Org. Chem.* **1998**, *63*, 8632.

(57) Krömer, J.; Rios-Carreras, I.; Fuhrmann, G.; Musch, C.; Wunderlin, M.; Debaerdemaeker, T.; Mena-Osteritz, E.; Bäuerle, P. *Angew. Chem., Int. Ed. Engl.* **2000**, *39*, 3481.

(58) Inoue, S.; Nakanishi, H.; Takimiya, K.; Aso, Y.; Otsubo, T. *Synth. Met.* **1997**, *84*, 341.

(59) Kunugi, Y.; Takimiya, K.; Yamane, K.; Yamashita, K.; Aso, Y.; Otsubo, T. *Chem. Mater.* **2003**, *15*, 6.

(60) Noda, T.; Imae, I.; Noma, N.; Shirota, Y. *Adv. Mater.* **1997**, *9*, 239.

(61) Noda, T.; Ogawa, H.; Noma, N.; Shirota, Y. *Adv. Mater.* **1997**, *9*, 720.

(62) Noda, T.; Ogawa, H.; Noma, N.; Shirota, Y. *J. Mater. Chem.* **1999**, *9*, 2177.

(63) Noda, T.; Shirota, Y. *J. Am. Chem. Soc.* **1998**, *120*, 9714.

(64) Fichou, D.; Horowitz, G.; Xu, B.; Garnier, F. *Synth. Met.* **1990**, *39*, 243.

(65) Havinga, E. E.; Rotte, I.; Meijer, E. W.; Hoeve, W. T.; Wynberg, H. *Synth. Met.* **1991**, *41*−*43*, 473.

(66) Hotta, S.; Waragai, K. *J. Mater. Chem.* **1991**, *1*, 835.

(67) Yassar, A.; Delabauglise, D.; Hmyene, M.; Nessak, B.; Horowitz, G.; Garnier, F. *Adv. Mater.* **1992**, *4*, 490.

(68) Tour, J. M.; Wu, R. *Macromolecules* **1992**, *25*, 1901.

(69) Guay, J.; Kasai, P.; Diaz, A.; Wu, R.; Tour, J. M.; Dao, L. H. *Chem. Mater.* **1992**, *4*, 1097.

(70) Bäuerle, P.; Segelbacher, U.; Maier, A.; Mehring, M. *J. Am. Chem. Soc.* **1993**, *115*, 10217.

(71) Fichou, D.; Bachet, B.; Demanze, F.; Billy, I.; Horowitz, G.; Garnier, F. *Adv. Mater.* **1996**, *8*, 500.

(72) Matsuura, Y.; Oshima, Y.; Misaki, Y.; Fujiwara, H.; Tanaka, K.; Yamabe, T.; Hotta, S. *Synth. Met.* **1996**, *82*, 155.

(73) Graf, D. D.; Campbell, J. P.; Miller, L. L.; Mann, K. R. *J. Am. Chem. Soc.* **1996**, *118*, 5480.

(74) Noma, N.; Kawaguchi, K.; Imae, I.; Nakano, H.; Shirota, Y. *J. Mater. Chem.* **1996**, *6*, 117.

(75) Noma, N.; Kawaguchi, K.; Imae, I.; Shirota, Y. *Synth. Met.* **1997**, *84*, 597.

(76) Funaoka, S.; Imae, I.; Noma, N.; Shirota, Y. *Synth. Met.* **1999**, *101*, 600.

(77) Noma, N.; Tsuzuki, T.; Shirota, Y. *Adv. Mater.* **1995**, *7*, 647.

(78) Horowitz, G.; Fichou, D.; Peng, X.; Xu, Z.; Garnier, F. *Solid State Commun.* **1989**, *72*, 381.

(79) Akimichi, H.; Waragai, K.; Hotta, S.; Kano, H.; Sakaki, H. *Appl. Phys. Lett.* **1991**, *58*, 1500.

(80) Horowitz, G.; Deloffre, F.; Garnier, F.; Hajlaoui, R.; Hmyene, M.; Yassar, A. *Synth. Met.* **1993**, *54*, 435.

(81) Hotta, S.; Waragai, K. *Adv. Mater.* **1993**, *5*, 896.

(82) Tsuzuki, T.; Kuwabara, Y.; Noma, N.; Shirota, Y.; Willis, M. R. *Jpn. J. Appl. Phys.* **1996**, *35*, L447.

(83) Gregg, B. A. *J. Phys. Chem.* **1996**, *100*, 852.

(84) Conboy, J. C.; Olson, E. J. C.; Adams, D. M.; Kerimo, J.; Zaban, A.; Gregg, B. A.; Barbara, P. F. *J. Phys. Chem. B* **1998**, *102*, 4516.

(85) Mascaro, D. J.; Thompson, M. E.; Smith, H. I.; Bulović, V. *Org. Electron.* **2005**, *6*, 211.
(86) Tamao, K.; Sumitani, K.; Kiso, Y.; Zembayashi, M.; Fujioka, A.; Kodama, S.; Nakajima, I.; Minato, A.; Kumada, M. *Bull. Chem. Soc. Jpn.* **1976**, *49*, 1958.
(87) Tamao, K.; Kodama, S.; Nakajima, I.; Kumada, M.; Minato, A.; Suzuki, K. *Tetrahedron* **1982**, *38*, 3347.
(88) Kagan, J.; Arora, S. K. *Heterocycles* **1983**, *20*, 1937.
(89) Wynberg, H.; Metselaar, J. *Synth. Commun.* **1984**, *14*, 1.
(90) Beny, J.-P.; Dhawan, S. N.; Kagan, J.; Sundlass, S. *J. Org. Chem.* **1982**, *47*, 2201.
(91) Shirota, Y.; Kobata, T.; Noma, N. *Chem. Lett.* **1989**, 1145.
(92) Higuchi, A.; Inada, H.; Kobata, T.; Shirota, Y. *Adv. Mater.* **1991**, *3*, 549.
(93) (a) Yoshikawa, S.; Kotani, Y.; Shirota, Y. Presented at the 69th Annual Meeting of the Chemical Society of Japan, Kyoto, Japan, 1995, prepr. no.2, p. 641. (b) Shirota, Y.; Moriwaki, K.; Yoshikawa, S.; Ujike, T.; Nakano, H. *J. Mater. Chem.* **1998**, *8*, 2579.
(94) Yoshiiwa, M.; Kageyama, H.; Shirota, Y.; Wakaya, F.; Gamo, K.; Takai, M. *Appl. Phys. Lett.* **1996**, *69*, 2605.
(95) Utsumi, H.; Nagahama, D.; Nakano, H.; Shirota, Y. *J. Mater. Chem.* **2002**, *12*, 2612.
(96) Tsujioka, T.; Kondo, H. *Appl. Phys. Lett.* **2003**, *83*, 937.
(97) Nakano, H.; Takahashi, T.; Kadota, T.; Shirota, Y. *Adv. Mater.* **2002**, *14*, 1157.
(98) Ueda, H.; Tanino, T.; Ando, H.; Nakano, H.; Shirota, Y. *Chem. Lett.* **2004**, *33*, 1152.
(99) Kadota, T.; Kageyama, H.; Wakaya, F.; Gamo, K.; Shirota, Y. *Chem. Lett.* **2004**, *33*, 706.
(100) Yang, D.; Chang, S. W.; Ober, C. K. *J. Mater. Chem.* **2006**, *16*, 1693.
(101) Ishikawa, W.; Inada, H.; Nakano, H.; Shirota, Y. *Chem. Lett.* **1991**, 1731.
(102) Ishikawa, W.; Inada, H.; Nakano, H.; Shirota, Y. *J. Phys. D* **1993**, *26*, B94.
(103) Ueta, E.; Nakano, H.; Shirota, Y. *Chem. Lett.* **1994**, 2397.
(104) Ishikawa, W.; Noguchi, K.; Kuwabara, Y.; Shirota, Y. *Adv. Mater.* **1993**, *5*, 559.
(105) Kageyama, H.; Itano, K.; Ishikawa, W.; Shirota, Y. *J. Mater. Chem.* **1996**, *6*, 675.
(106) Katsuma, K.; Shirota, Y. *Adv. Mater.* **1998**, *10*, 223.
(107) Kuwabara, Y.; Ogawa, H.; Inada, H.; Noma, N.; Shirota, Y. *Adv. Mater.* **1994**, *6*, 677.
(108) Higuchi, A.; Ohnishi, K.; Nomura, S.; Inada, H.; Shirota, Y. *J. Mater. Chem.* **1992**, *2*, 1109.
(109) Inada, H.; Ohnishi, K.; Nomura, S.; Higuchi, A.; Nakano, H.; Shirota, Y. *J. Mater. Chem.* **1994**, *4*, 171.
(110) Noda, T.; Ogawa, H.; Shirota, Y. *Adv. Mater.* **1999**, *11*, 283.
(111) Shirota, Y.; Kuwabara, Y.; Inada, H.; Wakimoto, T.; Nakada, H.; Yonemoto, Y.; Kawami, S.; Imai, K. *Appl. Phys. Lett.* **1994**, *65*, 807.
(112) Ishikawa, W.; Inada, H.; Nakano, H.; Shirota, Y. *Mol. Cryst. Liq. Cryst.* **1992**, *211*, 431.
(113) Inada, H.; Shirota, Y. *J. Mater. Chem.* **1993**, *3*, 319.
(114) Nishimura, K.; Kobata, T.; Inada, H.; Shirota, Y. *J. Mater. Chem.* **1991**, *1*, 897.
(115) Mäkinen, A. J.; Hill, I. G.; Kinoshita, M.; Noda, T.; Shirota, Y.; Kafafi, Z. H. *J. Appl. Phys.* **2002**, *91*, 5456.
(116) Salbeck, J.; Yu, N.; Bauer, J.; Weissörtel, F.; Bestgen, H. *Synth. Met.* **1997**, *91*, 209.
(117) Oldham, W. J., Jr.; Lachicotte, R. J.; Bazan, G. C. *J. Am. Chem. Soc.* **1998**, *120*, 2987.
(118) Ottmar, M.; Ichisaka, T.; Subramanian, L. R.; Hanack, M.; Shirota, Y. *Chem. Lett.* **2001**, 788.
(119) Imae, I.; Kawakami, Y. *Chem. Lett.* **2005**, *34*, 290.
(120) Thelakkat, M. *Macromol. Mater. Eng.* **2002**, *287*, 442.
(121) Louie, J.; Hartwig, J. F.; Fry, A. J. *J. Am. Chem. Soc.* **1997**, *119*, 11695.
(122) Shirota, Y.; Okumoto, K.; Inada, H. *Synth. Met.* **2000**, *111*−*112*, 387.
(123) Pang, J.; Tao, Y.; Freiberg, S.; Yang, X.-P.; D'Iorio, M.; Wang, S. *J. Mater. Chem.* **2002**, *12*, 206.
(124) Ohara, T.; Fujii, N.; Shirota, Y. Presented at the 76th Annual Meeting of the Chemical Society of Japan, Kanagawa, Japan, 1999, prepr. no.1, pp 372.
(125) Wu, C.-C.; Liu, T.-L.; Hung, W.-Y.; Lin, Y.-T.; Wong, K.-T.; Chen, R.-T.; Chen, Y.-M.; Chien, Y.-Y. *J. Am. Chem. Soc.* **2003**, *125*, 3710.
(126) Wu, C.-C.; Liu, W.-G.; Hung, W.-Y.; Liu, T.-L.; Lin, Y.-T.; Lin, H.-W.; Wong, K.-T.; Chien, Y.-Y.; Chen, R.-T.; Hung, T.-H.; Chao, T.-C.; Chen, Y.-M. *Appl. Phys. Lett.* **2005**, *87*, 052103.
(127) Geng, Y.; Katsis, D.; Culligan, S. W.; Ou, J. J.; Chen, S. H.; Rothberg, L. J. *Chem. Mater.* **2002**, *14*, 463.
(128) Wang, S.; Oldham, W. J., Jr.; Hudack, R. A., Jr.; Bazan, G. C. *J. Am. Chem. Soc.* **2000**, *122*, 5695.
(129) Sonntag, M.; Kreger, K.; Hanft, D.; Strohriegl, P.; Setayesh, S.; de Leeuw, D. *Chem. Mater.* **2005**, *17*, 3031.
(130) Yamamoto, T.; Nishiyama, M.; Koie, Y. *Tetrahedron Lett.* **1998**, *39*, 2367.
(131) Lyle, R. E.; DeWitt, E. J.; Nichols, N. M.; Cleland, W. *J. Am. Chem. Soc.* **1953**, *75*, 5959.
(132) Yu, W.-L.; Pei, J.; Huang, W.; Heeger, A. J. *Adv. Mater.* **2000**, *12*, 828.
(133) Shirota, Y.; Kuwabara, Y.; Okuda, D.; Okuda, R.; Ogawa, H.; Inada, H.; Wakimoto, T.; Nakada, H.; Yonemoto, Y.; Kawami, S.; Imai, K. *J. Lumin.* **1997**, *72*−*74*, 985.
(134) Inada, H.; Yonemoto, Y.; Wakimoto, T.; Imai, K.; Shirota, Y. *Mol. Cryst. Liq. Cryst.* **1996**, *280*, 331.
(135) Hamada, Y.; Sano, T.; Shibata, K.; Kuroki, K. *Jpn. J. Appl. Phys.* **1995**, *34*, L824.
(136) Van Slyke, S. A.; Chen, C. H.; Tang, C. W. *Appl. Phys. Lett.* **1996**, *69*, 2160.
(137) Elschner, A., Bruder, F., Heuer, H.-W., Jonas, F., Karbach, A., Kirchmeyer, S., Thurm, S.; Wehrmann, R. *Synth. Met.* **2000**, *111*−*112*, 139.
(138) Giebeler, C.; Antoniadis, H.; Bradley, D. D. C.; Shirota, Y. *Appl. Phys. Lett.* **1998**, *72*, 2448.
(139) Antoniadis, H.; Giebeler, C.; Bradley, D. D. C.; Shirota, Y. *Proc. SPIE*−*Int. Soc. Opt. Eng.* **1998**, *3476*, 142.
(140) Giebeler, C.; Antoniadis, H.; Bradley, D. D. C.; Shirota, Y. *J. Appl. Phys.* **1999**, *85*, 608.
(141) Mahapatro, A. K.; Ghosh, S. *Appl. Phys. Lett.* **2002**, *80*, 4840.
(142) Malliaras, G. G.; Scott, J. C. *J. Appl. Phys.* **1999**, *85*, 7426.
(143) Davids, P. S.; Campbell, I. H.; Smith, D. L. *J. Appl. Phys.* **1997**, *82*, 6319.
(144) Tse, S. C.; Tsang, S. W.; So, S. K. *J. Appl. Phys.* **2006**, *100*, 063708.
(145) Murata, H.; Merritt, C. D.; Inada, H.; Shirota, Y.; Kafafi, Z. H. *Appl. Phys. Lett.* **1999**, *75*, 3252.
(146) Ogawa, H.; Inada, H.; Shirota, Y. *Macromol. Symp.* **1997**, *125*, 171.
(147) Okumoto, K.; Shirota, Y. *Chem. Lett.* **2000**, 1034.
(148) Higuchi, A.; Shirota, Y. *Mol. Cryst. Liq. Cryst.* **1994**, *242*, 127.
(149) Chen, J. P.; Tanabe, H.; Li, X.-C.; Thoms, T.; Okamura, Y.; Ueno, K. *Synth. Met.* **2003**, *132*, 173.
(150) Chou, M.-Y.; Leung, M.-k.; Su, Y. O.; Chiang, C. L.; Lin, C.-C.; Liu, J.-H.; Kuo, C.-K.; Mou, C.-Y. *Chem. Mater.* **2004**, *16*, 654.
(151) Tokito, S.; Tanaka, H.; Noda, K.; Okada, A.; Taga, Y. *Appl. Phys. Lett.* **1997**, *70*, 1929.
(152) Tanaka, S.; Iso, T.; Doke, Y. *Chem. Commun.* **1997**, 2063.
(153) Wu, C.-C.; Lin, Y.-T.; Wong, K.-T.; Chen, R.-T.; Chien, Y.-Y. *Adv. Mater.* **2004**, *16*, 61.
(154) Ikai, M.; Tokito, S.; Sakamoto, Y.; Suzuki, T.; Taga, Y. *Appl. Phys. Lett.* **2001**, *79*, 156.
(155) Thelakkat, M.; Schmidt, H.-W. *Adv. Mater.* **1998**, *10*, 219.
(156) Higuchi, A.; Katsuma, K.; Shirota, Y. *Kobunshi Ronbunshu* **1996**, *53*, 829.
(157) Li, J.; Liu, D.; Li, Y.; Lee, C.-S.; Kwong, H.-L.; Lee, S. *Chem. Mater.* **2005**, *17*, 1208.
(158) Kundu, P.; Justin Thomas, K. R.; Lin, J. T.; Tao, Y.-T.; Chien, C.-H. *Adv. Funct. Mater.* **2003**, *13*, 445.
(159) Holmes, R. J.; Forrest, S. R.; Tung, Y.-J.; Kwong, R. C.; Brown, J. J.; Garon, S.; Thompson, M. E. *Appl. Phys. Lett.* **2003**, *82*, 2422.
(160) Hino, Y.; Kajii, H.; Ohmori, Y. *Org. Electron.* **2004**, *5*, 265.
(161) Okumoto, K.; Doi, H.; Shirota, Y. *J. Photopolym. Sci. Technol.* **2002**, *15*, 239.
(162) Shirota, Y.; Okumoto, K. *Jpn. Kokai Tokkyo Koho*, 2003-261473.
(163) Ohishi, H.; Tanaka, M.; Kageyama, H.; Shirota, Y. *Chem. Lett.* **2004**, *33*, 1266.
(164) Ko, C.-W.; Tao, Y.-T. *Synth. Met.* **2002**, *126*, 37.
(165) Tanaka, M.; Kageyama, H.; Shirota, Y. Presented at the 84th Annual Meeting of the Chemical Society of Japan, Hyogo, Japan, 2004, prepr. no.1, pp 432.
(166) Ogawa, H.; Ohnishi, K.; Shirota, Y. *Synth. Met.* **1997**, *91*, 243.
(167) Stolka, M.; Yanus, J. F.; Pai, D. M. *J. Phys. Chem.* **1984**, *88*, 4707.
(168) Adachi, C.; Tsutsui, T.; Saito, S. *Appl. Phys. Lett.* **1989**, *55*, 1489.
(169) Han, E.-M.; Do, L.-M.; Nidome, Y.; Fujihira, M. *Chem. Lett.* **1994**, 969.
(170) O'Brien, D. F.; Burrows, P. E.; Forrest, S. R.; Koene, B. E.; Loy, D. E.; Thompson, M. E. *Adv. Mater.* **1998**, *10*, 1108.
(171) Koene, B. E.; Loy, D. E.; Thompson, M. E. *Chem. Mater.* **1998**, *10*, 2235.
(172) Loy, D. E.; Koene, B. E.; Thompson, M. E. *Adv. Funct. Mater.* **2002**, *12*, 245.
(173) Okumoto, K.; Shirota, Y. *Mater. Sci. Eng.* **2001**, *B85*, 135.
(174) Tanaka, H.; Tokito, S.; Taga, Y.; Okada, A. *Chem. Commun.* **1996**, 2175.
(175) Hu, N.-X.; Xie, S.; Popovic, Z. D.; Ong, B.; Hor, A.-M. *Synth. Met.* **2000**, *111*−*112*, 421.

(176) Burrows, P. E.; Forrest, S. R.; Zhou, T. X.; Michalski, L. *Appl. Phys. Lett.* **2000**, *76*, 2493.
(177) Kwong, R. C.; Lamansky, S.; Thompson, M. E. *Adv. Mater.* **2000**, *12*, 1134.
(178) Baldo, M. A.; Thompson, M. E.; Forrest, S. R. *Nature* **2000**, *403*, 750.
(179) D'Andrade, B. W.; Thompson, M. E.; Forrest, S. R. *Adv. Mater.* **2002**, *14*, 147.
(180) Markham, J. P. J.; Lo, S.-C.; Magennis, S. W.; Burn, P. L.; Samuel, I. D. W. *Appl. Phys. Lett.* **2002**, *80*, 2645.
(181) Ohsedo, Y.; Yamate, T.; Okumoto, K.; Shirota, Y. *J. Photopolym. Sci. Technol.* **2001**, *14*, 297.
(182) (a) Okumoto, K.; Ohara, T.; Noda, T.; Shirota, Y. *Synth. Met.* **2001**, *121*, 1655. (b) Hashimoto, K.; Kageyama, H.; Shirota, Y. unpublished results.
(183) Shan, J.; Yap, G. P. A.; Richeson, D. S. *Can. J. Chem.* **2005**, *83*, 958.
(184) Yu, M.-X.; Duan, J.-P.; Lin, C.-H.; Cheng, C.-H.; Tao, Y.-T. *Chem. Mater.* **2002**, *14*, 3958.
(185) Hartmann, H.; Gerstner, P.; Rohde, D. *Org. Lett.* **2001**, *3*, 1673.
(186) Tabet, A.; Schroder, A.; Hartmann, H.; Rohde, D.; Dunsch, L. *Org. Lett.* **2003**, *5*, 1817.
(187) Liu, X.; Knupfer, M.; Dunsch, L.; Tabet, A.; Hartmann, H. *Org. Electron.* **2006**, *7*, 107.
(188) Zhang, Q.; Chen, J.; Cheng, Y.; Wang, L.; Ma, D.; Jing, X.; Wang, F. *J. Mater. Chem.* **2004**, *14*, 895.
(189) Grigalevicius, S.; Blazys, G.; Ostrauskaite, J.; Grazulevicius, J. V.; Gaidelis, V.; Jankauskas, V.; Montrimas, E. *Synth. Met.* **2002**, *128*, 127.
(190) Justin Thomas, K. R.; Lin, J. T.; Tao, Y.-T.; Ko, C.-W. *Adv. Mater.* **2000**, *12*, 1949.
(191) Jiang, K. J.; Sun, Y. L.; Shao, K. F.; Yang, L. M. *Chem. Lett.* **2004**, *33*, 50.
(192) Ostrauskaite, J.; Voska, V.; Buika, G.; Gaidelis, V.; Jankauskas, V.; Janeczek, H.; Sidaravicius, J. D.; Grazulevicius, J. V. *Synth. Met.* **2003**, *138*, 457.
(193) Kimura, M.; Inoue, S.; Shimada, K.; Tokito, S.; Noda, K.; Taga, Y.; Sawaki, Y. *Chem. Lett.* **2000**, 192.
(194) Bach, U.; De Cloedt, K.; Spreitzer, H.; Grätzel, M. *Adv. Mater.* **2000**, *12*, 1060.
(195) Bach, U.; Lupo, D.; Comte, P.; Moser, J. E.; Weissörtel, F.; Salbeck, J.; Spreitzer, H.; Grätzel, M. *Nature* **1998**, *395*, 583.
(196) Poplavskyy, D.; Nelson, J. *J. Appl. Phys.* **2003**, *93*, 341.
(197) Kimura, M.; Kuwano, S.; Sawaki, Y.; Fujikawa, H.; Noda, K.; Taga, Y.; Takagi, K. *J. Mater. Chem.* **2005**, *15*, 2393.
(198) Mi, B.-X.; Wang, P.-F.; Liu, M.-W.; Kwong, H.-L.; Wong, N.-B.; Lee, C.-S.; Lee, S.-T. *Chem. Mater.* **2003**, *15*, 3148.
(199) Zhang, L.-Z.; Chen, C.-W.; Lee, C.-F.; Wu, C.-C.; Luh, T.-Y. *Chem. Commun.* **2002**, 2336.
(200) Wu, C.-C.; Hung, W.-Y.; Liu, T.-L. *J. Appl. Phys.* **2003**, *93*, 5465.
(201) Sakai, J.; Kageyama, H.; Nomura, S.; Nakano, H.; Shirota, Y. *Mol. Cryst. Liq. Cryst.* **1997**, *296*, 445.
(202) Anderson, J. D.; McDonald, E. M.; Lee, P. A.; Anderson, M. L.; Ritchie, E. L.; Hall, H. K.; Hopkins, T.; Mash, E. A.; Wang, J.; Padias, A.; Thayumanavan, S.; Barlow, S.; Marder, S. R.; Jabbour, G. E.; Shaheen, S.; Kippelen, B.; Peyghambarian, N.; Wightman, R. M.; Armstrong, N. R. *J. Am. Chem. Soc.* **1998**, *120*, 9646.
(203) Seki, K.; Ito, E.; Ishii, H. *Synth. Met.* **1999**, *91*, 137.
(204) Hill, I. G.; Kahn, A. *J. Appl. Phys.* **1998**, *84*, 5583.
(205) Lee, S. T.; Wang, Y. M.; Hou, X. Y.; Tang, C. W. *Appl. Phys. Lett.* **1999**, *74*, 670.
(206) Hill, I. G.; Milliron, D.; Schwartz, J.; Kahn, A. *Appl. Surf. Sci.* **2000**, *166*, 354.
(207) Okumoto, K.; Wayaku, K.; Noda, T.; Kageyama, H.; Shirota, Y. *Synth. Met.* **2000**, *111*−*112*, 473.
(208) Borsenberger, P. M.; Shi, J. *Phys. Status Solidi B* **1995**, *191*, 461.
(209) Nomura, S.; Nishimura, K.; Shirota, Y. *Mol. Cryst. Liq. Cryst.* **1994**, *253*, 79.
(210) Salbeck, J.; Weissörtel, F. *Macromol. Symp.* **1997**, *125*, 121.
(211) Saragi, T. P. I.; Fuhrmann-Lieker, T.; Salbeck, J. *Adv. Funct. Mater.* **2006**, *16*, 966.
(212) Thelakkat, M.; Schmidt, H.-W. *Polym. Adv. Technol.* **1998**, *9*, 429.
(213) Hughes, G.; Bryce, M. R. *J. Mater. Chem.* **2005**, *15*, 94.
(214) Kulkarni, A. P.; Tonzola, C. J.; Babel, A.; Jenekhe, S. A. *Chem. Mater.* **2004**, *16*, 4556.
(215) Brinkmann, M.; Gadret, G.; Muccini, M.; Taliani, C.; Masciocchi, N.; Sironi, A. *J. Am. Chem. Soc.* **2000**, *122*, 5147.
(216) Wu, Q.; Esteghamatian, M.; Hu, N.-X.; Popovic, Z.; Enright, G.; Tao, Y.; D'Iorio, M.; Wang, S. *Chem. Mater.* **2000**, *12*, 79.
(217) Cui, Y.; Liu, Q.-D.; Bai, D.-R.; Jia, W.-L.; Tao, Y.; Wang, S. *Inorg. Chem.* **2005**, *44*, 601.
(218) Oyston, S.; Wang, C.; Hughes, G.; Batsanov, A. S.; Perepichka, I. F.; Bryce, M. R.; Ahn, J. H.; Pearson, C.; Petty, M. C. *J. Mater. Chem.* **2005**, *15*, 194.
(219) Kido, J.; Hongawa, K.; Okuyama, K.; Nagai, K. *Appl. Phys. Lett.* **1993**, *63*, 2627.
(220) Kido, J.; Matsumoto, T. *Appl. Phys. Lett.* **1998**, *73*, 2866.
(221) Naka, S.; Okada, H.; Onnagawa, H.; Tsutsui, T. *Appl. Phys. Lett.* **2000**, *76*, 197.
(222) Huang, J.; Pfeiffer, M.; Werner, A.; Blchwitz, J.; Leo, K.; Liu, S. *Appl. Phys. Lett.* **2002**, *80*, 139.
(223) Zhou, X.; Pfeiffer, M.; Huang, J. S.; Blochwitz-Nimoth, J.; Qin, D. S.; Werner, A.; Drechsel, J.; Maennig, B.; Leo, K. *Appl. Phys. Lett.* **2002**, *81*, 922.
(224) Bettenhausen, J.; Strohriegl, P. *Adv. Mater.* **1996**, *8*, 507.
(225) Ogawa, H.; Okuda, R.; Shirota, Y. *Mol. Cryst. Liq. Cryst.* **1998**, *315*, 187.
(226) Jandke, M.; Strohriegl, P.; Berleb, S.; Werner, E.; Brütting, W. *Macromolecules* **1998**, *31*, 6434.
(227) Gao, Z.; Lee, C. S.; Bello, I.; Lee, S. T.; Chen, R.-M.; Luh, T.-Y.; Shi, J.; Tang, C. W. *Appl. Phys. Lett.* **1999**, *74*, 865.
(228) Okumoto, K.; Shirota, Y. *Chem. Mater.* **2003**, *15*, 699.
(229) Inomata, H.; Goushi, K.; Masuko, T. Konno, T.; Imai, T.; Sasabe, H.; Brown, J. J.; Adachi, C. *Chem. Mater.* **2004**, *16*, 1285.
(230) Bettenhausen, J.; Greczmiel, M.; Jandke, M.; Strohriegl, P. *Synth. Met.* **1997**, *91*, 223.
(231) Kinoshita, M.; Shirota, Y. *Chem. Lett.* **2001**, 614.
(232) Okumoto, K.; Shirota, Y. *Appl. Phys. Lett.* **2001**, *79*, 1231.
(233) Sakamoto, Y.; Suzuki, T.; Miura, A.; Fujikawa, H.; Tokito, S.; Taga, Y. *J. Am. Chem. Soc.* **2000**, *122*, 1832.
(234) Yeh, H.-C.; Lee, R.-H.; Chan, L.-H.; Lin, T.-Y. J.; Chen, C.-T.; Balasubramaniam, E.; Tao, Y.-T. *Chem. Mater.* **2001**, *13*, 2788.
(235) Mäkinen, A. J.; Hill, I. G.; Noda, T.; Shirota, Y.; Kafafi, Z. H. *Appl. Phys. Lett.* **2001**, *78*, 670.
(236) Picciolo, L. C.; Murata, H.; Gondarenko, A.; Noda, T.; Shirota, Y.; Eaton, D. L.; Anthony, J. E.; Kafafi, Z. H. *Proc. SPIE*−*Int. Soc. Opt. Eng.* **2002**, *4464*, 383.
(237) Mazzeo, M.; Vitale, V.; Sala, F. D.; Anni, M.; Barbarella, G.; Favaretto, L.; Sotgiu, G.; Cingolani, R.; Gigli, G. *Adv. Mater.* **2005**, *17*, 34.
(238) Kinoshita, M.; Kita, H.; Shirota, Y. *Adv. Funct. Mater.* **2002**, *12*, 780.
(239) Tamao, K.; Uchida, M.; Izumizawa, T.; Furukawa, K.; Yamaguchi, S. *J. Am. Chem. Soc.* **1996**, *118*, 11974.
(240) Uchida, M.; Izumizawa, T.; Nakano, T.; Yamaguchi, S.; Tamao, K.; Furukawa, K. *Chem. Mater.* **2001**, *13*, 2680.
(241) Palilis, L. C.; Mäkinen, A. J.; Uchida, M.; Kafafi, Z. H. *Appl. Phys. Lett.* **2003**, *82*, 2209.
(242) Palilis, L. C.; Murata, H.; Uchida, M.; Kafafi, Z. H. *Org. Electron.* **2003**, *4*, 113.
(243) Murata, H.; Malliaras, G. G.; Uchida, M.; Shen, Y.; Kafafi, Z. H. *Chem. Phys. Lett.* **2001**, *339*, 161.
(244) Mäkinen, A. J.; Uchida, M.; Kafafi, Z. H. *Appl. Phys. Lett.* **2003**, *82*, 3889.
(245) Mäkinen, A. J.; Uchida, M.; Kafafi, Z. H. *J. Appl. Phys.* **2004**, *95*, 2832.
(246) Watkins, N. J.; Mäkinen, A. J.; Gao, Y.; Uchida, M.; Kafafi, Z. H. *J. Appl. Phys.* **2006**, *100*, 103706.
(247) Risko, C.; Kushto, G. P.; Kafafi, Z. H.; Brédas, J. L. *J. Chem. Phys.* **2004**, *121*, 9031; **2005**, *122*, 099901.
(248) Li, Z. H.; Tong, K. L.; Wong, M. S.; So, S. K. *J. Mater. Chem.* **2006**, *16*, 765.
(249) Oyamada, T.; Maeda, C.; Sasabe, H.; Adachi, C. *Chem. Lett.* **2003**, *32*, 388.
(250) Wu, C. C.; Lin, Y. T.; Chiang, H. H.; Cho, T. Y.; Chen, C. W.; Wong, K. T.; Liao, Y. L.; Lee, G. H.; Peng, S. M. *Appl. Phys. Lett.* **2002**, *81*, 577.
(251) Ono, K.; Yanase, T.; Ohkita, M.; Saito, K.; Matsushita, Y.; Naka, S.; Okada, H.; Onnagawa, H. *Chem. Lett.* **2004**, *33*, 276.
(252) Noda, T.; Ogawa, H.; Noma, N.; Shirota, Y. *Appl. Phys. Lett.* **1997**, *70*, 699.
(253) Maeda, M.; Yamate, T.; Okumoto, K.; Kageyama, H.; Shirota, Y.; unpublished results.
(254) Shirota, Y.; Kinoshita, M.; Noda, T.; Okumoto, K.; Ohara, T. *J. Am. Chem. Soc.* **2000**, *122*, 11021.
(255) Doi, H.; Kinoshita, M.; Okumoto, K.; Shirota, Y. *Chem. Mater.* **2003**, *15*, 1080.
(256) Moreno Castro, C.; Ruiz Delgado, M. C.; Hernández, V.; Shirota, Y.; Casado, J.; López Navarrete, J. T. *J. Phys. Chem. B* **2002**, *106*, 7163.
(257) Casado, J.; Ruiz Delgado, M. C.; Shirota, Y.; Hernández, V.; López Navarrete, J. T. *J. Phys. Chem. B* **2003**, *107*, 2637.
(258) Tang, H.; Li, F.; Shinar, J. *Appl. Phys. Lett.* **1997**, *71*, 2560.

(259) Guan, M.; Bian, Z. Q.; Zhou, Y. F.; Li, F. Y.; Li, Z. J.; Huang, C. H. *Chem. Commun.* **2003**, 2708.
(260) Yeh, H.-C.; Yeh, S.-J.; Chen, C.-T. *Chem. Commun.* **2003**, 2632.
(261) Yeh, H.-C.; Chan, L.-H.; Wu, W.-C.; Chen, C.-T. *J. Mater. Chem.* **2004**, *14*, 1293.
(262) Zhu, Y.; Kulkarni, A. P.; Jenekhe, S. A. *Chem. Mater.* **2005**, *17*, 5225.
(263) Huang, T.-H.; Lin, J. T.; Chen, L.-Y.; Lin, Y.-T.; Wu, C.-C. *Adv. Mater.* **2006**, *18*, 602.
(264) Zhang, H.; Huo, C.; Zhang, J.; Zhang, P.; Tian, W.; Wang, Y. *Chem. Commun.* **2006**, 281.
(265) Lee, S. H.; Jang, B.-B.; Kafafi, Z. H. *J. Am. Chem. Soc.* **2005**, *127*, 9071.
(266) Itano, K.; Ogawa, H.; Shirota, Y. *Appl. Phys. Lett.* **1998**, *72*, 636.
(267) Okumoto, K.; Shirota, Y. *J. Lumin.* **2000**, *87*−*89*, 1171.
(268) Ogawa, H.; Okuda, R.; Shirota, Y. *Appl. Phys. A* **1998**, *67*, 599.
(269) Cocchi, M.; Virgili, D.; Giro, G.; Fattori, V.; Di Marco, P.; Kalinowski, J.; Shirota, Y. *Appl. Phys. Lett.* **2002**, *80*, 2401.
(270) Li, G.; Kim, C. H.; Zhou, Z.; Shinar, J.; Okumoto, K.; Shirota, Y. *Appl. Phys. Lett.* **2006**, *88*, 253505.
(271) Chen, B.; Zhang, X. H.; Lin, X. Q.; Kwong, H. L.; Wong, N. B.; Lee, C. S.; Gambling, W. A.; Lee, S. T. *Synth. Met.* **2001**, *118*, 193.
(272) Chao, C.-I.; Chen, S.-A. *Appl. Phys. Lett.* **1998**, *73*, 426.
(273) Feng, J.; Li, F.; Gao, W.; Liu, S.; Liu, Y.; Wang, Y. *Appl. Phys. Lett.* **2001**, *78*, 3947.
(274) Thompson, J.; Blyth, R. I. R.; Mazzeo, M.; Anni, M.; Gigli, G.; Cingolani, R. *Appl. Phys. Lett.* **2001**, *79*, 560.
(275) Cha, S. W.; Jin, J.-I. *J. Mater. Chem.* **2003**, *13*, 479.
(276) Liu, Y.; Guo, J.; Zhang, H.; Wang, Y. *Angew. Chem., Int. Ed.* **2002**, *41*, 182.
(277) Hung, L. S.; Tang, C. W.; Mason, M. G. *Appl. Phys. Lett.* **1997**, *70*, 152.
(278) Zhou, X.; Blochwitz, J.; Pfeiffer, M.; Nollau, A.; Fritz, T.; Leo, K. *Adv. Funct. Mater.* **2001**, *11*, 310.
(279) Blochwitz, J.; Pfeiffer, M.; Hoffman, M.; Leo, K. *Synth. Met.* **2002**, *127*, 168.
(280) Ishihara, M.; Okumoto, K.; Tsuzuki, T.; Kageyama, H.; Nakano, H.; Shirota, Y. *Mol. Cryst. Liq. Cryst.* **2006**, *455*, 259.
(281) Itano, K.; Tsuzuki, T.; Ogawa, H.; Appleyard, S.; Willis, M. R.; Shirota, Y. *IEEE Trans. Electron Devices* **1997**, *44*, 1218.
(282) Cheng, G.; Zhang, Y.; Zhao, Y.; Liu, S.; Tang, S.; Ma, Y. *Appl. Phys. Lett.* **2005**, *87*, 151905.
(283) Kijima, Y.; Asai, N.; Tamura, S. *Jpn. J. Appl. Phys.* **1999**, *38*, 5274.
(284) O'Brien, D. F.; Baldo, M. A.; Thompson, M. E.; Forrest, S. R. *Appl. Phys. Lett.* **1999**, *74*, 442.
(285) Shirota, Y.; Kinoshita, M.; Okumoto, K. *Proc. SPIE*−*Int. Soc. Opt. Eng.* **2002**, *4464*, 203.
(286) Yu, G.; Xu, X.; Liu, Y.; Jiang, Z.; Yin, S.; Shuai, Z.; Zhu, D.; Duan, X.; Lu, P. *Appl. Phys. Lett.* **2005**, *87*, 222115.
(287) Ren, X.; Li, J.; Holmes, R. J.; Djurovich, P. I.; Forrest, S. R.; Thompson, M. E. *Chem. Mater.* **2004**, *16*, 4743.
(288) Yeh, S.-J.; Wu, M.-F.; Chen, C.-T.; Song, Y.-H.; Chi, Y.; Ho, M.-H.; Hsu, S.-F.; Chen, C. H. *Adv. Mater.* **2005**, *17*, 285.
(289) Murata, H.; Kafafi, Z. H.; Uchida, M. *Appl. Phys. Lett.* **2002**, *80*, 189.
(290) Adachi, C.; Kwong, R.; Forrest, S. R. *Org. Electron.* **2001**, *2*, 37.
(291) Lee, J. Y.; Kwon, J. H. *Appl. Phys. Lett.* **2005**, *86*, 063514.
(292) Shinar, J.; Shinar, R. *Mater. Res. Soc. Symp. Proc.* **2006** (Volume Date: 2005), *894*, 3−14.
(293) Peumans, P.; Yakimov, A.; Forrest, S. R. *J. Appl. Phys.* **2003**, *93*, 3693.
(294) Yu, G.; Gao, J.; Hummelen, J. C.; Wudl, F.; Heeger, A. J. *Science* **1995**, *270*, 1789.
(295) Shaheen, S. E.; Brabec, C. J.; Sariciftci, N. S.; Padinger, F.; Fromherz, T.; Hummelen, J. C. *Appl. Phys. Lett.* **2001**, *78*, 841.
(296) Li, G.; Shrotriya, V.; Yao, Y.; Yang, Y. *J. Appl. Phys.* **2005**, *98*, 043704.
(297) Peumans, P.; Uchida, S.; Forrest, S. R. *Nature* **2003**, *425*, 158.
(298) Uchida, S.; Xue, J.; Rand, B. P.; Forrest, S. R. *Appl. Phys. Lett.* **2004**, *84*, 4218.
(299) Heutz, S.; Sullivan, P.; Sanderson, B. M.; Schultes, S. M.; Jones, T. S. *Sol. Energy Mater. Sol. Cells* **2004**, *83*, 229.
(300) Rand, B. P.; Xue, J.; Uchida, S.; Forrest, S. R. *J. Appl. Phys.* **2005**, *98*, 124902.
(301) Suemori, K.; Miyata, T.; Yokoyama, M.; Hiramoto, M. *Appl. Phys. Lett.* **2005**, *86*, 063509.
(302) Yang, F.; Shtein, M.; Forrest, S. R. *J. Appl. Phys.* **2005**, *98*, 014906.
(303) Yang, F.; Shtein, M.; Forrest, S. R. *Nat. Mater.* **2005**, *4*, 37.
(304) Peumans, P.; Bulović, V.; Forrest, S. R. *Appl. Phys. Lett.* **2000**, *76*, 2650.
(305) Xue, J.; Uchida, S.; Rand, B. P.; Forrest, S. R. *Appl. Phys. Lett.* **2004**, *84*, 3013.
(306) Drechsel, J.; Männig, B.; Kozlowski, F.; Gebeyehu, D.; Werner, A.; Koch, M.; Leo, K.; Pfeiffer, M. *Thin Solid Films* **2004**, *451*−*452*, 515.
(307) Drechsel, J.; Männig, B.; Kozlowski, F.; Pfeiffer, M.; Leo, K.; Hoppe, H. *Appl. Phys. Lett.* **2005**, *86*, 244102.
(308) Yakimov, A.; Forrest, S. R. *Appl. Phys. Lett.* **2002**, *80*, 1667.
(309) Xue, J.; Uchida, S.; Rand, B. P.; Forrest, S. R. *Appl. Phys. Lett.* **2004**, *85*, 5757.
(310) Sariciftci, N. S.; Braun, D.; Zhang, C.; Srdano, V. I.; Heeger, A. J.; Stucky, G.; Wudl, F. *Appl. Phys. Lett.* **1993**, *62*, 585.
(311) Cremer, J.; Bäuerle, P. *J. Mater. Chem.* **2006**, *16*, 874.
(312) Cravino, A.; Roquet, S.; Alévêque, O.; Leriche, P.; Frère, P.; Roncali, J. *Chem. Mater.* **2006**, *18*, 2584.
(313) Roquet, S.; Cravino, A.; Leriche, P.; Alévêque, O.; Frère, P.; Roncali, J. *J. Am. Chem. Soc.* **2006**, *128*, 3459.
(314) de Bettignies, R.; Nicolas, Y.; Blanchard, P.; Levillain, E.; Nunzi, J.-M.; Roncali, J. *Adv. Mater.* **2003**, *15*, 1939.
(315) Rand, B. P.; Xue, J.; Yang, F.; Forrest, S. R. *Appl. Phys. Lett.* **2005**, *87*, 233508.
(316) Shirota, Y.; Kageyama, H.; Del Cano, T. *Abstracts of Papers*, 232nd ACS National Meeting, San Francisco, CA,, Sept. 10−14, 2006; American Chemical Society: Washington, DC, 2006; PMSE-022.
(317) Hong, Z. R.; Lee, C. S.; Lee, S. T.; Li, W. L.; Shirota, Y. *Appl. Phys. Lett.* **2002**, *81*, 2878.
(318) Gebeyehu, D.; Maennig, B.; Drechsel, J.; Leo, K.; Pfeiffer, M. *Sol. Energy Mater. Sol. Cells* **2003**, *79*, 81.
(319) Kinoshita, M.; Fujii, N.; Tsuzuki, T.; Shirota, Y. *Synth. Met.* **2001**, *121*, 1571.
(320) Kisselev, R.; Thelakkat, M. *Chem. Commun.* **2002**, 1530.
(321) Kushto, G. P.; Kim, W.; Kafafi, Z. H. *Appl. Phys. Lett.* **2005**, *86*, 093502.
(322) Xue, J.; Rand, B. P.; Uchida, S.; Forrest, S. R. *Adv. Mater.* **2005**, *17*, 66.
(323) Chu, C.-W.; Shao, Y.; Shrotriya, V.; Yang, Y. *Appl. Phys. Lett.* **2005**, *86*, 243506.
(324) Yoo, S.; Domercq, B.; Kippelen, B. *Appl. Phys. Lett.* **2004**, *85*, 5427.
(325) Wolberg, A.; Manassen, J. *J. Am. Chem. Soc.* **1970**, *92*, 2928.
(326) Darwent, J. R.; Douglas, P.; Harriman, A.; Porter, G.; Richoux, M.-C. *Coord. Chem. Rev.* **1982**, *44*, 83.
(327) Wöhrle, D.; Kreienhoop, L.; Schnurpfeil, G.; Elbe, J.; Tennigkeit, B.; Hiller, S.; Schlettwein, D. *J. Mater. Chem.* **1995**, *5*, 1819.
(328) Graaf, H.; Michaelis, W.; Schnurpfeil, G.; Jaeger, N.; Schlettwein, D. *Org. Electron.* **2004**, *5*, 237.
(329) Kang, S. J.; Yi, Y.; Kim, C. Y.; Cho, S. W.; Noh, M.; Jeong, K.; Whang, C. N. *Synth. Met.* **2006**, *156*, 32.
(330) Taima, T.; Sakai, J.; Yamanari, T.; Saito, K. *Jpn. J. Appl. Phys.* **2006**, *45*, L995.
(331) Lee, T.-W.; Byun, Y.; Koo, B.-W.; Kang, I.-N.; Lyu, Y.-Y.; Lee, C. H.; Pu, L.; Lee, S. Y. *Adv. Mater.* **2005**, *17*, 2180.
(332) Atienza, C. M.; Fernández, G.; Sánchez, L.; Martín, N.; Dantas, I. S.; Wienk, M. M.; Janssen, R. A. J.; Rahman, G. M. A.; Guldi, D. M. *Chem. Commun.* **2006**, 514.
(333) Shin, W. S.; Jeong, H.-H.; Kim, M.-K.; Jin, S.-H.; Kim, M.-R.; Lee, J.-K.; Lee, J. W.; Gal, Y.-S. *J. Mater. Chem.* **2006**, *16*, 384.
(334) Ma, W.; Yang, C.; Gong, X.; Lee, K.; Heeger, A. J. *Adv. Funct. Mater.* **2005**, *15*, 1617.
(335) Loi, M. A.; Denk, P.; Hoppe, H.; Neugebauer, H.; Meissner, D.; Winder, C.; Bradec, C. J.; Sariciftci, N. S.; Gouloumis, A.; Vázquez, P.; Torres, T. *Synth. Met.* **2003**, *137*, 1491.
(336) Hagen, J.; Schaffrath, W.; Otschik, P.; Fink, R.; Bacher, A.; Schmidt, H.-W.; Haarer, D. *Synth. Met.* **1997**, *89*, 215.
(337) Bao, Z.; Lovinger, A. J.; Dodabalapur, A. *Adv. Mater.* **1997**, *9*, 42.
(338) Bao, Z.; Lovinger, A. J.; Dodabalapur, A. *Appl. Phys. Lett.* **1996**, *69*, 3066.
(339) de Boer, R. W. I.; Stassen, A. F.; Craciun, M. F.; Mulder, C. L.; Molinari, A.; Rogge, S.; Morpurgo, A. F. *Appl. Phys. Lett.* **2005**, *86*, 262109.
(340) Zeis, R.; Siegrist, T.; Kloc, Ch. *Appl. Phys. Lett.* **2005**, *86*, 022103.
(341) Tang, Q.; Li, H.; He, M.; Hu, W.; Liu, C.; Chen, K.; Wang, C.; Liu, Y.; Zhu, D. *Adv. Mater.* **2006**, *18*, 65.
(342) Tada, H.; Touda, H.; Takada, M.; Matsushige, K. *Appl. Phys. Lett.* **2000**, *76*, 873.
(343) Ohta, H.; Kambayashi, T.; Nomura, K.; Hirano, M.; Ishikawa, K.; Takezoe, H.; Hosono, H. *Adv. Mater.* **2004**, *16*, 312.
(344) Podzorov, V.; Menard, E.; Borissov, A.; Kiryukhin, V.; Rogers, J. A.; Gershenson, M. E. *Phys. Rev. Lett.* **2004**, *93*, 086602.
(345) Horowitz, G.; Peng, X.; Fichou, D.; Garnier, F. *J. Appl. Phys.* **1990**, *67*, 528.
(346) Garnier, F.; Horowitz, G.; Peng, X. Z.; Fichou, D. *Synth. Met.* **1991**, *45*, 163.
(347) Horowitz, G.; Peng, X.-Z.; Fichou, D.; Garnier, F. *Synth. Met.* **1992**, *51*, 419.
(348) Dodabalapur, A.; Torsi, L.; Katz, H. E. *Science* **1995**, *268*, 270.

(349) Torsi, L.; Dodabalapur, A.; Rothberg, L. J.; Fung, A. W. P.; Katz, H. E. *Science* **1996**, *272*, 1462.
(350) Gundlach, D. J.; Lin, Y.-Y.; Jackson, T. N.; Schlom, D. G. *Appl. Phys. Lett.* **1997**, *71*, 3853.
(351) Hajlaoui, R.; Horowitz, G.; Garnier, F.; Arce-Broucher, A.; Laigre, L.; El Kassmi, A.; Demanze, F.; Kouki, F. *Adv. Mater.* **1997**, *9*, 389.
(352) Li, W.; Katz, H. E.; Lovinger, A. J.; Laquindanum, J. G. *Chem. Mater.* **1999**, *11*, 458.
(353) Halik, M.; Klauk, H.; Zschieschang, U.; Schmid, G.; Ponomarenko, S.; Kirchmeyer, S.; Weber, W. *Adv. Mater.* **2003**, *15*, 917.
(354) Facchetti, A.; Mushrush, M.; Katz, H. E.; Marks, T. J. *Adv. Mater.* **2003**, *15*, 33.
(355) Chesterfield, R. J.; Newman, C. R.; Pappenfus, T. M.; Ewbank, P. C.; Haukaas, M. H.; Mann, K. R.; Miller, L. L.; Frisbie, C. D. *Adv. Mater.* **2003**, *15*, 1278.
(356) Murphy, A. R.; Fréchet, J. M. J.; Chang, P.; Lee, J.; Subramanian, V. *J. Am. Chem. Soc.* **2004**, *126*, 1596.
(357) Locklin, J.; Li, D.; Mannsfeld, S. C. B.; Borkent, E.-J.; Meng, H.; Advincula, R.; Bao, Z. *Chem. Mater.* **2005**, *17*, 3366.
(358) Yoon, M.-H.; DiBenedetto, S. A.; Facchetti, A.; Marks, T. J. *J. Am. Chem. Soc.* **2005**, *127*, 1348.
(359) Zen, A.; Bilge, A.; Galbrecht, F.; Alle, R.; Meerholz, K.; Grenzer, J.; Neher, D.; Scherf, U.; Farrell, T. *J. Am. Chem. Soc.* **2006**, *128*, 3914.
(360) Mushrush, M.; Facchetti, A.; Lefenfeld, M.; Katz, H. E.; Marks, T. J. *J. Am. Chem. Soc.* **2003**, *125*, 9414.
(361) Yanagi, H.; Araki, Y.; Ohara, T.; Hotta, S.; Ichikawa, M.; Taniguchi, Y. *Adv. Funct. Mater.* **2003**, *13*, 767.
(362) Facchetti, A.; Letizia, J.; Yoon, M.-H.; Mushrush, M.; Katz, H. E.; Marks, T. J. *Chem. Mater.* **2004**, *16*, 4715.
(363) Noh, Y.-Y.; Azumi, R.; Goto, M.; Jung, B.-J.; Lim, E.; Shim, H.-K.; Yoshida, Y.; Yase, K.; Kim, D.-Y. *Chem. Mater.* **2005**, *17*, 3861.
(364) Ponomarenko, S. A.; Kirchmeyer, S.; Elschner, A.; Alpatova, N. M.; Halik, M.; Klauk, H.; Zschieschang, U.; Schmid, G. *Chem. Mater.* **2006**, *18*, 579.
(365) Videlot, C.; Ackermann, J.; Blanchard, P.; Raimundo, J.-M.; Frère, P.; Allain, M.; de Bettignies, R.; Levillain, E.; Roncali, J. *Adv. Mater.* **2003**, *15*, 306.
(366) Gorjanc, T. C.; Lévesque, I.; D'Iorio, M. *Appl. Phys. Lett.* **2004**, *84*, 930.
(367) Drolet, N.; Morin, J.-F.; Leclerc, N.; Wakim, S.; Tao, Y.; Leclerc, M. *Adv. Funct. Mater.* **2005**, *15*, 1671.
(368) Yasuda, T.; Fujita, K.; Tsutsui, T.; Geng, Y.; Culligan, S. W.; Chen, S. H. *Chem. Mater.* **2005**, *17*, 264.
(369) Nelson, S. F.; Lin, Y. -Y.; Gundlach, D. J.; Jackson, T. N. *Appl. Phys. Lett.* **1998**, *72*, 1854.
(370) Laquindanum, J. G.; Katz, H. E.; Lovinger, A. J. *J. Am. Chem. Soc.* **1998**, *120*, 664.
(371) Afzali, A.; Dimitrakopoulos, C. D.; Breen, T. L. *J. Am. Chem. Soc.* **2002**, *124*, 8812.
(372) Shtein, M.; Mapel, J.; Benziger, J. B.; Forrest, S. R. *Appl. Phys. Lett.* **2002**, *81*, 268.
(373) Klauk, H.; Halik, M.; Zschieschang, U.; Schmid, G.; Radlik, W.; Weber, W. *J. Appl. Phys.* **2002**, *92*, 5259.
(374) de Boer, R. W. I.; Klapwijk, T. M.; Morpurgo, A. F. *Appl. Phys. Lett.* **2003**, *83*, 4345.
(375) Sheraw, C. D.; Jackson, T. N.; Eaton, D. L.; Anthony, J. E. *Adv. Mater.* **2003**, *15*, 2009.
(376) Podzorov, V.; Sysoev, S. E.; Loginova, E.; Pudalov, V. M.; Gershenson, M. E. *Appl. Phys. Lett.* **2003**, *83*, 3504.
(377) Menard, E.; Podzorov, V.; Hur, S.-H.; Gaur, A.; Gershenson, M. E.; Rogers, J. A. *Adv. Mater.* **2004**, *16*, 2097.
(378) Ito, K.; Suzuki, T. *J. Appl. Phys.* **2004**, *95*, 5795.
(379) Choi, J.-M.; Hwang, D. K.; Kim, J. H.; Im, S. *Appl. Phys. Lett.* **2005**, *86*, 123505.
(380) De Angelis, F.; Cipolloni, S.; Mariucci, L.; Fortunato, G. *Appl. Phys. Lett.* **2005**, *86*, 203505.
(381) Singh, T. B.; Meghdadi, F.; Günes, S.; Marjanovic, N.; Horowitz, G.; Lang, P.; Bauer, S.; Sariciftci, N. S. *Adv. Mater.* **2005**, *17*, 2315.
(382) Ando, S.; Nishida, J.; Fujiwara, E.; Tada, H.; Inoue, Y.; Tokito, S.; Yamashita, Y. *Chem. Mater.* **2005**, *17*, 1261.
(383) Pisula, W.; Menon, A.; Stepputat, M.; Lieberwirth, I.; Kolb, U.; Tracz, A.; Sirringhaus, H.; Pakula, T.; Müllen, K. *Adv. Mater.* **2005**, *17*, 684.
(384) Seo, S.; Park, B.-N.; Evans, P. G. *Appl. Phys. Lett.* **2006**, *88*, 232114.
(385) Myny, K.; De Vusser, S.; Steudel, S.; Janssen, D.; Müller, R.; De Jonge, S.; Verlaak, S.; Genoe, J.; Heremans, P. *Appl. Phys. Lett.* **2006**, *88*, 222103.
(386) Bao, Z.; Lovinger, A. J.; Brown, J. *J. Am. Chem. Soc.* **1998**, *120*, 207.
(387) Noh, Y.-Y.; Kim, J.-J.; Yoshida, Y.; Yase, K. *Adv. Mater.* **2003**, *15*, 699.
(388) Kitamura, M.; Imada, T.; Kako, S.; Arakawa, Y. *Jpn. J. Appl. Phys.* **2004**, *43*, 2326.
(389) Aramaki, S.; Sakai, Y.; Ono, N. *Appl. Phys. Lett.* **2004**, *84*, 2085.
(390) de Oteyza, D. G.; Barrena, E.; Ossó, J. O.; Dosch, H.; Meyer, S.; Pflaum, J. *Appl. Phys. Lett.* **2005**, *87*, 183504.
(391) Hoshimono, K.; Fujimori, S.; Fujita, S.; Fujita, S. *Jpn. J. Appl. Phys.* **1993**, *32*, L1070.
(392) Haddon, R. C.; Perel, A. S.; Morris, R. C.; Palstra, T. T. M.; Hebard, A. F.; Fleming, R. M. *Appl. Phys. Lett.* **1995**, *67*, 121.
(393) Jarrett, C. P.; Pichler, K.; Newbould, R.; Friend, R. H. *Synth. Met.* **1996**, *77*, 35.
(394) Waldauf, C.; Schilinsky, P.; Perisutti, M.; Hauch, J.; Brabec, C. J. *Adv. Mater.* **2003**, *15*, 2084.
(395) Shibata, K.; Kubozono, Y.; Kanbara, T.; Hosokawa, T.; Fujiwara, A.; Ito, Y.; Shinohara, H. *Appl. Phys. Lett.* **2004**, *84*, 2572.
(396) Kunugi, Y.; Takimiya, K.; Negishi, N.; Otsubo, T.; Aso, Y. *J. Mater. Chem.* **2004**, *14*, 2840.
(397) Singh, T. B.; Marjanović, N.; Matt, G. J.; Sariciftci, N. S.; Schwödiauer, R.; Bauer, S. *Appl. Phys. Lett.* **2004**, *85*, 5409.
(398) Kumashiro, R.; Tanigaki, K.; Ohashi, H.; Tagmatarchis, N.; Kato, H.; Shinohara, H.; Akasaka, T.; Kato, K.; Aoyagi, S.; Kimura, S.; Takata, M. *Appl. Phys. Lett.* **2004**, *84*, 2154.
(399) Amriou, S.; Mehta, A.; Bryce, M. R. *J. Mater. Chem.* **2005**, *15*, 1232.
(400) Tapponnier, A.; Biaggio, I.; Günter, P. *Appl. Phys. Lett.* **2005**, *86*, 112114.
(401) Nagano, T.; Sugiyama, H.; Kuwahara, E.; Watanabe, R.; Kusai, H.; Kashino, Y.; Kubozono, Y. *Appl. Phys. Lett.* **2005**, *87*, 023501.
(402) Ogawa, K.; Kato, T.; Ikegami, A.; Tsuji, H.; Aoki, N.; Ochiai, Y.; P. Bird, J. *Appl. Phys. Lett.* **2006**, *88*, 112109.
(403) Horowitz, G.; Kouki, F.; Spearman, P.; Fichou, D.; Nogues, C.; Pan, X.; Garnier, F. *Adv. Mater.* **1996**, *8*, 242.
(404) Laquindanum, J. G.; Katz, H. E.; Dodabalapur, A.; Lovinger, A. J. *J. Am. Chem. Soc.* **1996**, *118*, 11331.
(405) Malenfant, P. R. L.; Dimitrakopoulos, C. D.; Gelorme, J. D.; Kosbar, L. L.; Graham, T. O. *Appl. Phys. Lett.* **2002**, *80*, 2517.
(406) Yoo, B.; Jung, T.; Basu, D.; Dodabalapur, A.; Jones, B. A.; Facchetti, A.; Wasielewski, M. R.; Marks, T. J. *Appl. Phys. Lett.* **2006**, *88*, 082104.
(407) Sirringhaus, H.; Friend, R. H.; Li, X. C.; Moratti, S. C.; Holmes, A. B.; Feeder, N. *Appl. Phys. Lett.* **1997**, *71*, 3871.
(408) Lanquindanum, J. G.; Katz, H. E.; Lovinger, A. J.; Dodabalapur, A. *Adv. Mater.* **1997**, *9*, 36.
(409) Kunugi, Y.; Takimiya, K.; Yamashita, K.; Aso, Y.; Otsubo, T. *Chem. Lett.* **2002**, 958.
(410) Takimiya, K.; Kunugi, Y.; Konda, Y.; Niihara, N.; Otubo, T. *J. Am. Chem. Soc.* **2004**, *126*, 5084.
(411) Wu, Y.; Li, Y.; Gardner, S.; Ong, B. S. *J. Am. Chem. Soc.* **2005**, *127*, 614.
(412) Cicoira, F.; Santato, C.; Melucci, M.; Favaretto, L.; Gazzano, M.; Muccini, M.; Barbarella, G. *Adv. Mater.* **2006**, *18*, 169.
(413) Sun, Y. M.; Ma, Y. Q.; Liu, Y. Q.; Lin, Y. Y.; Wang, Z. Y.; Wang, Y.; Di, C. A.; Xiao, K.; Chen, X. M.; Qiu, W. F.; Zhang, B.; Yu, G.; Hu, W. P.; Zhu, D. B. *Adv. Funct. Mater.* **2006**, *16*, 426.
(414) Sun, Y.; Liu, Y.; Ma, Y.; Di, C.; Wang, Y.; Wu, W.; Yu, G.; Hu, W.; Zhu, D. *Appl. Phys. Lett.* **2006**, *88*, 242113.
(415) Nam, M.-S.; Ardavan, A.; Cava, R. J.; Chaikin, P. M. *Appl. Phys. Lett.* **2003**, *83*, 4782.
(416) Mas-Torrent, M.; Durkut, M.; Hadley, P.; Ribas, X.; Rovira, C. *J. Am. Chem. Soc.* **2004**, *126*, 984.
(417) Mas-Torrent, M.; Hadley, P.; Bromley, S. T.; Crivillers, N.; Veciana, J.; Rovira, C. *Appl. Phys. Lett.* **2005**, *86*, 012110.
(418) Xue, J.; Forrest, S. R. *Appl. Phys. Lett.* **2001**, *79*, 3714.
(419) Ponomarenko, S. A.; Kirchmeyer, S.; Elschner, A.; Huisman, B.-H.; Karbach, A.; Drechsler, D. *Adv. Funct. Mater.* **2003**, *13*, 591.
(420) Sun, Y. M.; Xiao, K.; Liu, Y. Q.; Wang, J. L.; Pei, J.; Yu, G.; Zhu, D. B. *Adv. Funct. Mater.* **2005**, *15*, 818.
(421) Muccini, M. *Nat. Mater.* **2006**, *5*, 605.
(422) Hepp, A.; Heil, H.; Weise, W.; Ahles, M.; Schmechel, R.; von Seggern, H. *Phys. Rev. Lett.* **2003**, *91*, 157406.
(423) Rost, C.; Karg, S.; Riess, W.; Loi, M. A.; Murgia, M.; Muccini, M. *Appl. Phys. Lett.* **2004**, *85*, 1613.
(424) Dinelli, F.; Capelli, R.; Loi, M. A.; Murgia, M.; Muccini, M.; Facchetti, A.; Marks, T. J. *Adv. Mater.* **2006**, *18*, 1416.
(425) Schein, L. B.; Brown, D. W. *Mol. Cryst. Liq. Cryst.* **1982**, *87*, 1.
(426) Frankevich, E.; Maruyama, Y.; Ogata, H. *Chem. Phys. Lett.* **1993**, *214*, 39.
(427) Warta, W.; Stehle, R.; Karl, N. *Appl. Phys. A* **1985**, *36*, 163.
(428) Adam, D.; Closs, F.; Frey, T.; Funhoff, D.; Haarer, D.; Ringsdorf, H.; Schuhmacher, P.; Siemensmeyer, K. *Phys. Rev. Lett.* **1993**, *70*, 457.
(429) Adam, D.; Schuhmacher, P.; Simmerer, J.; Häussling, L.; Siemensmeyer, K.; Etzbach, K. H.; Ringsdorf, H.; Haarer, D. *Nature* **1994**, *371*, 141.

(430) van de Craats, A. M.; Warman, J. M.; Müllen, K.; Geerts, Y.; Brand, J. D. *Adv. Mater.* **1998**, *10*, 36.
(431) Borsenberger, P. M.; Pautmeier, L. T.; Bässler, H. *Phys. Rev. B* **1992**, *46*, 12145.
(432) Shirota, Y.; Okumoto, K.; Ohishi, H.; Tanaka, M.; Nakao, M.; Wayaku, K.; Nomura, S.; Kageyama, H. *Proc. SPIE−Int. Soc. Opt. Eng.* **2005**, *5937*, 593717.
(433) Tse, S. C.; Fong, H. H.; So, S. K. *J. Appl. Phys.* **2003**, *94*, 2033.
(434) Shirota, Y.; Nomura, S.; Kageyama, H. *Proc. SPIE−Int. Soc. Opt. Eng.* **1998**, *3476*, 132.
(435) Strohriegl, P.; Grazulevicius, J. V. *Adv. Mater.* **2002**, *14*, 1439.
(436) Nishimura, K.; Inada, H.; Kobata, T.; Matsui, Y.; Shirota, Y. *Mol. Cryst. Liq. Cryst.* **1992**, *217*, 235.
(437) Nomura, S.; Nishimura, K.; Shirota, Y. *Thin Solid Films* **1996**, *273*, 27.
(438) Deng, Z.; Lee, S. T.; Webb, D. P.; Chan, Y. C.; Gambling, W. A. *Synth. Met.* **1999**, *107*, 107.
(439) Lee, J. Y.; Kwon, J. H. *Appl. Phys. Lett.* **2006**, *88*, 183502.
(440) Saudigel, J.; Stössel, M.; Steuber, F.; Simmerer, J. *Appl. Phys. Lett.* **1999**, *75*, 217.
(441) Kageyama, H.; Ohnishi, K.; Nomura, S.; Shirota, Y. *Chem. Phys. Lett.* **1997**, *277*, 137.
(442) Tse, S. C.; Kwok, K. C.; So, S. K. *Appl. Phys. Lett.* **2006**, *89*, 262102.
(443) Heun, S.; Borsenberger, P. M. *Chem. Phys.* **1995**, *200*, 245.
(444) Malliaras, G. G.; Shen, Y.; Dunlap, D. H.; Murata, H.; Kafafi, Z. H. *Appl. Phys. Lett.* **2001**, *79*, 2582.
(445) Fong, H.; Lun, K.; So, S. *Jpn. J. Appl. Phys.* **2002**, *41*, L1122.
(446) Fong, H. H.; So, S. K. *J. Appl. Phys.* **2005**, *98*, 023711.
(447) Fong, H. H.; So, S. K. *J. Appl. Phys.* **2006**, *100*, 094502.
(448) Kepler, R. G.; Beeson, P. M.; Jacobs, S. J.; Anderson, R. A.; Sinclair, M. B.; Valencia, V. S.; Cahill, P. A. *Appl. Phys. Lett.* **1995**, *66*, 3618.
(449) Chen, B. J.; Lai, W. Y.; Gao, Z. Q.; Lee, C. S.; Lee, S. T.; Gambling, W. A. *Appl. Phys. Lett.* **1999**, *75*, 4010.
(450) Yasuda, T.; Yamaguchi, Y.; Zou, D.-C.; Tsutsui, T. *Jpn. J. Appl. Phys.* **2002**, *41*, 5626.
(451) Tokuhisa, H.; Era, M.; Tsutsui, T.; Saito, S. *Appl. Phys. Lett.* **1995**, *66*, 3433.
(452) Kawabe, Y.; Abe, J. *Appl. Phys. Lett.* **2002**, *81*, 493.
(453) Bettenhausen, J.; Strohriegl, P.; Brütting, W.; Tokuhisa, H.; Tsutsui, T. *J. Appl. Phys.* **1997**, *82*, 4957.
(454) Mihailetchi, V. D.; van Duren, J. K. J.; Blom, P. W. M.; Hummelen, J. C.; Janssen, R. A. J.; Kroon, J. M.; Respens, M. T.; Verhees, W. J. H.; Wienk, M. M. *Adv. Funct. Mater.* **2003**, *13*, 43.
(455) Matsusue, N.; Suzuki, Y.; Naito, H. *Jpn. J. Appl. Phys.* **2005**, *44*, 3691.
(456) Borsenberger, P. M.; Fitzgerald, J. J. *J. Phys. Chem.* **1993**, *97*, 4815.
(457) Borsenberger, P. M.; Magin, E. H.; Shi, *J. Phys. B* **1996**, *217*, 212.

CR050143+